Phosphorylation of the Cell Surface Receptor Golden Goal and Layer-Specific Targeting in *Drosophila*

Dissertation

Klaudiusz Mann

Phosphorylation of the Cell Surface Receptor Golden Goal and Layer-Specific Targeting in *Drosophila*

Dissertation
zur Erlangung des Doktorgrades der Naturwissenschaften

an der Fakultät für Biologie
der Ludwigs-Maximilians-Universität München
Angefertigt am Max Planck Institut für Neurobiologie
Arbeitsgruppe Neuronale Konnektivität

Vorgelegt von
Klaudiusz Mann

München, 14. November 2011

Erstgutachter:	Prof. Dr. Rüdiger Klein
Zweitgutachter:	Prof. Dr. John Parsch
Tag der mündlicher Prüfung	03. April 2012

Ehrenwörtliche Versicherung

Hiermit, erkläre ich, dass ich die vorliegende Dissertation selbständig und ohne unerlaubte Hilfe angefertigt habe. Ich habe mich dabei keiner anderen als der von mir ausdrücklich bezeichneten Hilfen und Quellen bedient.

Erklärung

Ich erkläre hiermit, dass ich mich nicht anderweitig ohne Erfolg einer Doktorprüfung unterzogen habe. Die Dissertation wurde in ihrer jetzigen oder ähnlichen Form bei keiner anderen Hochschule eingereicht und hat noch keinen sonstigen Prüfungszwecken gedient.

München, Oktober 2011

____

Klaudiusz Mann

Die vorliegende Arbeit wurde zwischen October 2007 und Dezember 2011 unter der Leitung von Dr. Takashi Suzuki am Max-Planck-Institut für Neurobiologie in Martinstried durchgeführt.

The following article has been published based on my thesis:

Mann K, Wang M, Luu S-H, Ohler S, Hakeda-Suzuki S, Suzuki T (2012)
A putative tyrosine phosphorylation site of the cell surface receptor Golden goal is involved in synaptic layer selection in the visual system. *Development* 139(4):760-71

Mojej Rodzinie

Table of content

List of abbreviations 4
Index of figures 5
Index of tables 6
Summary 7

1. Introduction 9
1.1 Cellular and molecular mechanisms of axon guidance 9
1.2 Mechanisms of layer-specific axon targeting 14
1.3 The *Drosophila* visual system 18
1.4 Development of the fly visual system 20
1.5 Molecular mechanisms of lamination in the *Drosophila* visual system 22
1.6 Golden goal and synaptic-layer recognition 24
1.7 Objectives of the thesis project 27

2. Results 29
2.1 Gogo requires the cytoplasmic middle part for its function 29
2.2 The YYD motif has a crucial function 32
2.3 The YYD motif is a potential phosphorylation site 32
2.4 Gogo undergoes phosphorylation 35
2.5 The additional phosphorylation sites 37
2.6 The phospho-Gogo specific antibody 40
2.7 The YYD motif is phosphorylated during the pupal development 43
2.8 YYD motif and M1 layer targeting 44

2.9 Gogo phosphorylation is not entirely required for M1 layer recognition..... 47
2.10 YYD motif and *flamingo* in M3 layer targeting 49
2.11 Fmi-Gogo collaboration and Gogo phosphorylation.................................. 51
2.12 DInR regulates Gogo phosphorylation *in vivo* 53
2.13 *dinr* and *gogo* interact genetically in photoreceptor axon targeting 56
2.14 DInR enzymatic activity is required for potentiating *gogo* overexpression phenotypes 58
2.15 Loss of *dinr* does not affect R8 targeting 61
2.16 Downregulation of insulin signaling suppresses R8 axons adhesion to the M1 layer... 64

3. Discussion 67
3.1 The functional elements in the Gogo cytoplasmic domain 68
3.2 Gogo is a tyrosine phosphorylated axon guidance receptor 69
3.3 The model 70
3.4 Gogo phosphorylation and visual system development 71
3.5 *gogo* and *dinr* 74
3.6 Gogo dephosphorylation as a permissive signal in axon guidance 78
3.7 Concluding remarks.. 80

4. Materials and Methods 81
4.1 Materials 81
4.1.1 Chemicals.. 81
4.1.2 Buffers and solutions 82
4.1.3 Fly maintenance 83
4.1.4 Equipment 84
4.1.5 Consumables and other reagents.. 85
4.1.6 Antibodies 86
4.1.7 Fly stocks 88
4.1.8 Plasmids 89
4.1.9 Oligonucleotides 91
4.2 Methods 92
4.2.1 Molecular cloning 92
4.2.2 Transformation and plasmid preparation 94
4.2.3 Cell culture and transfection 94
4.2.4 Cell aggregation assay and immunocytochemical staining 95
4.2.5 Co-immunoprecipitation 95

4.2.6 Immunoblotting 96
4.2.7 Fly maintenance 96
4.2.8 *Drosophila* genetics 97
4.2.9 *Drosophila* transgenesis 98
4.2.10 Genomic DNA isolation 100
4.2.11 Whole mount brain staining 101
4.2.12 Assessment of the R8 photoreceptor axonal phenotypes 101
4.2.13 Summary of experimental genotypes 102

5. Appendix 107

6. Bibliography 109

Acknowledgements 119
Curriculum vitae 121

List of abbreviations

The following list includes only the frequently used abbreviations. All other abbreviations are explained in the main text.

APF	(hours) after pupal formation
D	aspartic acid
DInR (*dinr*)	*Drosophila* Insulin Receptor
DILP (*dilp*)	*Drosophila* Insulin-Like Peptide
*ey*FLP	*eyless* Flipase
F	phenylalanine
Fmi (*fmi*)	Flamingo
GOF	gain of function
Gogo (*gogo*)	Golden goal
GMR	glass multiple reporter
IIS	insulin/IGF (insulin-like growth factor)-signaling
IP	immunoprecipitation
LOF	loss of function
UAS	upstream regulatory sequence
pY	phosphotyrosine
RGC	retinal ganglion cells
S2	Schneider’s line 2 cells
Y	tyrosine

Index of figures

Figure 1-1: The general mechanisms of axon guidance
Figure 1-2: General mechanisms governing layer-specific axon targeting in the *Drosophila* visual system
Figure 1-3: *Drosophila* visual system structure
Figure 1-4: Development of the *Drosophila* visual system
Figure 1-5: Genetic regulation of target layer selection in the *Drosophila* visual system
Figure 1-6: Gogo: protein structure and function
Figure 2-1: Gogo requires the cytoplasmic middle part for its function
Figure 2-2: The YYD motif has a crucial function
Figure 2-3: Gogo is tyrosine-phosphorylated *in vivo*
Figure 2-4: The YYD motif is phosphorylated *in vivo*
Figure 2-5: Location of the additional phosphorylation sites
Figure 2-6: The YYD motif is the “key phosphorylation site”
Figure 2-7: The phospho-Gogo specific antibody
Figure 2-8: The YYD motif is phosphorylated during early pupal development
Figure 2-9: The YYD motif plays a role in the interaction of R8 axons with the M1 layer
Figure 2-10: Gogo phosphorylation and the temporal layer recognition
Figure 2-11: Gogo - Fmi collaboration to recognize the M3 layer requires Gogo dephosphorylation
Figure 2-12: Fmi-Gogo interaction and Gogo phosphorylation
Figure 2-13: *dinr* positively regulates Gogo phosphorylation
Figure 2-14: *gogo* interacts genetically with *dinr* during R8 axons targeting
Figure 2-15: DInR enzymatic activity is required for potentiating Gogo overexpression phenotypes
Figure 2-16: Mutation in the YYD motif suppress the genetic interaction with *dinr*
Figure 2-17: Loss of *dinr* does not affect R8 axon targeting
Figure 2-18: Downregulation of insulin signaling suppresses R8 axons interaction to the temporary layer
Figure 3-1: Model explaining R8 axons defects upon Gogo hyperphosphorylation
Figure 3-2: Signaling “A” and “B” model
Figure 5-1: Gogo expression level comparison between different lines used in the study

Index of tables

Table 4-1: Chemicals
Table 4-2: Equipment
Table 4-3: Consumables and other reagents
Table 4-4: Primary antibodies
Table 4-5: Secondary antibodies
Table 4-6: Fly stocks
Table 4-7: Plasmids
Table 4-8: Oligonucleotides
Table 5-1: Candidate kinases tested for the enhancement of *gogo* gain of function phenotype

Summary

Golden goal (Gogo) is a cell-surface protein critical for proper synaptic layer targeting of photoreceptors in the *Drosophila melanogaster* visual system. In collaboration with the seven-transmembrane cadherin Flamingo (Fmi), Gogo mediates both temporal and final layer targeting of R cell axons and its cytoplasmic domain is required. However, it is not known how Gogo activity is regulated. I show in my Dissertation that a conserved tripeptide Tyr-Tyr-Asp (YYD motif) in Gogo cytoplasmic domain is required for photoreceptor axon targeting. Deleting the YYD motif is sufficient to completely abolish Gogo function. I demonstrate that the YYD motif is a phosphorylation site and that mutations in the YYD tripeptide impair synaptic layer targeting. Gogo phosphorylation results in premature axon stopping and dephosphorylation is crucial for the collaboration with Fmi during the final target layer targeting. Therefore, both temporal and final layer targeting strongly depend on Gogo phosphorylation status. *Drosophila* Insulin Receptor (DInR) has been reported to regulate wiring of photoreceptors in the fly. I show that insulin signaling is a positive regulator of YYD motif phosphorylation in a direct or indirect way. My findings suggest a novel mechanism of the regulation of Gogo activity by phosphorylation which can be induced by insulin signaling. I propose the model that a constant phosphorylation signal is antagonized by a presumably temporal dephosphorylation signal, which creates a permissive signal that could govern developmental timing in axon targeting.

1. Introduction

1.1 Cellular and molecular mechanisms of axon guidance

The structure of the nervous system forms the basis for synaptic communication between specific neurons enabling proper perception and behavior (Huberman et al., 2010). Therefore, the pattern and fidelity of precise connections between neurons shape the functional capabilities of the nervous system. The structural complexity of the nervous system can be observed at different anatomical levels, for instance: topographic maps, synaptic layers, sets of synapses (Mast et al., 2006). To achieve this level of complexity, nerve cells, unlike most cells whose parts stay at the same place, are able to extend their axons at very long distances. Thus, understanding how neuronal cells find specific synaptic targets to achieve a stereotyped pattern of connections is one of the central questions in developmental neurobiology (Sanes and Zipursky, 2010).

Two models provided a conceptual framework for our understanding of the development of precise synaptic connections in the central nervous system. First, the Langley's hypothesis of "chemical relations" between synaptically connected neurons (Langley, 1892), second, Sperry's "chemoaffinity" hypothesis (Sperry, 1963). The notion of Sperry that the molecular interactions between neurons and the extracellular environment (including between and amongst axons and dendrites) ensure for the connections between "proper" synaptic partners (Sperry, 1963) was confirmed by experimental work over the last four decades and many molecular cues that provide the synaptic specificity were identified (Benson et al., 2001; Huberman et al., 2010; Raper and Mason, 2010). Sperry in his work postulated that *"the cells and fibers of the brain and cord must carry some kind of individual identification tags, presumably cytochemical in nature, by which they are distinguished one from another almost in many regions, to the level of the single neuron; and further, that the growing fibers are extremely particular when it comes to establishing synaptic connections, each axon linking only with certain neurons to which it becomes selectively attached by specific chemical affinities"* (Sperry, 1963). Thus, each pair of neurons – source and target – should have its own, unique, self-recognizing chemical identity; this is the principle of the guiding mechanism (Benson et al., 2001). However, contemporary models do not propose a point-for-point specificity between each axon and its target. Rather gradients of adhesivity or repulsion play a role in determining the areas that the axon can enter (Gilbert, 1997).

How a neuronal process can recognize and respond to chemical cues which guide them to a particular target cells? It is the growth cone - a highly motile and sensitive structure at the tips of axons and dendrites - which is the locomotory apparatus and enables neurites to navigate through the environment (Dickson, 2001) (**Figure 1-1A**). The environmental cues that guide axons (and dendrites) can function at both long and short ranges; and as chemoattractants or chemorepellents. They can influence the bundling of axons together into nerves or fascicles (fasciculation) or mediate interactions between nerves and substrates (Dickson, 2002; Kolodkin and Tessier-Lavigne, 2011) (**Figure 1-1B**). The pathways that axons have to follow show very often an astonishing complexity and this requires that neurites change the responsiveness to certain cues from attraction to repulsion or completely extinguish responses to certain cues and acquire responsiveness to other at key choice points (Kolodkin and Tessier-Lavigne, 2011).

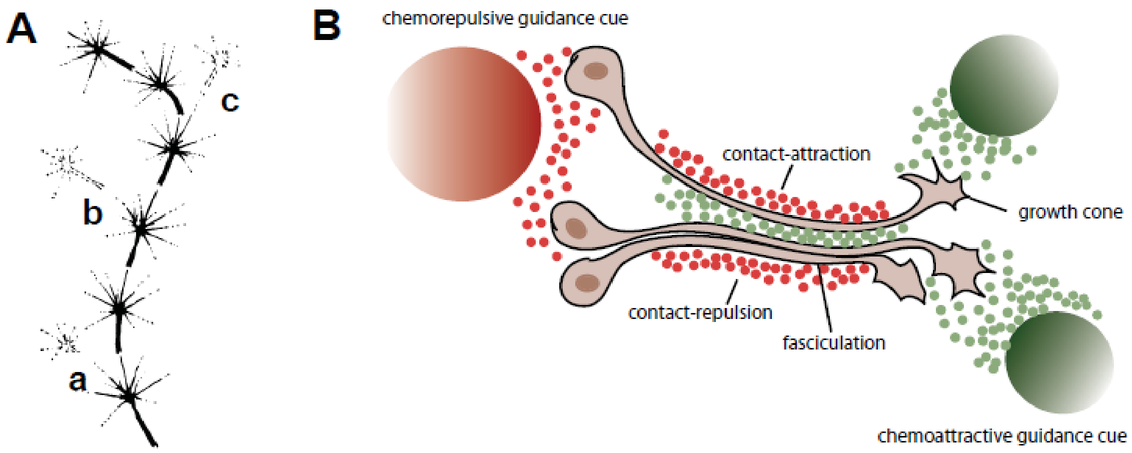

Figure 1-1: The general mechanisms of axon guidance

(A) Schematic of sequential steps in guidance of a growing nerve fiber. The growth cone constantly tests the surrounding in all directions; the critical factors will prevail to set the course in a certain direction. Numerous alternative possible paths, as represented at ‘a’, ‘b’ and ‘c’ are possible at each point but fail to develop because of differential chemical attraction. Adapted from (Sperry, 1963).

(B) Schematic representation of main guidance mechanisms: chemorepulsion, chemoattraction, contact-repulsion and contact-attraction. Axons are repelled from the source of the repellent (red), whereas growth cones are attracted towards cells expressing the attractant (green). Commonly axons travel through the environment in the form of a fascicle. Adapted from (TessierLavigne and Goodman, 1996).

Four major families of “canonical” guidance cues were identified over the last two decades: Netrins, Slits, Semaphorins and Ephrins (Dickson, 2002). Additionally morphogens, growth factors, and certain cell-adhesion molecules (CAMs) are involved in neuronal guidance and connectivity (Kolodkin and Tessier-Lavigne, 2011).

Netrins

Netrins constitute a small family of conserved cues of about 70-80 kDa. They are bifunctional, capable of attracting some axons and repelling others (Colamarino and Tessier-Lavigne, 1995) which explains their well studied function in guiding axons both toward and away from the midline (Harris et al., 1996). Netrins play a role in axon guidance across the animal kingdom in many aspects of nervous system development (Moore et al., 2007), acting at both “long-range” and “short-range” (Kolodkin and Tessier-Lavigne, 2011). The attractive responses are mediated through their receptors of the DCC (Deleted in Colorectal Carcinomas) family (Dickson, 2002; Bashaw and Klein, 2010), whereas repulsive responses are mediated primarily by UNC-5 and UNC5-DCC signaling (Lai Wing Sun et al., 2011).

Slits

Slits are large secreted molecules functioning in axonal repulsion (Dickson, 2002) which act through receptors of the Roundabout (Robo) family (Kidd et al., 1998). Some of the large Slits can be cleaved to yield an amino-terminal fragment that can also bind to Robo (Kolodkin and Tessier-Lavigne, 2011). Furthermore, Slits can stimulate axon branching and elongation (Wang et al., 1999).

Semaphorins

Semaphorins are large, conserved protein family that includes both secreted and transmembrane guidance molecules (Yazdani and Terman, 2006). Semaphorins contain a signature Semaphorin domain composed of approximately 500 amino acids signature that plays a key role in mediating physical binding of these proteins with signaling receptors belonging to the Plexin family. Semaphorin signaling acts repulsively during neural development: either as repellents in a surrounding repulsion fashion or, when expressed on axon bundles, to facilitate the unbundling, or defasciculation of individual axonal processes (Tran et al., 2007; Kolodkin and Tessier-Lavigne, 2011). The major receptors for Semaphorins are members of the Plexin family which are mostly bound directly by Semaphorins, but sometimes secreted Semaphorins bind to the obligate co-receptors Neuropilin-1 or Neuropilin-2 forming an active holoreceptor complex (Kolodkin and Tessier-Lavigne, 2011). Some Semaphorins under certain circumstances serve both as attractants and repellents (Tran et al., 2007).

Ephrins

Two subfamilies constitute the Ephrins family: the five class A Ephrins (tethered to the cell surface via GPI linkages) and three class B Ephrins (transmembrane molecules) (Klein, 2004). Ephrins undergo a clustering to activate their receptors and are not active if released from the cell surface; thus they act as short-range guidance cues (Klein, 2009). In organization of topographic maps Ephrins function as attractants for some axons and repellents for other, as well as positive or negative regulators of axonal branching (Klein, 2004; Kolodkin and Tessier-Lavigne, 2011). Ephrins also participate in “reverse” signaling, functioning as receptors to regulate topographic mapping, axon guidance and synaptogenesis (Egea and Klein, 2007; Klein, 2009).

Morphogens and growth factors

Among the morphogens Hedgehog (Hh), morphogens from the Wnt pathway, and Transforming Growth Factor b (TGFb)/bone morphogenetic protein (BMP) families and a variety of growth factors were shown to be implicated in axon guidance (Kolodkin and Tessier-Lavigne, 2011). It is worth to note, that the same molecular gradient can be used both as a morphogen and as a guidance cue (Butler and Dodd, 2003). In axon guidance the function of Wnts is best known: it acts in *Drosophila via* Derailed, the homolog of the Ryk receptor tyrosine kinase in mediating repulsive responses of axons, whereas in mammals Wnt4 is implicated in attracting commissural axons in the anterior direction after midline crossing (Kolodkin and Tessier-Lavigne, 2011). Functions for various Wnts in axon attraction and repulsion, moreover in topographic mapping and synapse formation in diverse organisms were reported (Salinas and Zou, 2008). The function of Hh family members in axons guidance (both as repellents and attractants) has been documented only in vertebrates so far (Kolodkin and Tessier-Lavigne, 2011). TGFb/BMP family members were shown to act as repellents. However, for instance in *C. elegans* the UNC-129 gene is not a guidance cue but rather modulates the response of the axons to the Netrin signal (Kolodkin and Tessier-Lavigne, 2011).

Growth factors were implicated in attraction of axons in the peripheral and central nervous system. Examples include: hepatocyte growth factor, the neurotrophins brain-derived neurotrophic factor and neurotrophin-3, fibroblast growth factor, glial-derived neurotrophic factor, neuregulin, and stem cell factor (Kolodkin and Tessier-Lavigne, 2011). However, the full understanding of growth factor function in axon guidance is far from being complete.

Cell-adhesion molecules

The majority of recent findings support the model in which the members of the cell-adhesion molecule families regulate outgrowth stimulation or attraction by functioning as signaling molecules, usually in heterophilic combinations (Kolodkin and Tessier-Lavigne, 2011). Examples include for instance: Beaten Path (Beat) and Sidestep in *Drosophila* (Siebert et al., 2009), and others like NrCAM, L1 (members of the

IgCAMs) (Kolodkin and Tessier-Lavigne, 2011). A fascinating example is the *Drosophila* DsCAM which can be generated in over 19,000 isoforms through alternative splicing (Grueber and Sagasti, 2010).

1.2 Mechanisms of layer-specific axon targeting

The organization of neuronal networks into columns and layers is a typical feature of many areas of the nervous system in invertebrates and vertebrates. Why mechanisms allowing for the formation of columns and layers in the nervous system have evolved?

Typically axons bearing signals from adjacent points in space target to adjacent areas in the brain forming topographic maps. An extensively studied example is here the visual system (Feldheim and O'Leary, 2010). However, not only the position in space but also other attributes of a visual stimulus (for instance color, brightness, movement) have to be processes in parallel. If position is encoded by localized activation within a two-dimensional field of neurons, these other features are encoded by local circuit modules (often envisioned as “columns”) that act both in series and in parallel and are reiterated many times across the field. “Columns” lie orthogonal to the topographic map; each level of the “column” represents a different, specific visual feature within the same point in space, for instance color etc. (Huberman et al., 2010). Thus, the visual system (and other parts of the brain), show not only a columnar but also a laminar (layered) structure. How the columns acquire a laminated structure is an intriguing question. Several factors can contribute to the formation of layers in the nervous system: cell-cell recognition (1), cell-extracellular matrix and cell-secreted cues interaction (2) and neural activity (3) (Huberman et al., 2010).

1) Layer-specific targeting by cell-cell recognition

Four models were proposed which could explain how layers are specified during development (Huberman et al., 2010).

1) Pre- and postsynaptic cells use a combinatorial code of cell-surface molecules. Pre- and postsynaptic partners express matching complements of ligands and receptors, so that only contacts between the correct cells are stabilized (**Figure 1-2A**).

2) The expression of ubiquitous cell-adhesion molecules is temporally dynamically regulated and is switched on and off as axons are growing toward the target (**Figure 1-2B**).
3) Neurites in the layer express attractive or repulsive axon guidance molecules, drawing appropriate axons toward (or away) from their target (**Figure 1-2C**).
4) The quantitative differences in adhesive factors are used by incoming axons to sort into layers (**Figure 1-2D**).

Certainly new variations of the mechanisms proposed above are possible.

2) Layer-specific targeting by matrix cues

The extracellular matrix was postulated to be prepatterned to guide axons into their target layers. The guidance cues which are attached to the matrix can act both as attractants or repellents, and can be expressed in form of bands (labeling unique vertical positions) or gradients (Huberman et al., 2010). The guidance cues can be anchored to the membrane (for instance growing retinal ganglion cells, RGC) neurons require cues attached to the collagen IV, (Xiao et al., 2005; Xiao and Baier, 2007)), or molecules deposited in the matrix on their own can help to organize neurons into layers (for instance in the case of layer-specific targeting of the RGCs to the optic tectum: the large glycoproteins Tenascin-C, Tenascin-R, Reelin and the chondroitin sulfate proteoglycan Versican (Sakakibara et al., 2003; Yamagata and Sanes, 2005; Baba et al., 2007), Nel (Jiang et al., 2009)

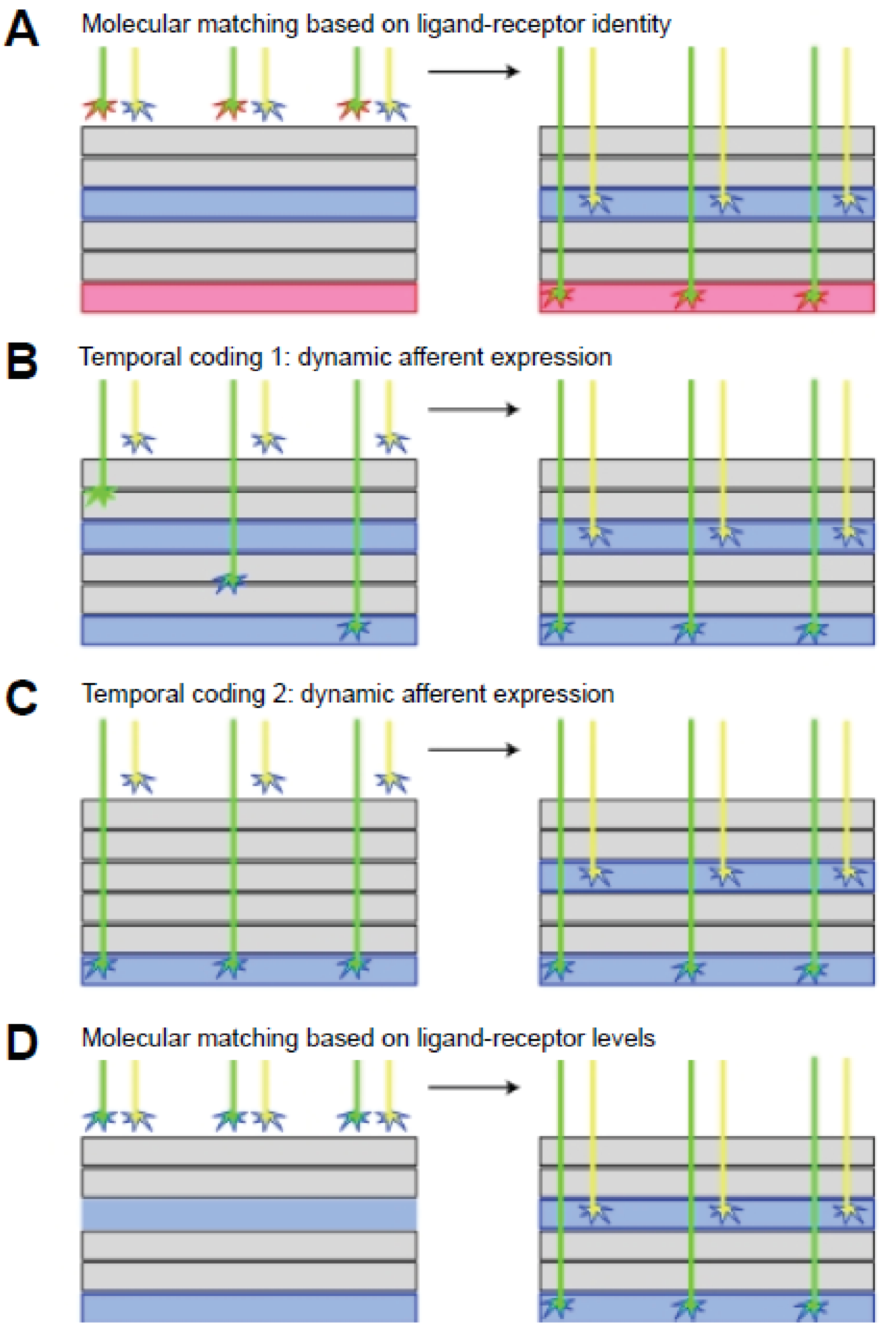
A
Molecular matching based on ligand-receptor identity
B
Temporal coding 1: dynamic afferent expression
C
Temporal coding 2: dynamic afferent expression
D
Molecular matching based on ligand-receptor levels

Figure 1-2: General mechanisms governing layer-specific axon targeting in the *Drosophila* visual system

(A) The precise match between axons expressing two different molecular recognition signals (red and blue) is achieved because the target layers express different recognition cues (red and blue).

(B) A set of neurons passes by the more distal layer and recognizes the deeper destination layer because the expression of a specific surface recognition cue (blue) is switched on after they leave to distally located target structure. Later in the development, a second population of neuronal processes which already express the recognition molecules (blue) projects to the first target layer which expresses the matching guidance determinants (blue).

3) Neural activity and layer-specific targeting

The involvement of neuronal activity on targeting-specificity remains unclear since it was shown that connectivity is a predetermined process that occurs in the absence of neural activity (Benson et al., 2001). On the other hand studies on the retina have shown that the spontaneous activity of the retina is important for topographic and eye-specific mapping of RGC axons in the primary relay centers (for instance lateral geniculate nucleus, LGN) since activity can disintegrate eye-specific connections in the LGN after they form (Chapman, 2000; Demas et al., 2006). However, eye specific "layers" are different from the functionally distinct laminar-specific targeting since they do not reflect cell-type-specific targeting choices (Huberman et al., 2010). Therefore, some authors suggest that the involvement of neural activity on layer formation is questionable and could be a result of a species-specific variations (Huberman et al., 2010). In summary, it was proposed that early in the development the correct targeting is activity-independent, however, once the connections are formed, activity is needed to maintain their laminar specificity. It is well accepted that activity influences the final synapse formation and number (Benson et al., 2001). Thus, wiring occurs initially by an activity-independent guidance mechanism, and these early formed connections are subsequently refined through electrical signaling among neurons (Kolodkin and Tessier-Lavigne, 2011).

In *Drosophila*, in contrast to mammals, formation of neuronal circuits is believed to be genetically "hard wired" and activity-independent (Hiesinger et al., 2006).

(C) Axons from different populations (green and yellow) of neurons already express the appropriate recognition molecule (blue). However, the expression of the guidance determinants in the target area is dynamically regulated and the later arriving axons (yellow) form connections within the distal targeting layer.

(D) The layer-specific targeting depends on the expression level of ligands and receptors. The highly expressing growth cones (green) recognize the high expressing target layer (dark blue); whereas the low expressing growth cones (yellow) target the low expressing target (light blue). Figure from (Huberman et al., 2010).

1.3 The *Drosophila* visual system

The astonishing complexity of the *Drosophila melanogaster* compound eye was described for the first time in 1915 by Ramón y Cajal (Clandinin and Zipursky, 2002). Flies share with other invertebrates and vertebrates several basic features of the eye organization, including a retinotopic map and layer-specific connectivity (Ting and Lee, 2007). Therefore, they are useful as models to study the principles of the nervous system development. The *Drosophila* compound eye comprises an array of 800 simple eyes (ommatidia), each containing eight photoreceptors (R cells) arranged in a stereotyped fashion, forming a crystal-like structure (**Figure 1-3**) (Clandinin and Zipursky, 2002). Four neuropiles constitute the optic lobe underlying each of the fly's compound eyes: the lamina, medulla, lobula and the lobula plate (**Figure 1-3A**). Photoreceptors from a single ommatidium form a bundle to innervate the lamina and the medulla in a retinotopic fashion. The photoreceptors are categorized in two subclasses: the R1-R6 cells, responsible for motion detection (so called outer photoreceptors) and the R7/R8 cells, responsible for color vision (inner photoreceptors).

Within the lamina, R1-R6 axons defasciculate and each axon projects to a unique target, thereby redistributing their inputs to separate post-synaptic targets (**Figure 1-3B**). It has a critical functional consequence: due to the curvature of the fly eye R-cells that look at the same point in space can converge onto a common target. Each target comprises five lamina monopolar neurons, called L1-L5. Together, these cells and the associated R cell axons form an axon fascicle called cartridge (**Figure 1-3D**) (Meinertzhagen and O'Neil, 1991).

The medulla contains a number of different cell types and is subdivided into ten layers (M1-M10) (Fischbach K.F., 1989). The photoreceptors R7 and R8 extend through the lamina and terminate at two distinct layers in the medulla: M6 and M3 layer respectively (**Figure 1-3A, C**). Here each point in space is represented by a single column comprised of R7/R8 cell axons and the indirect inputs from R1-R6 cells *via* lamina neurons from lamina cartridges (Mast et al., 2006). The layer-specific connections made by R7, R8 and lamina neurons are reminiscent of those observed in the vertebrate cortex (Ting and Lee, 2007). The precise pattern of neuronal connections within the lamina and medulla was described at the level of individual neurons (Meinertzhagen and O'Neil, 1991; Takemura et al., 2008).

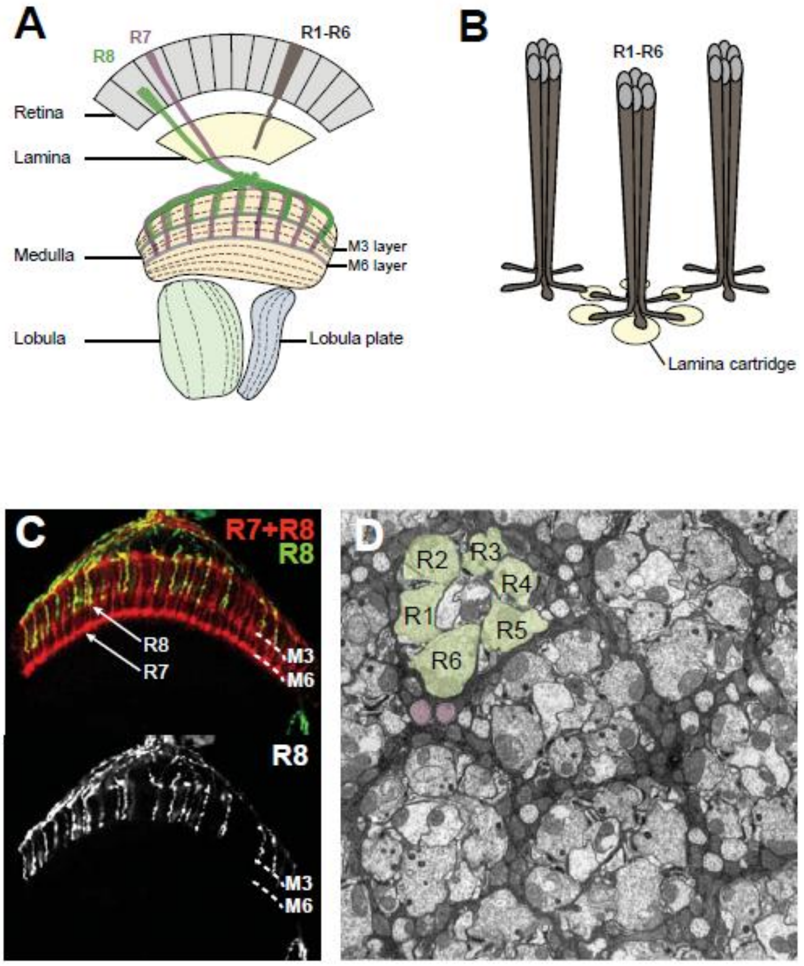
A
R7
R8
R1-R6
Retina
Lamina
Medulla
M3 layer
M6 layer
Lobula
Lobula plate
B
R1-R6
Lamina cartridge
C
R7+R8
R8
R8
R7
M3
M6
R8
M3
M6
D
R2
R3
R4
R1
R5
R6

Figure 1-3: ***Drosophila* visual system structure**

(A) The crystal-like structure of the compound eye retina is formed by 800 simple eyes (ommatidia), each containing R1-R8 photoreceptors. Below the retina four neuropiles form the optic lobes: the lamina, medulla, lobula and lobula plate. R1-R6 cells (grey) terminate in the lamina. The medulla is composed of ten distinct layers and R7 (red) / R8 (green) axons terminate in the M6 and M3 layers respectively.

(B) In the lamina R1-R6 photoreceptors defasciculate redistributing their inputs to separate targets (cartridges).

(C) *In vivo* confocal image of a wild type medulla R8 axons (labeled with *Rh6-GFP*, green) terminate in the M3 layer, whereas R7 axons target the M6 layer. Medulla layers are indicated by white dashed lines. Both R7 and R8 are labeled with mAb24B10 staining (red).

(D) Electron microscopy section of the fly’s wild type lamina. An array of cartridges is visible. Each of the photoreceptors can be identified based on the morphology and the relative position to the neighboring cells. A single cartridge is pseudocolored (R1-R6 in green and R7/8 in red).

1.4 Development of the fly visual system

The *Drosophila* adult eye derives from the larval eye imaginal disc, an epithelial structure that begins to differentiate during the third instar larval stage when the morphogenetic furrow (a visible indentation that demarcates the boundary between developing photoreceptors and undifferentiated cells) moves from the posterior to the anterior edge of the eye disc inducing sequential differentiation of photoreceptor neurons (**Figure 1-4A**). Next, differentiated photoreceptors send their processes into the brain through the optic stalk (a tube-like structure connecting the eye disc with the brain), where they orchestrate the development of the optic lobe. Photoreceptors migration towards the brain relies on the glia cells migration. The R8 photoreceptors differentiate first and project axons to the medulla as the pioneering axons. They are followed by the R1-R6 axons which stop at the lamina neuropil (**Figure 1-4B**). In order to induce proliferation and differentiation of lamina neurons first photoreceptors deliver Hedgehog and Spitz (epidermal growth factor (EGF) – like ligand). Lamina neurons then together with photoreceptors will form lamina cartridges. The R7 cells differentiate as the last ones and send their processes towards the brain in one bundle with the pioneering R8 axon followed by the R1-R6 axons (Tayler and Garrity, 2003; Ting and Lee, 2007).

As mentioned before during the larval development the R7/R8 cells past the lamina and terminate at the medulla ganglion (**Figure 1-4A, B**). Their targeting occurs in a step-wise fashion (**Figure 1-4C**). During the first (early pupal) stage, the R8, R7 and lamina axons sequentially project to their temporary layers. During the second (late pupal) stage their growth cones progress synchronously to their destinated layers. The R-cell growth cones begin to segregate into discrete layers at 17% after pupal formation (Ting et al., 2005). First, the R8 cell extends its axon into the superficial medulla (M1 layer, R8-temporary layer). The R7s which differentiate 24 hours after R8 project axons which pass the R8 growth cones and pause at a deeper layer (R7-temporary layer). The second step starts at 50 APF. At this stage the R8 growth cones project to the R7 temporary layer, which later becomes the R8-recipient layer (M3). R7s extend further into the medulla and reach their final targeting layer (M6) (Ting et al., 2005).

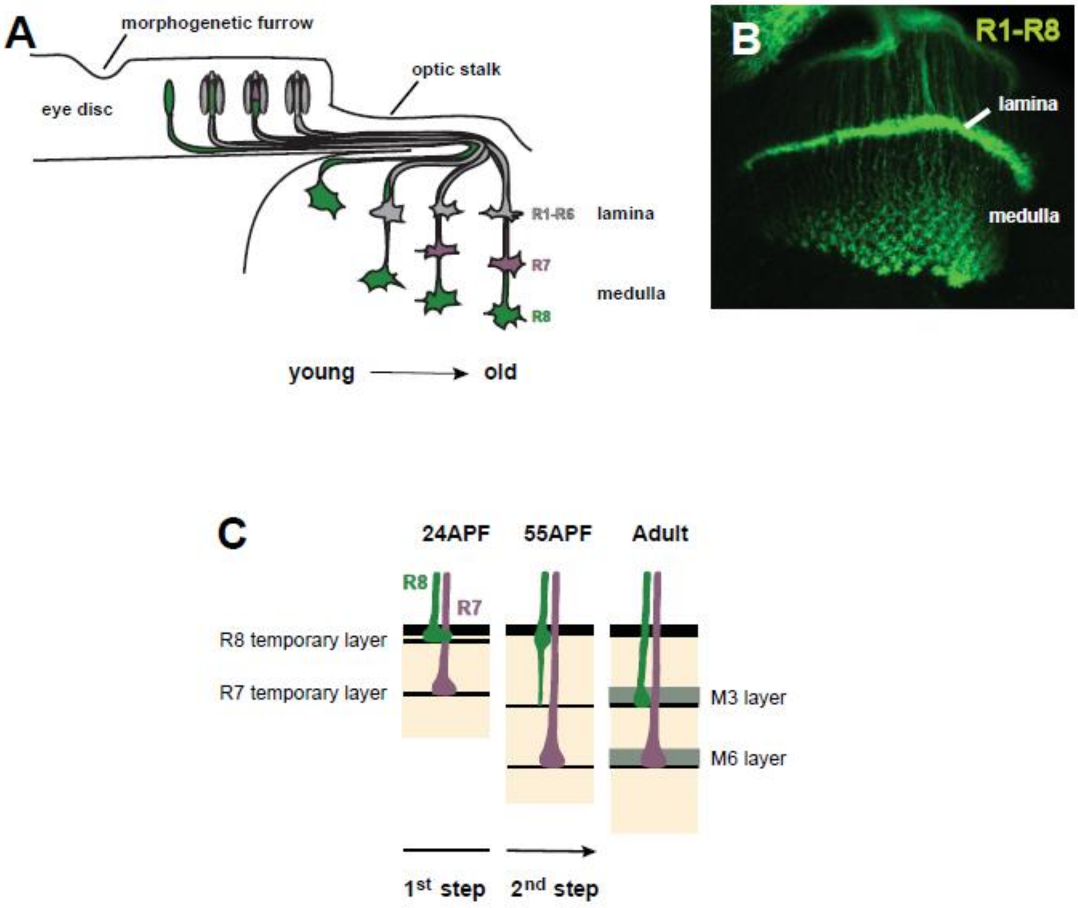
A
morphogenetic furrow
eye disc
optic stalk
R1-R6
lamina
R7
medulla
R8
young
old
B
R1-R8
lamina
medulla
C
24APF
55APF
Adult
R8
R7
R8 temporary layer
R7 temporary layer
M3 layer
M6 layer
1st step
2nd step

Figure 1-4: Development of the *Drosophila* visual system

(A) The larval development. The photoreceptors differentiate in the eye disc and send their processes through the optic stalk towards the brain. R1-R6 axons stop in the region where the future lamina will be formed (lamina plexus) and R7/8 grow deeper to form the medulla. It is a dynamical process thus a gradient of early and late differentiated axons is clearly visible. Adapted from (Tayler and Garrity, 2003).

(B) Confocal image stack from a third instar larval stage lamina. All photoreceptors were labeled with mAb24B10 (green).

(C) Targeting of R7/8 photoreceptors during pupal development occurs in two distinct steps. In the young pupae (24APF, 1st step), R7/8 axons reach their temporal layers where they pause until about 50 APF. At this time they start to project to their recipient layers (2nd step). The development is completed at the end of the pupal stage.

1.5 Molecular mechanisms of lamination in the *Drosophila* visual system

All optic ganglions in the *Drosophila* visual system (lamina, medulla, lobula and lobula plate) have a layered structure. However, here I will focus only on the layer formation during the medulla development, specifically on the target layer selection by R8 and R7 photoreceptors.

R8 photoreceptors

Three cell surface molecules – the leucine-rich repeat cell adhesion molecule Capricious (Caps) (Shinza-Kameda et al., 2006), the seven-transmembrane cadherin Flamingo (Fmi) (Lee et al., 2003; Senti et al., 2003) and Golden goal (Gogo) (Tomasi et al., 2008; Hakeda-Suzuki et al., 2011) have been implicated in establishing synaptic-layer targeting specifically in R8 photoreceptors.

The homophilic molecule Caps is expressed in R8 cells and target neurons in the distal medulla including M3 layer, but not M6 layer. Thus Caps is used to recognize and stabilize the contact between R8 axons and the target layer (Shinza-Kameda et al., 2006). Overexpression of Caps in R7 redirects them to the M3 layer whereas *caps*-deficient R8 cells terminate in layers deeper than M3.

Both Fmi and Gogo are dynamically expressed in all R-cell subtypes. Animals mutant for *fmi* and *gogo* share phenotypic similarities: in both cases the R8 axons remain at the distal border of the medulla neuropil, where they normally pause during early pupal development. The exact function of *gogo* in R8 targeting and the involvement of *fmi* will be explained in the next paragraph (**Introduction 1.6**).

During the targeting process the afferent axons and the target neurons have to act in a coordinated manner. For instance the secreted low-density lipoprotein (LDL) receptor repeat containing ligand Jelly belly (Jeb) and the Anaplastic receptor tyrosine kinase (Alk) control afferent-target interaction during layer-specific (and column-specific) targeting of R8 axons within the medulla. Jeb upon release from the photoreceptor cells activates Alk signaling in the target neurons and so directly or undirectly regulates expression of guidance molecules (Fmi, Dumbfounded/Kin of Irre and Roughest/IrreC) thereby promoting target recognition by the environment (Bazigou et al., 2007).

R7 photoreceptors

N-cadherin (Ncad) – an adhesion molecule widely distributed in the brain – is involved in synaptic layer recognition by R7 axons acting as a permissive adhesion factor. In brains mutant for *Ncad* R7 incorrectly target the M3 instead of the M6 layer. Ncad mediates afferent-target interactions and acts cell-autonomously in R7 cells (Lee et al., 2001; Nern et al., 2005; Ting et al., 2005; Yonekura et al., 2007). Additionally two receptor protein tyrosine phosphatases Ptp69D and Lar, as well as Liprin-α were shown to regulate R7 targeting (Newsome et al., 2000; Clandinin et al., 2001; Maurel-Zaffran et al., 2001; Hofmeyer et al., 2006; Hofmeyer and Treisman, 2009). Surprisingly, R7 axon targeting does not depend on Lar phosphatase activity, but on the wedge domain which mediates dimerization and facilitates the recruitment of other components such as Ncad and Liprin-α (Hofmeyer et al., 2006).

The number of expressed guidance determinants is restricted. Thus, additional mechanisms are required to achieve a layer-specificity of the complex neuronal connections. One of the possibilities used in nature is a precise spatio-temporal control of expression of guidance determinants. The transient expression of transcription factors enables to control and coordinate the expression of guidance determinants. For instance Sequoia (Seq) is transiently expressed first in R8 and then R7 cells when they extend to their temporary layers (Petrovic and Hummel, 2008). The *seq* gene controls the expression of Ncad (thereby regulating afferent-target interactions), Rhodopsin expression and target-layer specificity by suppression of alternate R7/R8 specific fates (Morey et al., 2008). Another prominent example is the transcription regulator Senseless (Sens) which directly activates both the expression of the R8-specific Rh5/Rh6 opsins and Caps, while repressing the R7-specific opsins Rh3/Rh4. The transcription factor NF-YC cell-autonomously repress upregulation of Sens; it acts in parallel with the transcription factor Prospero that suppresses the expression of R8-cell-specific opsins while promoting R7-cell-specific guidance molecules (Morey et al., 2008).

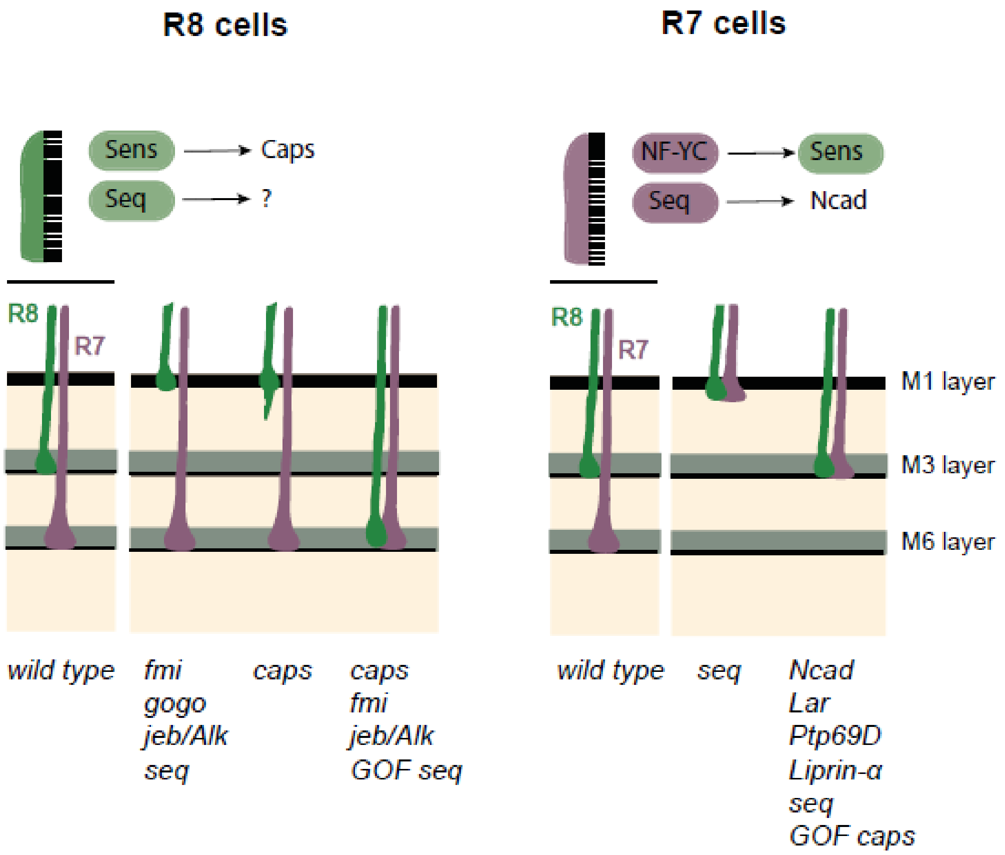
R8 cells
R7 cells
Sens
Caps
Seq
?
NF-YC
Sens
Seq
Ncad
R8
R7
R8
R7
M1 layer
M3 layer
M6 layer
wild type
fmi
gogo
jeb/Alk
seq
caps
caps
fmi
jeb/Alk
GOF seq
wild type
seq
Ncad
Lar
Ptp69D
Liprin-α
seq
GOF caps

Figure 1-5: Genetic regulation of target layer selection in the *Drosophila* visual system
Layer-specific targeting of R8 (left) and R7 axons (right) is regulated by distinct, however partially overlapping molecular mechanisms. On the left side of each panel the wild type targeting is schematically depicted; the right site shows the typical loss of function mutant phenotypes; GOF – gain of function. Adapted from (Salecker et al., 2011).

1.6 Golden goal and synaptic-layer recognition

The *golden goal* (*gogo*) gene was identified in a large scale genetic screen for genes involved in axon pathfinding in the *Drosophila* visual system (Berger et al., 2008; Tomasi et al., 2008). Three *gogo* mutants were recovered ([D869], [D1600], [H1675]), each of them is a single nucleotide mutation (**Figure 1-6A**). In *gogo* animals in which photoreceptor (R) cells are mutant for *gogo* (*gogo*$^-$ *ey*FLP flies) a number of defects is visible, mutant animals show axon guidance defects in both lamina and medulla (R1-R6, R7/R8 cells). In the lamina R1-R6 photoreceptor synaptic target selection is affected (Hakeda-Suzuki et al., 2011). The medulla rotation is incomplete resulting in the formation of abnormal bundles through an ectopic chiasm at the posterior side of the lamina. The array of R7 axons is generally disrupted, resulting in crossings and a low frequency of undershooting the medulla layer M6. The R8 axons cross and bundle each other, often overshoot their correct target layer M3 or stall at the temporary layer M1 (Tomasi et al., 2008).

Gogo is an evolutionary conserved single transmembrane molecule which has a Tsp1 (Trombospondin1), a CUB domains and a GOGO domain on the extracellular side (**Figure 1-6A**). The Gogo and Tsp1 domains, but not the CUB domain, are required for Gogo function (Tomasi et al., 2008). Gogo protein is dynamically expressed in the visual system (Tomasi et al., 2008). Specifically during the pupal stages Gogo is highly expressed in all photoreceptors. From the midpupal stage onward Gogo expression becomes reduced, but a faint staining is seen on R axons at the M3 layer. In later stages of pupal development, Gogo seems to be expressed in R neurons at a relatively small level (Tomasi et al., 2008).

The only known molecule which physically interacts with Gogo is Hu-li tai shao (Hts), the *Drosophila* homologue of Adducin (Ohler et al., 2011). It was proposed that Gogo both positively and negatively regulates Hts regulating the Actin-Spectrin cytoskeleton in growth cone filopodia and thereby guiding R axons (Ohler et al., 2011).

Based on the phenotypical analysis and other experiments Gogo was proposed to function specifically in R8 axons (but not R7) to promote repulsive axon-axons interactions between R axons to maintain their proper spacing. Moreover, Gogo is one of the key regulators of layer-specific targeting and it promotes axon-target recognition at the M1 temporary layer allowing R8 axons to enter their correct columns in the medulla and its prolonged expression causes R8 axon terminals to form blob-like structures at the medulla neuropil border, indicating an enhanced axon-target interaction (**Figure 1-6B**) (Tomasi et al., 2008; Hakeda-Suzuki et al., 2011). On the other hand loss of *gogo* results in axons stalling at the medulla surface: the stalling occurs because the axon-target interaction in this case is abolished (**Figure 1-6B**). Later it was shown that a seven-transmembrane cadherin Flamingo (Fmi) may interact antagonistically with Gogo at the M1 temporary layer and that Gogo and Fmi cooperate to mediate targeting of R8 photoreceptor axons to the M3 layer (Hakeda-Suzuki et al., 2011). Thus Gogo alone promotes adherence between R8 photoreceptor axons and the M1 layer, and then at midpupal stages, Fmi antagonizes M1 adhesion and collaborates with Gogo to mediate R8 targeting to the M3 layer. Gogo and Fmi interact in *cis in vivo* and the Gogo cytoplasmic domain is crucial for the M3 layer targeting since the M3 layer targeting information is transmitted to downstream components through the cytoplasmic domain of Gogo (Hakeda-Suzuki et al., 2011).

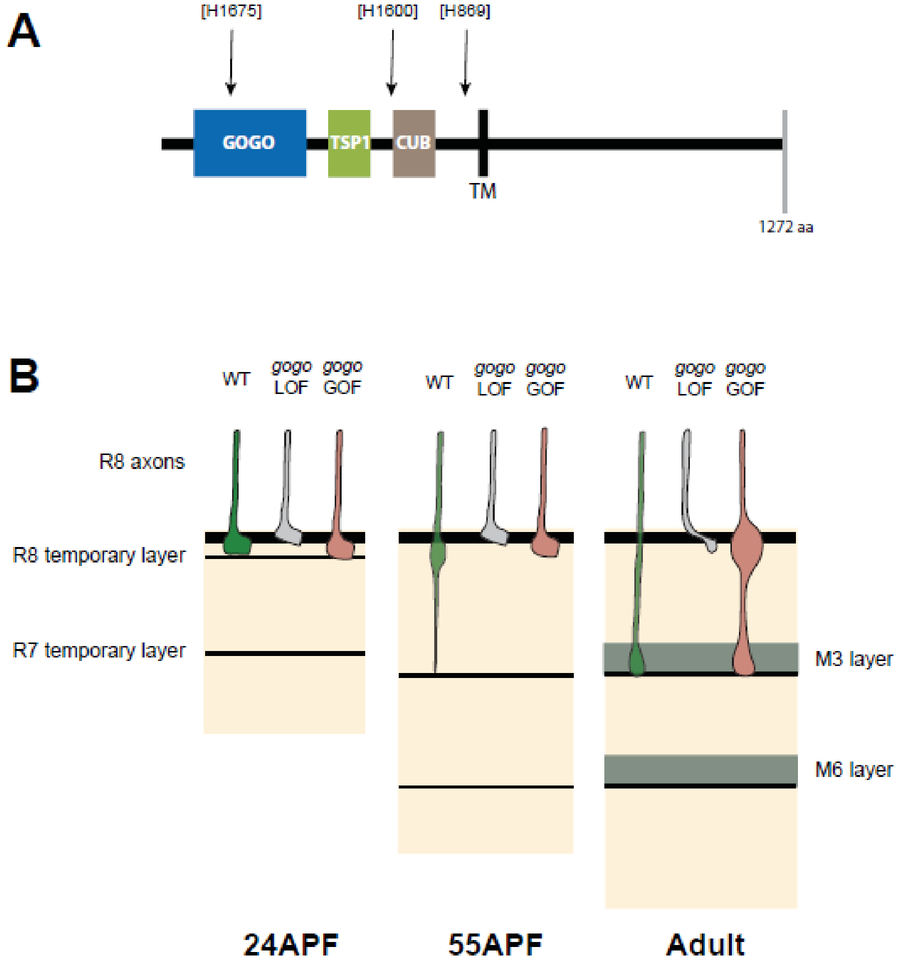
A
[H1675]
[H1600]
[H869]
GOGO
TSP1
CUB
TM
1272 aa
B
WT
gogo LOF
gogo GOF
WT
gogo LOF
gogo GOF
WT
gogo LOF
gogo GOF
R8 axons
R8 temporary layer
R7 temporary layer
M3 layer
M6 layer
24APF
55APF
Adult

Figure 1-6: Gogo: protein structure and function

(A) Gogo protein structure. The extracellular part contains the GOGO, Tsp1 and CUB domains, followed by a transmembrane domain (TM). No domains are identified on the intracellular side. The available mutant alleles with their locations are indicated with arrows; aa, amino acid.

(B) Gogo functions in both temporal and final layer recognition in R8 photoreceptors. In *gogo* LOF the first targeting step (24 APF) is affected: R8 axons stall at the medulla surface. In the mid pupae the second targeting stage starts and wild type axons form filopodia projecting towards the R7 temporary layer which will become the future R8 final target layer (M3). However, loss of Gogo results in axon stalling at the temporary layer since the mutant axons cannot recognize the positive cue which is present there. On the contrary, axons which overexpress Gogo form a blob-like structure at the M1 indicating a strong adhesive interaction.

1.7 Objectives of the thesis project

Although the functional requirement of *gogo* was characterized, it is still not known how Gogo protein activity on a molecular level is regulated. Moreover, the fact that the intracellular fragment does not contain any defined domains but is necessary for protein function (Tomasi et al., 2008) leads to the speculation that it could be involved in transmission of information to the downstream components (Hakeda-Suzuki et al., 2011) or, alternatively, is a target for signaling which could modulate Gogo activity.

Therefore, the goal of this project was to identify the functional domains in the cytoplasmic domain of Gogo and to characterize in details their requirement and function. To investigate this problem, I used a set of molecular genetics, histochemistry and cell culture based assays. In my thesis, I show that the middle part of Gogo cytoplasmic domain includes the minimal intracellular fragment necessary and sufficient for Gogo function. It contains a conserved YYD tripeptide which is a phosphorylation site. Gogo phosphorylation status is critical for the proper targeting of R8 axons to the temporal and final target layers.

Two people significantly contributed to the experimental part of this work: Si-Hong Luu performed the preliminary experiment on the requirement of the cytoplasmic middle part and the YYD motif for Gogo (his data are not shown here) and Mengzhe Wang who helped me with generation of many transgenic flies (indicated in **Materials and Methods** as M. W.), overexpression of *UAS-gogo* lines (Figure 2-7) and conducted the Gogo-Fmi co-overexpression experiment (Figure 2-11).

2. Results

2.1 Gogo requires the cytoplasmic middle part for its function

The GOGO domain and the Tsp1 domain, but not the CUB-like domain, are necessary and sufficient for Gogo activity on the extracellular site (Tomasi et al., 2008). Furthermore, it was shown that the intracellular region of Gogo is crucial for its function since Gogo protein which lacks the entire cytoplasmic domain (GogoΔC) does not rescue the *gogo*$^-$ mutant phenotype (Tomasi et al., 2008). However, the role of the cytoplasmic part of Gogo and its involvement in intracellular signaling is unknown. The necessity of the Gogo cytoplasmic domain for the protein activity motivated us to identify the functional elements in it. To obtain initial clues about the functional units, the cytoplasmic domain was divided into three sections of similar size: C1, C2 and C3 (covering amino acids: 726 – 953, 954 – 1105 and 1106 – 1272 respectively) (**Figure 2-1A**). Next, Gogo expression constructs covering the entire Gogo extracellular domain, transmembrane domain (with the following 20 amino acids to ensure the proper transmembrane localization of the modified proteins) and different deletions of Gogo cytoplasmic parts C1, C2 and C3 (GogoC1, GogoC2, GogoC3 respectively) were cloned (Ohler et al., 2011). In the following step mosaic animals which have an eye mutant for *gogo* in an otherwise wild type background (*gogo*$^-$ *ey*FLP mutant) were generated and the transgenes were expressed in *gogo*$^-$ *ey*FLP mutant background, under control of the photoreceptor specific *GMR* (*glass multiple reporter*) promoter to test their rescuing ability of the mutant phenotype. Since it could be possible that the functional elements are located in more than just one of these fragments or between them, additionally the following deletion constructs were generated: GogoC1C2, GogoC2C3 and GogoC1C3. They were tested in a rescue experiment similar to the one described above (**Figure 2-1C-J**).

In a wild type brain R7 and R8 photoreceptors target M6 and M3 layers respectively, resulting in formation of a regular array of columns and layers in the medulla (**Figure 2-1B**). The *ey*FLP *gogo*$^-$ mutant animals display a very severe phenotype with incomplete medulla rotation, combined with the formation of abnormal bundles through an ectopic chiasm (**Figure 2-1C**) (Tomasi et al., 2008). This mutant phenotype can be completely rescued when a transgene encoding the full length Gogo sequence is expressed (**Figure 2-1D**).

Expression of the GogoC2 construct completely rescues the *ey*FLP *gogo*- mutant phenotype. On the contrary, both GogoC1 and GogoC3 were nonfunctional since the *gogo*$^-$ phenotype was not rescued to any extent. In line with this GogoC1C2 and GogoC2C3, but not GogoC1C3 were able to rescue the *gogo*$^-$ phenotype, since both of them contain the rescuing C2 fragment (**Figure 2-1E-J**).

These results strongly suggest that the middle part of Gogo cytoplasmic domain (C2) includes the minimal intracellular fragment necessary and sufficient for Gogo cytoplasmic function.

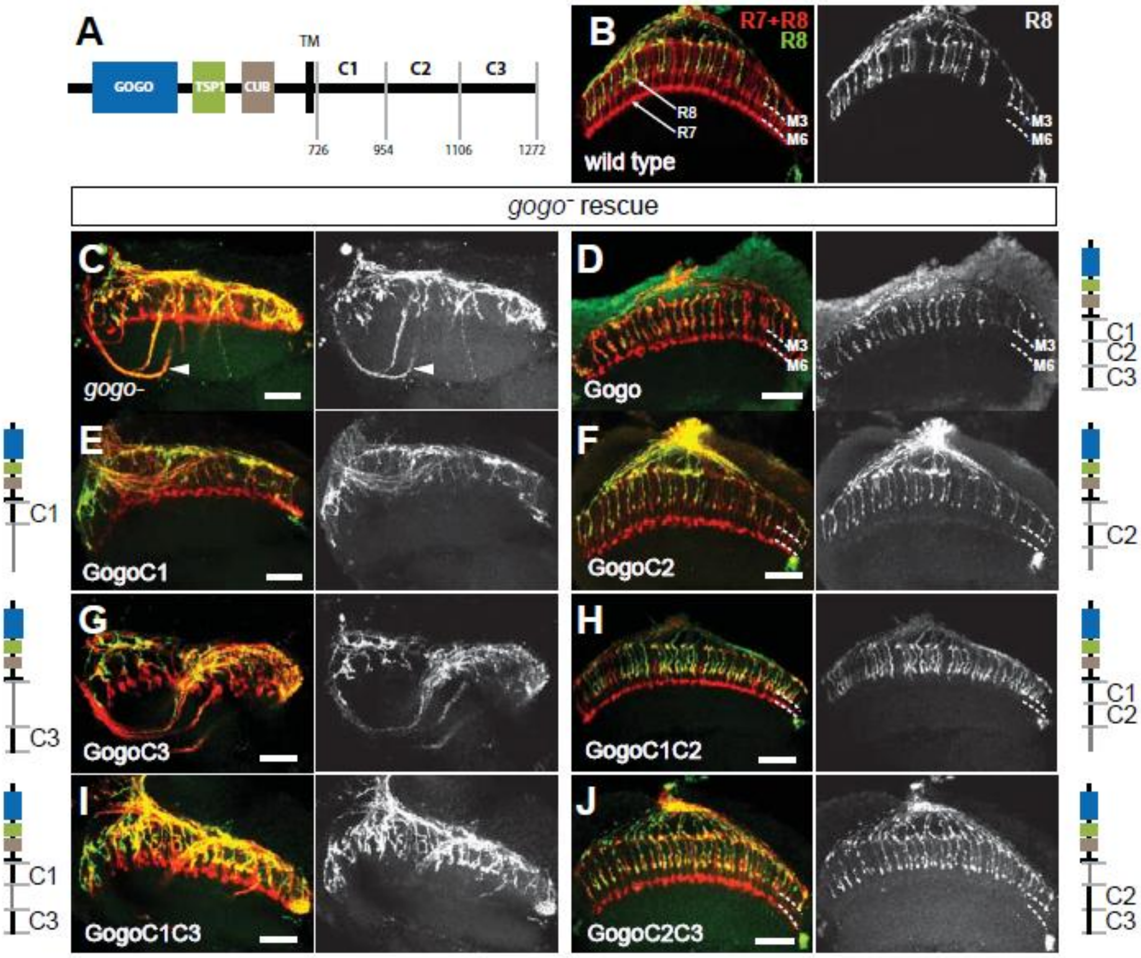
A
TM
GOGO
TSP1
CUB
C1
C2
C3
726
954
1106
1272
B
R7+R8
R8
R8
R7
M3
M6
wild type
R8
M3
M6
gogo⁻ rescue
C
gogo-
D
M3
M6
Gogo
C1
C2
C3
E
C1
GogoC1
F
GogoC2
C2
G
C3
GogoC3
H
GogoC1C2
C1
C2
I
C1
C3
GogoC1C3
J
GogoC2C3
C2
C3

Figure 2-1: Gogo requires the cytoplasmic middle part for its function

(A) Gogo intracellular domain was divided into three sections which were defined arbitrary: C1, C2 and C3. The numbers indicate the amino acid location.

(B) Wild type medulla. All R8 axons (*Rh6-GFP*, green) terminate in the M3 layer, whereas R7 axons target the M6 layer. R7/R8 photoreceptors were stained with mAb24B10.

(C-J) The *gogo* transgenes covering Gogo truncations indicated in each panel were expressed using the eye specific *GMR* promoter in eye-specific *gogo*$^-$ mutant flies. Eyes mutant for *gogo* (C) show a severe phenotype with medulla rotation defects (arrowhead) and misguided axons. The *gogo*$^-$ mutant phenotype is rescued by full length Gogo and all transgenes containing the C2 section, GogoC2, GogoC1C2, GogoC2C3 but not by GogoC1, GogoC3 and GogoC1C3. Gogo schematics next to the panels depict the protein truncations used. The labeling is the same as in (B). Dashed lined mark the location of M3, M6 layers. Scale bars represent 20 µm.

2.2 The YYD motif has a crucial function

To investigate in a more details the function of the cytoplasmic section C2, a bioinformatical study was performed (Tomasi et al., 2008). A series of PSI-BLAST searches within the NCBI non-redundant databases revealed that, although there is no overall conservation within the cytoplasmic domains, the C2 fragment contains a motif specific for *gogo* orthologues: a short sequence containing a highly conserved tripeptide motif, Tyr^{1019}-Tyr^{1020}-Asp^{1021} (YYD), was identified (referred later as the YYD motif, **Figure 2-2A**). The conservation of the YYD motif indicates that it may serve as a putative regulatory site and/or protein interaction domain.

To elucidate whether the YYD motif has a function in axonal pathfinding, a transgenic fly line expressing the full-length *gogo* but lacking the YYD motif (*gogoΔYYD*) under control of the *GMR* promoter was generated. The *gogoΔYYD* construct was inserted into the attP40 locus in the fly genome using the PhiC31 integrase – mediated transgenesis system to ensure the same expression level as of other constructs used later in this study (**Materials and Methods 4.2.9** and **Figure 5-1A, B**). Interestingly, in contrast to the wild type Gogo, GogoΔYYD could not rescue the mutant phenotype (**Figure 2-2B-D**). This indicates that indeed the YYD motif is necessary for Gogo cytoplasmic activity.

2.3 The YYD motif is a potential phosphorylation site

Having confirmed the necessity of the YYD tripeptide for Gogo function, I sought to determine the role of these residues. Since changes in tyrosine phosphorylation of proteins are a commonly used mechanism of modulating protein activity (Maher and Pasquale, 1988; Alonso et al., 2004; Liu et al., 2004; Tarrant and Cole, 2009), it raises the possibility that this could be also the case for Gogo. Typical analysis of the effects of protein phosphorylation at a particular site involves site-directed mutagenesis of the residue of interest (Tarrant and Cole, 2009). In particular, replacement of tyrosine with phenylalanine (F) in recombinant proteins was shown to be useful to mimic the unphosphorylated status (Xia et al., 2008; Tarrant and Cole, 2009).

Similarly, acidic substitutions (ex. aspartic acid, D) were shown to be useful as phosphomimetics (Zang et al., 2008; Tarrant and Cole, 2009). I took advantage of this approach to determine the functional role of the tyrosine residues located in the YYD motif.

I examined *in vivo* the ability of *gogo* phosphomimetic constructs to rescue the mutant phenotype. In order to exclude the possibility that the observed phenotypes are manifested due to different functional properties of the expressed proteins and that they are not influenced by differences in expression levels between fly lines, all transgenes were inserted in the same locus using the PhiC31 integrase-mediated transgenesis system and a similar expression level was confirmed by anti-Gogo staining (**Figure 5-1A-D**). The following *gogo* transgenes (under the control of the eye specific *GMR* promoter) were tested: *gogo* (wild type sequence), *gogoFFD* (non-phospho-Gogo) and *gogoDDD* (phospho-Gogo). Since I did not succeed in inserting the *gogoFFD* transgene into the landing site-locus I used a random insertion whose expression level was similar to the rest of the transgenes (**Figure 5-1C**). As I mentioned before expression of wild type Gogo completely rescues the mutant phenotype (**Figure 2-2C**). Interestingly, only the non-phosphorylatable GogoFFD, but not GogoDDD, is able to reconstitute the wild type function of *gogo* when expressed in *gogo*$^{-}$ *ey*FLP mutant eye (**Figure 2-2B, E, F**). Differences in the rescuing ability indicate that the Gogo phosphorylation status might be crucial for regulating Gogo activity.

Since the second tyrosine in the YYD motif is conserved not only in invertebrates but also in vertebrates (**Figure 2-2A**), in contrast to the first one, I was interested whether both of them are equally important for Gogo function, or rather only one of them (presumably the more conserved one) is functional. To test this, I mutated each of the tyrosines separately and performed a rescue experiment similar to the one described above. Flies expressing the following *gogo* transgenes were tested: *gogoFYD*, *gogoYFD*, *gogoDYD*, *gogoYDD*. None of the single phospho-mutants (DYD, YDD) can rescue the mutant phenotype whereas both of the single non-phospho-mimetic mutants (FYD, YFD) can (**Figure 2-2B, G-J**). Thus, I conclude that both tyrosines in the YYD motif are crucial for Gogo function.

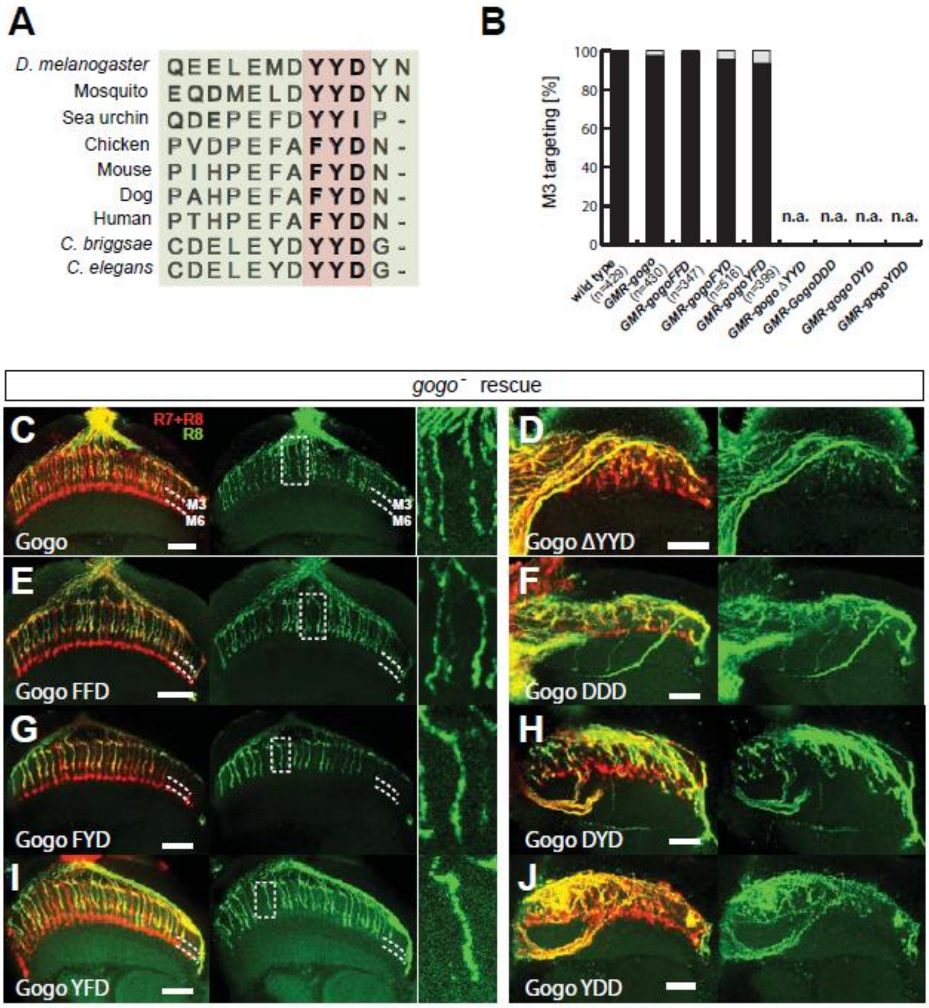
A
D. melanogaster QEELEMDYYDYN
Mosquito EQDMELDYYDYN
Sea urchin QDEPEFDYYIP-
Chicken PVDPEFAFYDN-
Mouse PIHPEFAFYDN-
Dog PAHPEFAFYDN-
Human PTHPEFAFYDN-
C. briggsae CDELEYDYYDG-
C. elegans CDELEYDYYDG-
B
M3 targeting [%]
100
80
60
40
20
0
n.a.
n.a.
n.a.
n.a.
wild type (n=429)
GMR-gogo (n=430)
GMR-gogoFFD (n=347)
GMR-gogoFYD (n=516)
GMR-gogoYFD (n=399)
GMR-gogo ΔYYD
GMR-GogoDDD
GMR-gogo DYD
GMR-gogoYDD
gogo⁻ rescue
C
R7+R8
R8
M3
M6
Gogo
D
Gogo ΔYYD
E
Gogo FFD
F
Gogo DDD
G
Gogo FYD
H
Gogo DYD
I
Gogo YFD
J
Gogo YDD

Figure 2-2: The YYD motif has a crucial function

(A) The cytoplasmic middle part (C2) contains a tripeptide YYD motif which is highly conserved among invertebrate and vertebrate species (red shadow).

(B-J) The requirement of the YYD motif was confirmed in a series of rescue experiments. All transgenes were expressed under the control of the eye specific *GMR* promoter and were inserted in the same locus to ensure the same expression level; the *gogoFFD* transgene is a random insertion whose expression level is similar to the rest of the constructs. R8 axons express *Rh6-GFP*, all photoreceptors were stained with mAb24B10. Scale bars represent 20 µm.

(B) Quantification of the rescue experiments. The percentage of R8 axons targeting the M3 layer was determined for the rescuing constructs. For the non-rescuing constructs, the R8 targeting could not be assessed because of the severity of the mutant phenotype (n.a).

(C, D) The *gogo*$^-$ phenotype (*ey3.5*FLP mosaics) is completely rescued by *GMR-Gogo* (wild type), but not when the YYD tripeptide is removed (*GMR-GogoΔYYD*).

(E, G, I) Transgenes having Y-F mutations in the YYD motif substitute for the functional protein (GogoFFD, GogoFYD, GogoYFD).

(F, H, J) Phospho- mimics (GogoDDD, GogoDYD, GogoYDD), similarly to GogoΔYYD, do not rescue the mutant phenotype.

2.4 Gogo undergoes phosphorylation

The studies on the function of Gogo phospho mimics strongly suggest that the Tyr^{1019}and Tyr^{1020} (YYD motif) are phosphorylation sites, since the phospho-status of Gogo seems to be highly important for photoreceptor axon guidance. Interestingly, they rather indicate that the dephosphorylation event is important, because the non-phosphorylatable Gogo rescues completely the *gogo* mutant phenotype. It raises an obvious question whether Gogo is tyrosine-phosphorylated *in vivo*? Therefore, I aimed to test in a more direct way whether Gogo is phosphorylated at Tyr^{1019} and Tyr^{1020}.

In the first step, the tyrosine-specific phosphorylation of Gogo was probed *in vivo*. For this purpose, the myc-tagged Gogo was expressed specifically in the visual system (*GMR-gogo-myc*) and co-immunoprecipitated from *Drosophila* third instar larval brains. Indeed, a phosphorylation of the myc-tagged full length Gogo is clearly visible (probed with the anti-phosphotyrosine specific antibody, 4G10, **Figure 2-3A**). Similarly, I could observe a clear tyrosine phosphorylation during the pupal development when I probed for the phosphorylation in the young pupae at 24 APF (**Figure 2-3B**).

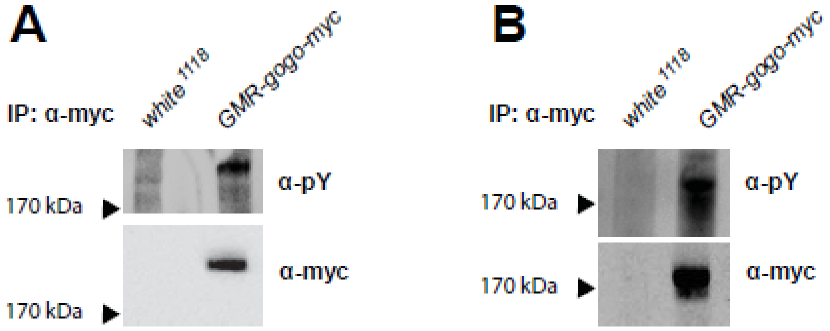

Figure 2-3: Gogo is tyrosine-phosphorylated *in vivo*

Gogo expressed in the photoreceptors (*GMR-Gogo-myc*) shows a tyrosine specific phosphorylation detected with the 4G10 antibody. Gogo-myc was immunoprecipitated (IP) from 25-30 larval (A) and pupal (B) brains. Brain lysate from *white*^{1118} flies was used as a negative control.

In the next step I utilized the *Drosophila* S2 cell line to dissect the phosphorylation of Gogo intracellular domain in more detail (**Figure 2-4**). I observed that Gogo is tyrosine phosphorylated when expressed in S2 cells (**Figure 2-4B**). However, the YYD motif is not the only phosphorylation site (data not shown). The C2 fragment contains nine tyrosines (**Figure 2-4A**) but the full length Gogo with all of them mutated to phenylalanine (Gogo^{9F}) does not show any tyrosine phosphorylation (**Figure 2-4B**). Therefore the additional potential tyrosine phosphorylation site(s) should be included among them.

I decided to restrict my analysis to a short fragment of the C2 part (GogoC2^{short}) which covers only five tyrosines, including the YYD motif (amino acids 982 – 1052), and constitutes the most conserved part of GogoC2 section (**Figure 2-4C**). Using this Gogo truncation I tested whether specifically the YYD motif is a phosphorylation site. If both tyrosines in the YYD motif are mutated to phenylalanine and the rest of the tyrosines are intact (GogoC2$^{short\ FFD}$) the phosphorylation signal is abolished, indicating that only the YYD motif is tyrosine-phosphorylated in the C2 short fragment (**Figure 2-4D**). However, when each of the tyrosine residues in the YYD motif is mutated separately (GogoC2$^{short\ FYD}$, GogoC2$^{short\ YFD}$), the phosphorylation of the non-mutated amino acid occurs (**Figure 2-4D**). Thus both Tyr$^{1019,\ 1020}$ are phosphorylation sites.

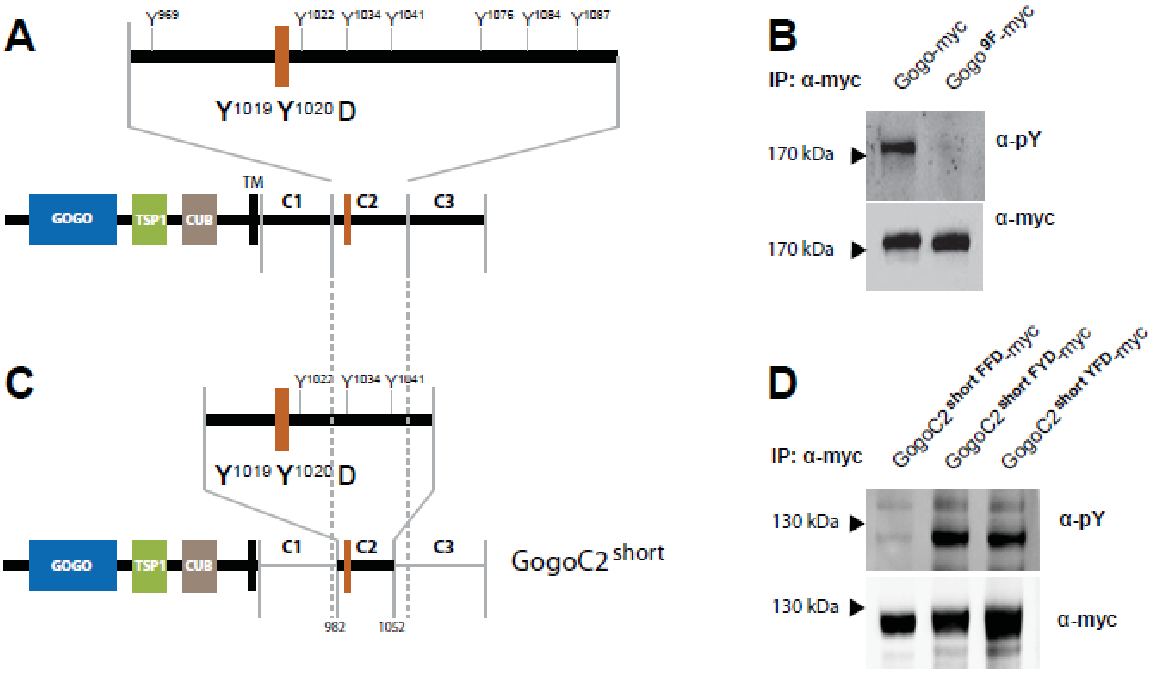
A
Y969
Y1022
Y1034
Y1041
Y1076
Y1084
Y1087
Y1019 Y1020 D
TM
GOGO
TSP1
CUB
C1
C2
C3
B
IP: α-myc
Gogo-myc
Gogo 9F-myc
170 kDa
α-pY
170 kDa
α-myc
C
Y1022
Y1034
Y1041
Y1019 Y1020 D
GOGO
TSP1
CUB
C1
C2
C3
GogoC2 short
982
1052
D
IP: α-myc
GogoC2 short FFD-myc
GogoC2 short FYD-myc
GogoC2 short YFD-myc
130 kDa
α-pY
130 kDa
α-myc

Figure 2-4: The YYD motif is phosphorylated *in vivo*

(A) Gogo C2 section contains nine tyrosines including the YYD motif (Y^{1019}Y^{1020}D).

(B) To test whether all Gogo phosphorylation sites are included in the C2 section all nine tyrosines were mutated to F (Gogo^{9F}). Next, *UAS-Gogo-myc* (wild type sequence) or *UAS-Gogo^{9F}-myc* were tested for tyrosine phosphorylation in S2 cells. Y-F mutations prevent from phosphorylation indicating that Gogo has tyrosine phosphorylation sites in the C2 fragment.

(C) GogoC2^{short} truncation contains only five tyrosines.

(D) Both tyrosines in the YYD motif are phosphorylation sites since Y-F mutations in both of them completely suppresses the phosphorylation of the GogoC2^{short} truncation (Gogo$^{short\ FFD}$), whereas single-tyrosine mutants (Gogo$^{short\ FYD}$, Gogo$^{short\ YFD}$) show a clear pY signal coming from the non-mutated residue.

(B, D) S2 cells were co-transfected with *Act-Gal4* driver and indicated *UAS-Gogo* construct. Subsequently, Gogo-myc was immunoprecipitated (IP), pY signal was detected with the 4G10 antibody.

2.5 The additional phosphorylation sites

Using the GogoC2^{short} deletion I could show that the YYD is indeed a phosphorylation site. However a question remains open where the additional potential phospho- sites are located and finally whether they play a significant role in axon targeting?

For sure they are among the nine tyrosines in the C2 fragment since the Gogo^{9F} mutant is not phosphorylated. Obviously it could be either the “first” N-terminally to the “short” fragment located tyrosine (Y^{969}). Alternatively, phospho- site(s) could be also located within the “last” three C-terminally located tyrosines in the C2 fragment (Y$^{1076, 1084, 1087}$, **Figure 2-4A, C**). To distinguish between these two possibilities I cloned appropriate Gogo constructs to test this: Gogo$^{\text{short FFD – C}}$ (including Tyr$^{1076, 1084, 1087}$) and Gogo$^{\text{short FFD – N}}$ (including Tyr^{969}, **Figure 2-5A**). Both of this constructs have the YYD motif mutated to FFD to make sure that only the additional phosphorylation sites are detected. Each of these constructs and the positive/negative controls (Gogo-myc, Gogo^{9F}-myc respectively) were expressed in S2 cells and tested for phosphorylation. Among the three tested deletions only Gogo$^{\text{short FFD – C}}$ is phosphorylated indicating that the additional phosphorylation site(s) are among Tyr$^{1076, 1084, 1087}$ (**Figure 2-5B**).

What is the impact of the potential additional phosphorylation site(s) on Gogo function? They were only poorly conserved during evolution, thus are they substantial for Gogo function? To verify this I decided to test whether *gogo*$^{-}$ mutant phenotype is rescued by the GogoC2$^{\text{short FFD}}$ fragment which covers only the most conserved part of Gogo cytoplasmic domain.

When I expressed *GMR-GogoC2*$^{\textit{short FFD}}$ in the mutant background, the transgene rescues most of the features typical for *gogo*$^{-}$: the medulla rotation is completely rescued, and the R8 targeting phenotype is partially rescued (70% of R8 axons targets properly, n=372), some axons show a bundling phenotype (**Figure 2-6**). Thus, I conclude that the additional potential phosphosite(s) might not play a substantial role for Gogo function since they are not entirely required for the mutant phenotype rescue.

In summary, the Tyr$^{1019, 1020}$ (YYD motif) both are phosphorylation sites and the potential additional tyrosine phosphorylation site(s) are not substantial for Gogo function since *gogo* transgene which lacks these tyrosines is still functional. I concluded that the YYD tripeptide is therefore the “key phosphorylation site”.

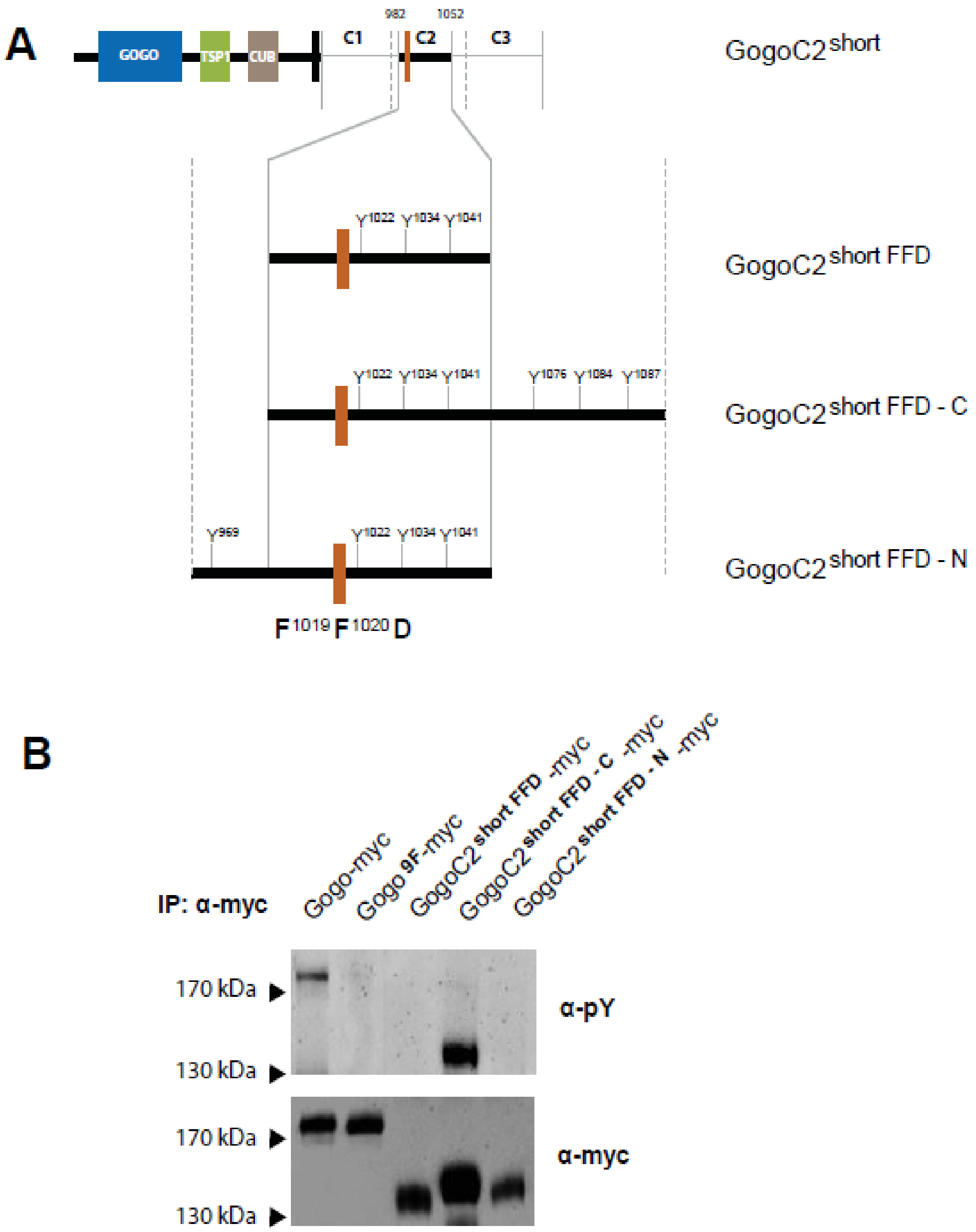
A
GOGO
TSP1
CUB
C1
C2
C3
982
1052
GogoC2 short
Y1022 Y1034 Y1041
GogoC2 short FFD
Y1022 Y1034 Y1041 Y1076 Y1084 Y1087
GogoC2 short FFD - C
Y969 Y1022 Y1034 Y1041
GogoC2 short FFD - N
F1019 F1020 D
B
IP: α-myc
Gogo-myc
Gogo 9F-myc
GogoC2 short FFD -myc
GogoC2 short FFD - C -myc
GogoC2 short FFD - N -myc
170 kDa
130 kDa
α-pY
170 kDa
130 kDa
α-myc

Figure 2-5: Location of the additional phosphorylation sites

(A) Tyrosine-phosphorylation sites (additional to the YYD motif) are located within the three C-terminally locates tyrosines in the C2 section. To narrow down the location of phospho sites Gogo deletions depicted here schematically were cloned and tested for phosphorylation in S2 cells (GogoC2 $^{\text{short FFD}}$, GogoC2 $^{\text{short FFD-C}}$, GogoC2 $^{\text{short FFD-N}}$). All of them have FFD mutations in the YYD motif to make sure that only the additional phosphorylation sites are detected.

(B) Gogo-myc (positive control) but not Gogo^{9F} (negative control) are phosphorylated when expressed in S2 cells. Only the GogoC2 $^{\text{short FFD-C}}$ deletion which contains the three C-terminally located tyrosines in the C2 section undergoes phosphorylation. The Tyr$^{1076,\ 1084,\ 1087}$ are additional potential phosphorylation sites. Gogo-myc was immunoprecipitated (IP), pY signal was detected with the 4G10 antibody.

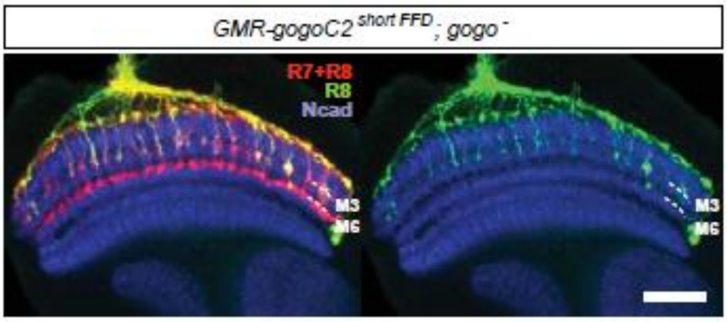

Figure 2-6: The YYD motif is the "key phosphorylation site"
Non-phospho mimetic version GogoC2^{shortFFD} is sufficient to partially rescue the *gogo*$^-$ phenotype. M3 and M6 layers are indicated with dashed lines. R8 axons were visualized with *Rh6-GFP*, all photoreceptors were stained with mAb24B10 and the neuropiles with anti-*D*Ncadherin staining. Scale bar represents 20 µm.

2.6 The phospho-Gogo specific antibody

The fact that the YYD site is phosphorylated in S2 cells, combined with the *gogo*$^-$ rescue experiments presented in previous sections strongly suggest that the YYD motif undergoes phosphorylation not only in cell culture but also in animals. Is it possible to show that the YYD motif is phosphorylated in a more direct way? In order to solve this problem I aimed to raise a polyclonal antibody which would detect specifically the YYD motif in the phosphorylated status. This tool could allow to show directly that the phosphotyrosine signal detected previously in Gogo isolated from the fly (**Figure 2-3**) is at least partially coming from the YYD motif and not only from the additional phosphorylation sites. Several phospho-Gogo peptides were generated and injected into rabbits to obtain YYD specific phospho-Gogo polyclonal antibodies. Only one of the obtained antibodies (Ab2795-D01) gave positive results.

For the Ab2795-D01 generation, three Gogo peptides comprising twelve amino acids, including the YYD motif, were synthetized (**Figure 2-7A; Materials and Methods 4.1.6**). Each of them had a different phosphorylation status: pYYD, YpYD, pYpYD. The antibody Ab2795-D01 was raised against a mixture of these three peptides. After the animals were immunized, the serum was affinity-purified against the non-phosphorylated peptide, YYD. The specificity of this antibody was tested first *in vitro* by verifying the binding to Gogo peptides showing different phosphorylation status (YYD, pYYD, YpYD and pYpYD) using an ELISA assay (**Figure 2-7B**, performed by Peptide Institute Inc., Japan). The Ab2795-D01 binds to all Gogo peptides which have at least one tyrosine phosphorylated (the strongest binding occurs to pYYD) but does not bind to non-phosphorylated YYD site.

In the next steps, I tested whether the generated antibody is useful for western blot analysis. Does the antibody recognize specifically the phosphorylated YYD motif? In a preliminary experiment, S2 cells were transfected with *UAS-gogo* and the sodium orthovanadate treatment (**Materials and Methods 4.2.3**) was used to increase Gogo phosphorylation (**Figure 2-7C, D**). Indeed, the Ab2795-D01 detects the increase in Gogo phosphorylation. In order to test whether the antibody binds specifically to the YYD motif sequence, I performed a similar experiment using GogoFFD as a negative control. Since the FFD mutation abolishes phosphorylation, the antibody should not detect it at all. The Ab2795-D01 shows a clear and reproducible difference in reactivity between phospho- and non-phospho-Gogo (**Figure 2-7E, F**). However the negative control is not completely clean since some unspecific signal is visible.

Nevertheless, a clear qualitative difference in the recognition of Gogo vs. GogoFFD allows the conclusion that the Ab2795-D01 detects mostly the phosphotyrosine signal coming from the YYD motif.

The Ab2795-D01 turned out to be not applicable for immunhistological staining and detection of Gogo from cell lysates on western blots (without immunoprecipitation). The obtained signals in these cases are indistinguishable from the background (data not shown).

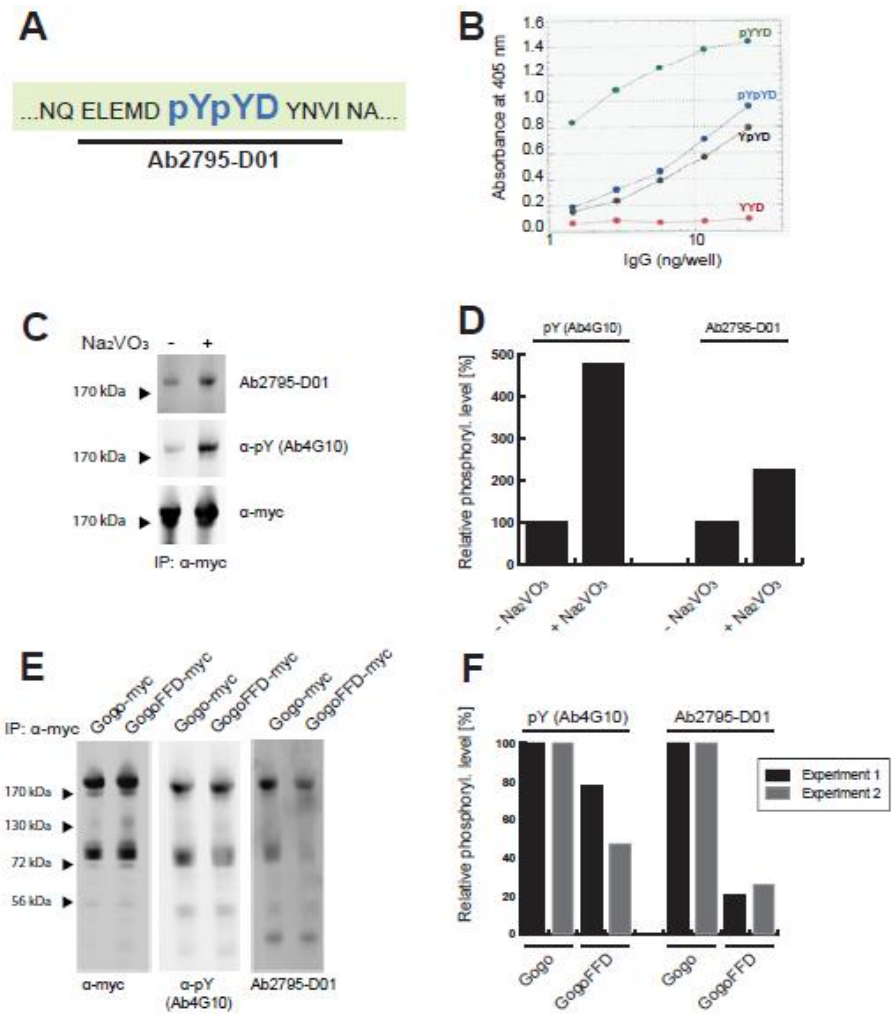

Figure 2-7: The phospho-Gogo specific antibody

(A) The anti-phospho-Gogo specific polyclonal antibody (Ab2795-D01) was raised against phosphorylated peptides composed of the underlined amino acids (Peptide Institute Inc., Japan).

(B) The specificity was first tested *in vitro* using the ELISA assay. The binding to synthetized Gogo peptides having one, two or no phospho-tyrosine (pYYD, YpYD, pYpYD, YYD) was measured (performed by Peptide Institute Inc., Japan).

(C, D) The Ab2795-D01 detects increase in Gogo phosphorylation after sodium orthovanadate treatment. The band intensity was quantified with ImageJ; the Gogo phosphorylation (without Na_2VO_3) was used as 100%.

(E, F) The Ab2795-D01 recognizes phosphorylated Gogo as compared to GogoFFD indicating that the antibody recognizes the YYD motif phosphorylation at least to some degree. A slight difference in phosphorylation is visible with the 4G10 antibody and it increases when the Ab2795-D01 is used. The quantification from two different experiments is shown. The band intensity was quantified with ImageJ; the Gogo (wild type) phosphorylation was used as 100%. Gogo-myc / GogoFFD-myc migrate in this case also as a smaller band (about 80 kDa), which is probably a degradation product. Sodium orthovanadate treatment was used for all samples.

2.7 The YYD motif is phosphorylated during the pupal development

Since the phospho-Gogo specific antibody (Ab2795-D01) recognizes the phosphorylated YYD motif (visible upon comparison with GogoFFD), I decided to use the same approach to test for phosphorylation in the early pupal stages. For this purpose, Gogo-myc was immunoprecipitated from 24 APF brains. The detected Gogo phosphorylation signal was quantified and compared with GogoFFD-myc. The *white*^{1118} flies were used as negative control (**Figure 2-8**). The Ab2795-D01 detects wild type Gogo much better than GogoFFD (**Figure 2-8A**). The quantification showed that there is a dramatic difference in the phosphorylation between Gogo and GogoFFD when detected with the general phosphotyrosine specific 4G10 antibody (decrease by about 60%) and even more profound difference when detected with the Ab2795-D01 (decrease by about 90%, **Figure 2-8B**).

In summary, presented evidence strongly suggest that also in the animal the YYD motif is a phosphorylation site.

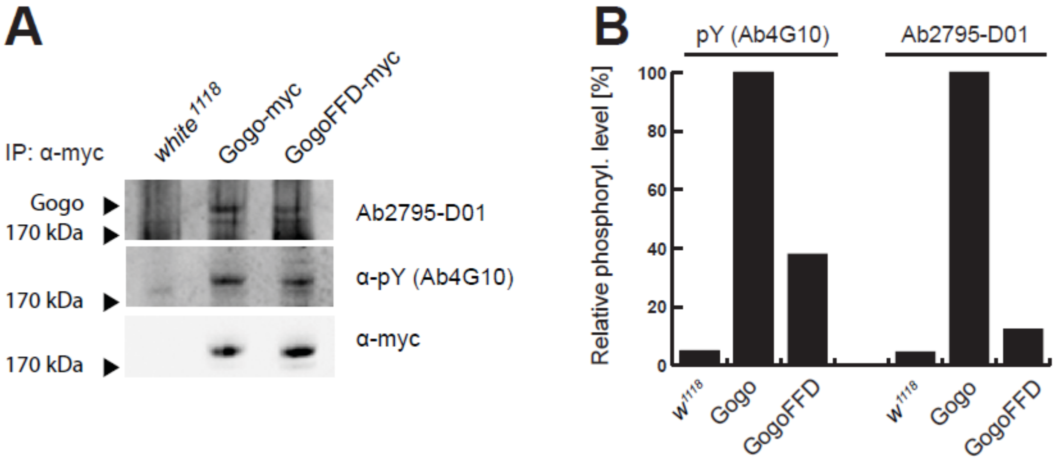

Figure 2-8: The YYD motif is phosphorylated during early pupal development

(A) Gogo-myc and GogoFFD-myc were expressed specifically in photoreceptors (*GMR* promoter) and immunoprecipitated from 25 pupa; brains at stage 24 APF; *white*^{1118} fly was used as a negative control. The Ab2795-D01 recognizes Gogo-myc. Mutation in the YYD motif (GogoFFD) lowers the affinity of the Ab2795-D01 to Gogo strongly suggesting that the YYD site is phosphorylated.

(B) Quantification of the western blot. A difference in phosphorylation detected with the 4G10 antibody is visible and a more profound decrease when the Ab2795-D01 is used. The band intensity was quantified with ImageJ; Gogo (wild type) phosphorylation was used as 100%.

2.8 YYD motif and M1 layer targeting

When Gogo is overexpressed in a wild type background, R8 photoreceptors show the formation of blob-like structures at the medulla M1 layer (**Figure 2-9A**). Based on this observation and other experiments, Gogo was proposed to have an adhesive function at the M1 layer during the early pupal stages, when the R8 axons make a temporal stop at the surface of the medulla (**Figure 1-6B**, Tomasi et al., 2008; Hakeda-Suzuki et al., 2011). It leads to a speculation that the blob formation could be related to Gogo phosphorylation. Does the YYD tripeptide phosphorylation have a role in M1 layer recognition during the first targeting step? First, I asked whether the YYD motif could be required for the M1 layer targeting. To answer this question I tested whether mutations in the YYD motif interfere with the M1 layer targeting. Because of the specific phenotype of the wild type Gogo overexpression, a gain of function experiment was a suitable approach to test this.

To ensure that the observed phenotypes are not caused by differences in expression levels between different insertions, all of the constructs used here (*UAS* promoter) were inserted into the same locus using the PhiC31 integrase-mediated transgenesis system (**Materials and Methods 4.2.9**) and similar expression level of all constructs was confirmed with anti-Gogo staining (**Figure 5-1E-H**). Surprisingly, the overexpression of GogoΔYYD (*GMR-Gal4, UAS-GogoΔYYD*) in a wild type background leads to stopping of R8 axons at the M1 layer. In contrast, the stopping never occurs when wild type Gogo is overexpressed (**Figure 2-9A, B, I**). The R7 targeting seems to be normal as deduced from the mAb24B10 staining. The stopping of R8 axons at the M1 layer strongly suggests that the ΔYYD mutation affects the interaction of R8 axons with the temporal targeting layer M1 during the mid pupal stage. It indicates that the YYD motif is required for allowing R8 photoreceptor axons to leave the M1 layer and to proceed to final targeting (M3 layer). If this function of Gogo is blocked (GogoΔYYD), R8 axons stop at the M1 layer and they fail to innervate the deeper medulla layers.

Since the YYD motif is essential for the proper interaction with the M1 layer and Gogo phospho/non-phospho-mutants show different behavior in rescue conditions, it raises the possibility that function of the YYD motif in M1 targeting could depend on Gogo phosphorylation status. In order to check it, I overexpressed *gogo* phospho-mutants in a wild type background (**Figure 2-9C-I**). For this purpose, *UAS* constructs driven by *GMR-Gal4* were used. Interestingly, as it was the case for the rescue experiments, the phospho- vs. non-phospho-Gogo constructs showed different behaviors. The phospho-Gogo (DDD) showed a similar M1 stopping phenotype as the inactive GogoΔYYD, whereas non-phosphorylatable Gogo (FFD) did not show any obvious mutant phenotype and the photoreceptor targeting was wild type. This result was further confirmed by overexpression of transgenes having only single tyrosines in the YYD motif mutated. Even if only one of the tyrosines was substituted with a phospho-amino acid (DYD, YDD) I observed R8 stopping at the M1 layer. In contrary, it was never the case when non-phosphorylatables were used (FYD, YFD). Combined with my previous result that Gogo is phosphorylated when expressed in photoreceptor cells, it suggests that Gogo is phosphorylated at the early stages of the development. After the M1 targeting is finalized Gogo dephosphorylation could permit the R8 axon to leave the M1 layer and target the M3 layer. Thus I could observe a blob phenotype only when I expressed the wild type Gogo but never when I overexpressed GogoFFD, since the phosphorylation in this case is impossible.

In summary, the YYD tripeptide plays an essential role during the M1 temporal layer targeting. Deletion of the YYD motif or by mimicking phosphorylation is sufficient to stop the targeting of R8 photoreceptors at the temporal targeting stage.

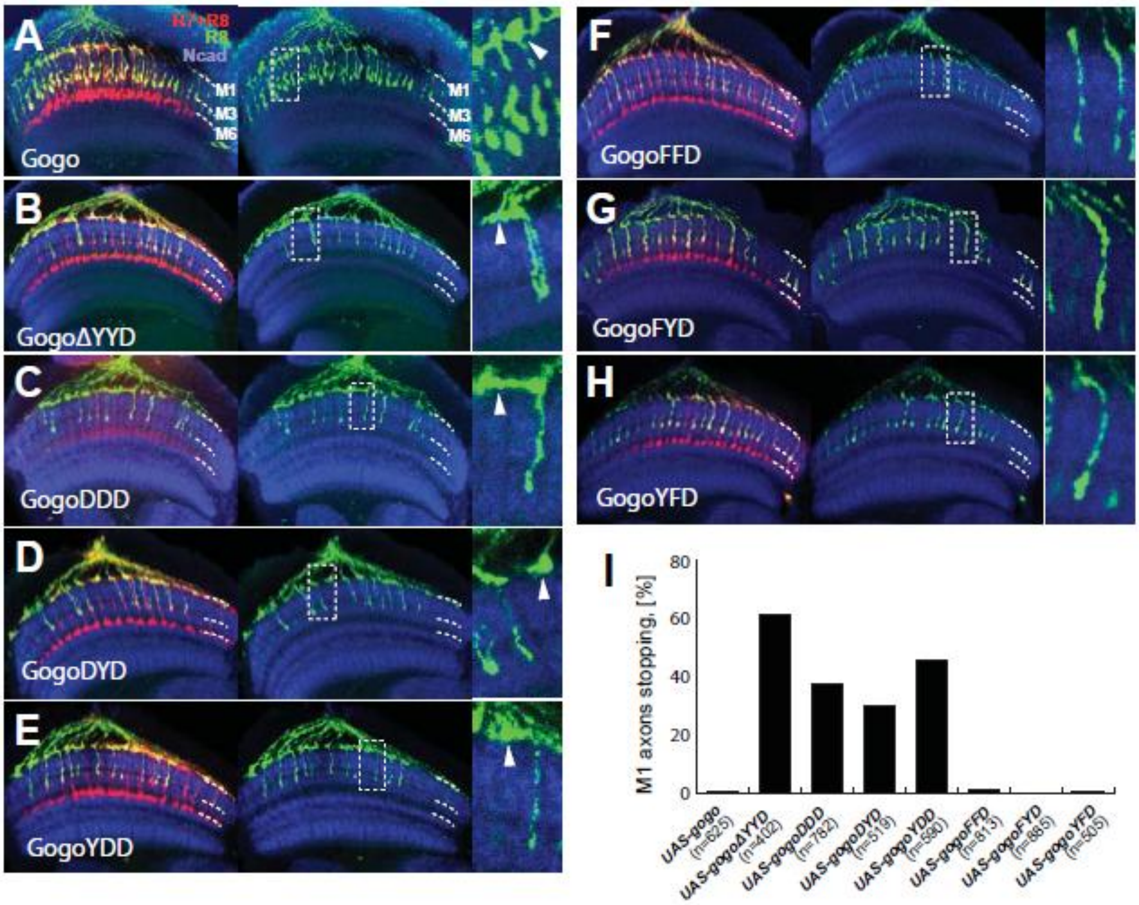
A
R7+R8
R8
Ncad
M1
M3
M6
Gogo
B
GogoΔYYD
C
GogoDDD
D
GogoDYD
E
GogoYDD
F
GogoFFD
G
GogoFYD
H
GogoYFD
I
M1 axons stopping, [%]
80
60
40
20
0
UAS-gogo (n=625)
UAS-gogoΔYYD (n=402)
UAS-gogoDDD (n=782)
UAS-gogoDYD (n=519)
UAS-gogoYDD (n=590)
UAS-gogoFFD (n=813)
UAS-gogoFYD (n=885)
UAS-gogoYFD (n=505)

Figure 2-9: The YYD motif plays a role in the interaction of R8 axons with the M1 layer

(A-H) Phenotypes of R8 photoreceptors overexpressing wild type Gogo (A), Gogo lacking the YYD motif, GogoΔYYD (B), Gogo phospho mimics (C-E) and non-phosphorylatable Gogo forms (F-H). Expression of *UAS-Gogo* constructs was driven by the *GMR-Gal4* driver. R8 axons are visualized with *Rh6-GFP* expression (green), all photoreceptors are stained with mAb24B10 (red) and the neuropiles with anti-*D*Ncadherin staining (Ncad). Single axons in the boxed area are magnified in each panel (right).

(A) Overexpression of wild type Gogo results in the formation of blobs at the medulla surface (arrowhead) which indicate enhanced adhesiveness of R8 axons to the M1 layer.

(B-E) Removing the YYD motif (B) or mimicking phosphorylation (C-E) results in R8 axons stopping at the temporary targeting layer. Arrowheads indicate premature axon stopping.

(F-H) Overexpression of Gogo having Y-F mutation in the YYD motif does not affect the R8 axons targeting.

(I) Quantification of R8 axons stopping at the M1 layer.

2.9 Gogo phosphorylation is not entirely required for M1 layer recognition

Removal of the YYD motif or insertion of the DDD mutation is sufficient to cause axon stopping at the temporary M1 layer indicating the function of these residues for the recognition of the temporal target. However this experiment does not answer the question whether Gogo phosphorylation is necessary for the interaction with the M1 layer. The fact that a dephosphorylated form of Gogo (FFD) is able to rescue the *gogo*$^-$ phenotype and that GogoFFD does not cause any obvious overexpression phenotype when overexpressed in a wild type background indicates, that Gogo phosphorylation might not be entirely required for the recognition of the M1 temporary layer. In order to verify this, I checked whether there are any defects during the pupal stages when *gogo*$^-$ is rescued by GogoFFD. If Gogo dephosphorylation is suppressing the adhesion between the R8 axon and the positive cue at the M1 layer then one could imagine that the R8 axons which express only the dephosphorylated Gogo (FFD) might for instance prematurely extend their processes to the M3 layer, because they lack the adhesive properties.

To verify this I checked in more detail how the targeting of R8 axons occurs during the pupal development. In order to visualize the R8 axons in the pupae the *atonal-tau-myc* marker (**Materials and Methods 4.2.8**) in combination with anti-tau staining was used. As a negative control an eye-specific *gogo*$^-$ mosaic was used. *GMR-gogoFFD* and *GMR-gogo* (positive control) were expressed in the mutant background. The phenotype was tested at 30, 50 and 55 APF to enable observation of the phenotype when the transition from the 1st to the 2nd targeting step occurs (**Figure 1-4C and 2-10**). At 30 APF in *gogo*$^-$ and in a rescue situation (both Gogo and GogoFFD) axons reach the temporary layer (**Figure 2-10A, D, G**). In the mid pupae (50 APF) the *gogo*$^-$ phenotype is clearly visible (rotation defect, an extensive axon bundling and occasional overshooting of R8 axons, **Figure 2-10B**). When Gogo or GogoFFD were expressed in a mutant background R8 photoreceptor adhere to the temporary layer (**Figure 2-10E, H**). At 55 APF axons expressing Gogo or GogoFFD already formed filopodia towards the final targeting layer (**Figure 2-10C, F, I**).

Thus, it indicates that although Gogo dephosphorylation is necessary for leaving the M1 layer, in a physiological situation the phosphorylation is not entirely necessary for the adhesion to the M1 layer.

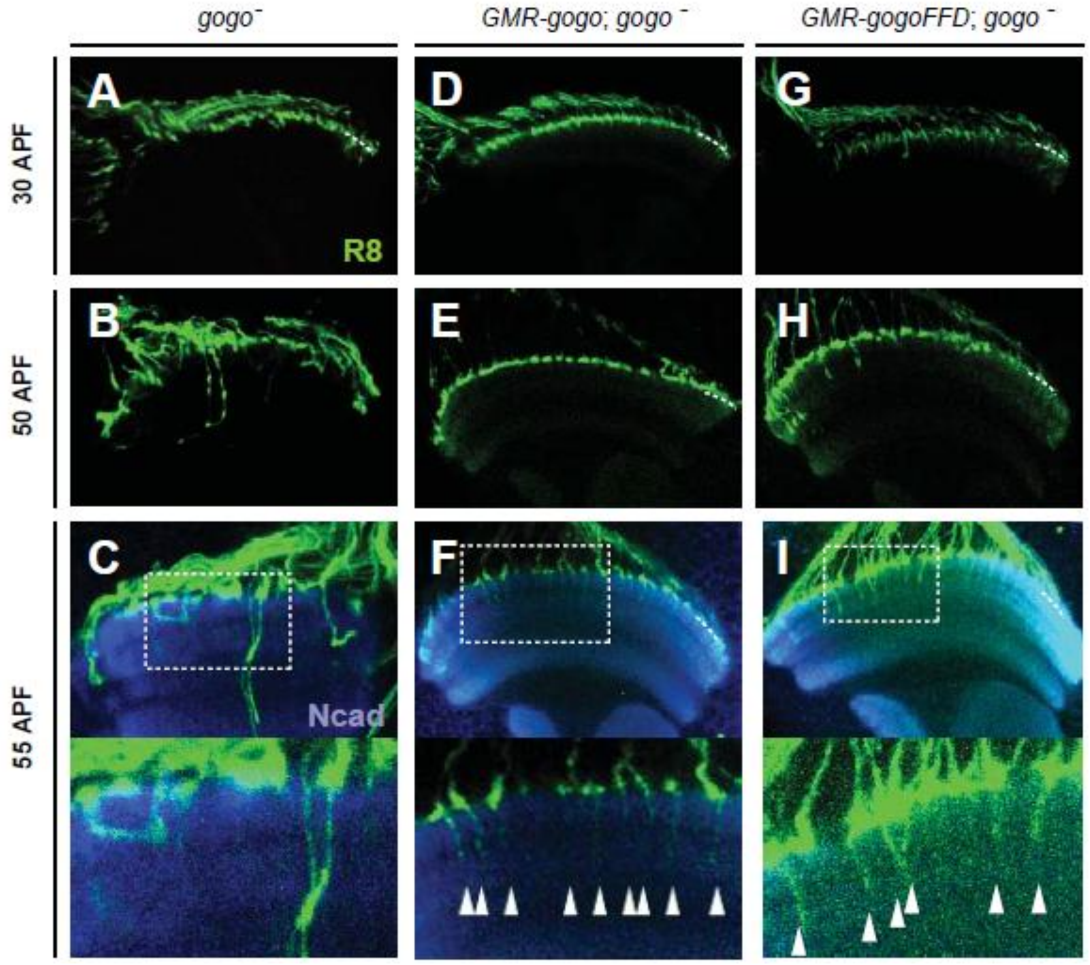

Figure 2-10: Gogo phosphorylation and the temporal layer recognition

The requirement of Gogo phosphorylation for interaction with the temporary layer was tested in details before and during the mid pupal stages. Eye-specific *gogo*$^{-}$ mosaic was used as a genetic background. The R8 axons were expressing the *atonal-tau-myc* marker (stained anti-tau, green), the neuropiles were stained with anti-*D*Ncadherin antibody (blue). Pupae 30, 50 and 55 APF of the indicated genotypes were analyzed; dashed line: R8 temporary layer; for 55 APF the boxed area is magnified to better visualize thin filopodial processes.

(A-C) Axons mutant for *gogo* fail to recognize the M1 layer and stall at the medulla surface, occasional overshooting is visible.

(D-F) When *gogo*$^{-}$ is rescued with wild type Gogo the targeting is not affected and at 55 APF processes towards the future M3 layer are already formed (arrowheads).

(G-I) Even if Gogo YYD motif is continuously dephosphorylated (GogoFFD) the targeting occurs similarly to the control situation (D-F) and neurons form extensions towards the M3 layer (arrowheads).

2.10 YYD motif and *flamingo* in M3 layer targeting

It was shown before that Gogo and Fmi act together to recognize and adhere to the M3 layer, since *gogo* and *fmi* co-overexpression in R7 cells induces their mistargeting to the R8-recipient layer (M3), whereas the mistargeting never occurs when *gogo* or *fmi* are overexpressed alone (Hakeda-Suzuki et al., 2011). Is it possible that this interaction also depends on Gogo phosphorylation status?

In order to answer this question *gogo* and *fmi* were co-overexpressed – however instead of wild type proteins Gogo phospho mimics were used. All transgenic insertions used here were inserted in the same landing site locus (attP40) and showed similar expression level. The phenotypes in flies when different Gogo phospho variants are overexpressed together with Fmi in a wild type background were analyzed (**Figure 2-11**). Half of the R7 could be redirected to the M3 layer when Fmi was overexpressed together with wild type Gogo and GogoFFD mimic (Gogo + Fmi, 50% of axons redirected, n = 196 axons; GogoFFD + Fmi, 51% of axons redirected, n = 406, **Figure 2-11A-D, F**). In contrary, I did not observe a R7 phenotype when Fmi was overexpressed together with GogoDDD (0%, n = 380, **Figure 2-11E, F**).

These findings indicate that Gogo/Fmi collaboration to recognize and adhere to the M3 layer strongly depends on the YYD motif and they suggest that it occurs only when Gogo is dephosphorylated.

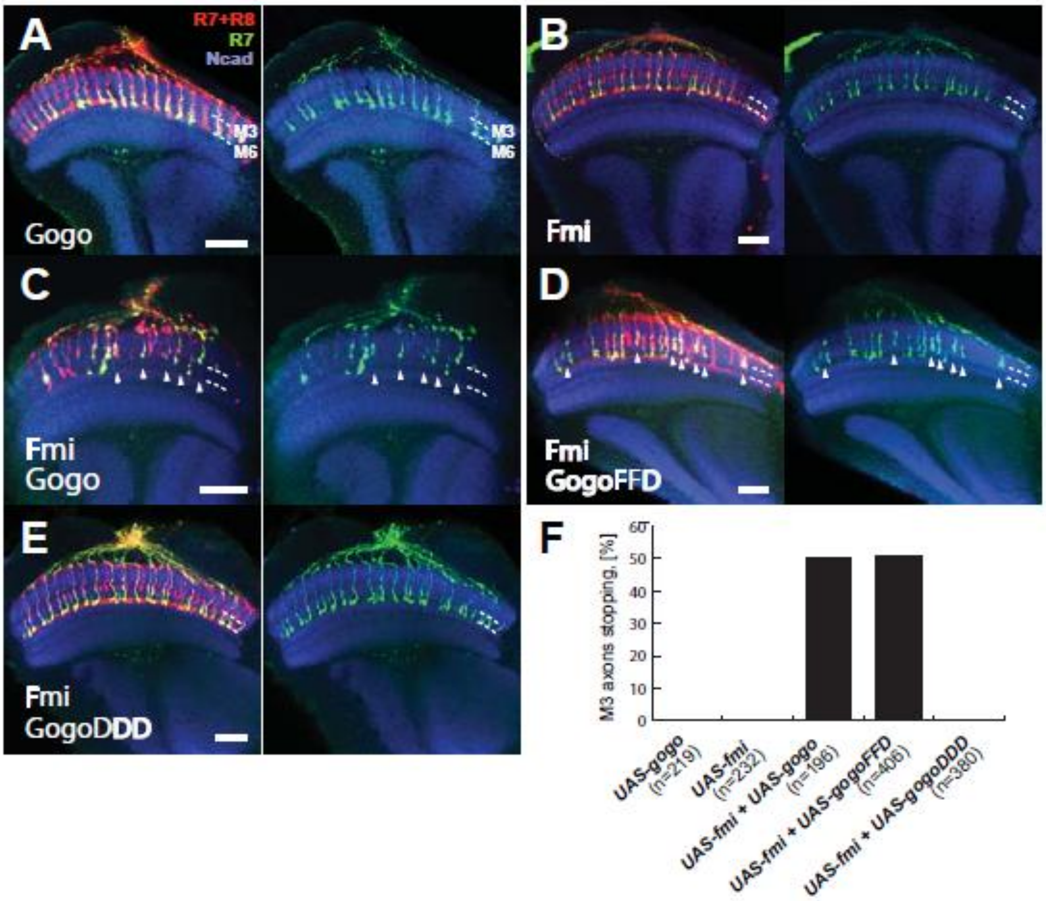
A
R7+R8
R7
Ncad
M3
M6
M3
M6
Gogo
B
Fmi
C
Fmi
Gogo
D
Fmi
GogoFFD
E
Fmi
GogoDDD
F
M3 axons stopping, [%]
60
50
40
30
20
10
0
UAS-gogo (n=219)
UAS-fmi (n=232)
UAS-fmi + UAS-gogo (n=196)
UAS-fmi + UAS-gogoFFD (n=406)
UAS-fmi + UAS-gogoDDD (n=380)

Figure 2-11: Gogo -Fmi colaboration to recognize the M3 layer requires Gogo dephosphorylation

(A-E) Phenotypes of R7 photoreceptors overexpressing Gogo, Fmi and combinations of Fmi with Gogo phospho-variants. All constructs were inserted in the same locus. R7 cells were visualized with *Rh4-GFP*, all photoreceptors with mAb24B10 and neuropiles with anti-*D*Ncadherin staining (blue). Dashed line indicates M3 and M6 layers. Scale bars represent 20 µm.

(A, B) Overexpression of Gogo or Fmi alone does not affect photoreceptor targeting and all R7 axons target normally (M6 layer).

(C-E) Overexpression of Fmi in combination with Gogo (C) or non-phospho-Gogo, (GogoFFD) (D), but not GogoDDD (E) results in R7 axons stopping at the M3 layer where R8 axons normally target. Arrowheads indicate premature R7 axon stopping at the M3 layer.

(F) Quantification of the R7 photoreceptor stopping phenotype at the M3 layer.

2.11 Fmi-Gogo collaboration and Gogo phosphorylation

Two evidence support the notion that Fmi-Gogo collaboration could rely on Gogo phosphorylation status:

1) Fmi functions in M3 layer targeting only with the non-phosphorylatable form of Gogo (see above)
2) Fmi antagonizes Gogo adhesion to the M1 layer (which presumably depends on Gogo phosphorylation), since changing the balance of Gogo and Fmi activity level in R8 photoreceptors affects the affinity to M1 layer: when *gogo* is overexpressed in *fmi* hypomorph background more R8 axons stop at the M1 layer compared with the moderate *gogo* overexpression. On the contrary, when *fmi* expression was mildly elevated (with *GMR-fmi*) in the Gogo overexpression background, M1 blobs were strongly reduced (Hakeda-Suzuki et al., 2011).

Moreover it was postulated that Fmi has to form a close interaction with Gogo to function (Hakeda-Suzuki et al., 2011). Formation of this functional complex can be studied in cell culture using an aggregation assay: Fmi expressed in S2 cells interacts homophilically resulting in formation of cell aggregates and shows accumulation at cell-cell contact sites. Cells transfected only with Gogo do not form aggregates since Gogo does not interact homophilically. However, when Gogo and Fmi are co-transfected they colocalize at cell-cell contacts and the colocalization is mediated by their transmembrane or extracellular domains (Hakeda-Suzuki et al., 2011). I speculated that Gogo phosphorylation status affects its recruitment to the complex. If this is true Gogo and Fmi should not colocalize at cell-cell contacts when Gogo is phosphorylated and therefore non-functional.

In order to check whether the interaction at the cell-cell contact depends on Gogo phosphorylation status, S2 cells were co-transfected with *UAS-fmi* in combination with *gogo/gogoFFD/gogoDDD*; subsequently an aggregation assay was performed. Analysis of the aggregates revealed that Fmi colocalizes with both phospho- and non-phosphomimetic form of Gogo (**Figure 2-12**).

Thus Fmi can probably form a complex with both dephosphorylated and phosphorylated Gogo. Therefore lack of the Fmi-GogoDDD interaction *in vivo* is not due to impairment in colocalization and consequently functional complex formation by these molecules.

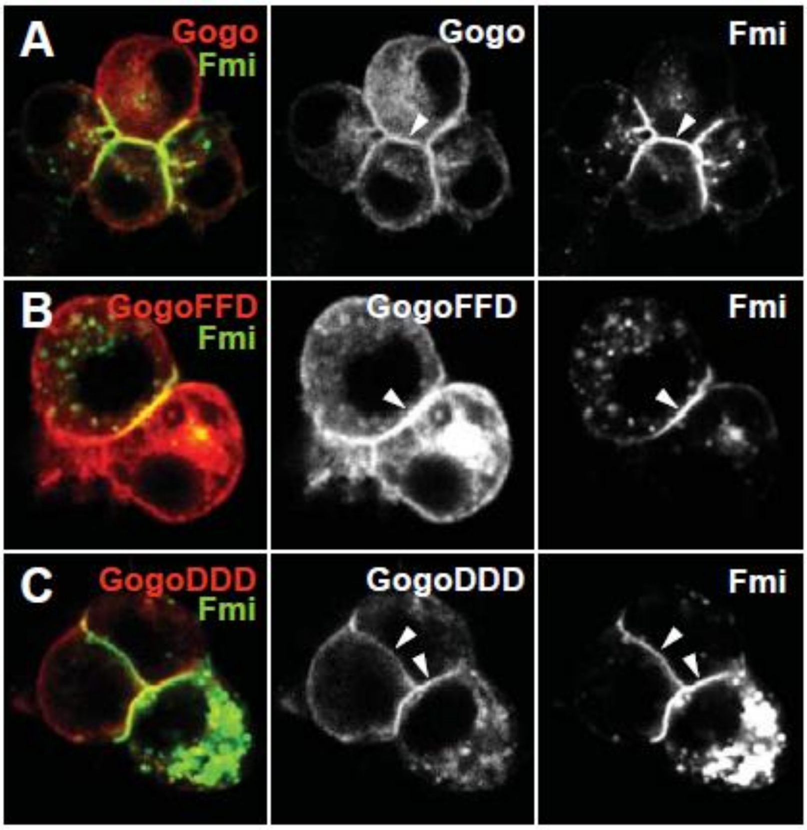

Figure 2-12: Fmi-Gogo interaction and Gogo phosphorylation

S2 cells were co-transfected with *UAS-fmi-EYFP* (green) and *UAS-gogo-myc*, *UAS-gogoFFD-myc*, *UAS-gogoDDD-myc* (stained anti-myc, red) and subsequently an aggregation assay was performed. The co-localization of Gogo and Fmi in the cell-cell contact area which occurs when wild type proteins are expressed (A) is not hampered when Gogo phospho- mimics are used: FFD (B) and DDD (C).

2.12 DInR regulates Gogo phosphorylation *in vivo*

The presented results support the notion that Gogo is a tyrosine-phosphorylated protein and they shed light on the function of phosphorylation. In this context it is an intriguing scientific problem to find the enzymes that modulate Gogo phosphorylation status (kinases, phosphatases). To approach this question a set of candidate genes was analyzed (briefly discussed in **Discussion 3.5**). Based on this preliminary data I decided to focus on the promising candidate: *Drosophila* Insulin Receptor (DInR, *dinr*).

DInR has a tyrosine kinase activity and was shown to be required for photoreceptor axon targeting (Song et al., 2003). The *dinr* expression is enriched in R-cell projections and DInR has a transmembrane localization (Song et al., 2003). These two properties make it a very interesting candidate for being a modulator of Gogo phosphorylation. To investigate whether DInR can influence Gogo phosphorylation, I examined the phosphorylation of Gogo co-overexpressed with DInR in S2 cell line. A tyrosine phosphorylation, albeit low, can be detected when Gogo is expressed alone. Gogo phosphorylation increases dramatically when DInR is co-overexpressed (**Figure 2-13A**). Moreover, the positive effect of DInR on Gogo phosphorylation is dose dependent. It suggests that DInR activity could be required for a positive regulation of Gogo phosphorylation and thereby *gogo* function.

The YYD motif is probably not the only phosphorylation site (**Figure 2-5**), thus does DInR specifically regulate the phosphorylation of the YYD motif? In order to solve this question, I modified the Gogo^{short} construct in such a way that the YYD motif is intact but other tyrosines on the cytoplasmic site are mutated (Y^{1022}F / Y^{1034}F / Y^{1041}F, **Figure 2-13B**). I refer to this construct as Gogo$^{short\ YYD\ FFF}$. Thus, the detected phosphorylation comes for sure only from the YYD motif. The Gogo$^{short\ YYD\ FFF}$ deletion shows a basal phosphorylation which increases dramatically when DInR is co-expressed (**Figure 2-13B**). I conclude that the YYD tripeptide phosphorylation is enhanced by DInR activity.

Is it possible to modulate Gogo phosphorylation not only by increasing the *dinr* expression but also by stimulating the receptor activity with its ligand? In the

Drosophila genome, there are seven insulin-like peptides (DILPs) which could be ligands for DInR. DILPs are evolutionary conserved and can act redundantly (Gronke et al., 2010). On the other hand, it has been reported that the *Drosophila* DInR signaling can be activated by human insulin (Fernandez et al., 1995). To further confirm that DInR signaling modulates Gogo phosphorylation, S2 cells were transfected with Gogo and treated with human insulin for 20 hours. Consistent with the previous result, Gogo phosphorylation is enhanced by insulin treatment. Moreover, insulin-triggered phosphorylation induction is dose dependent (dose used was between 0 – 50 μg / ml) confirming involvement of the DInR signaling (**Figure 2-13C**).

Taken together, these results suggest that the Gogo YYD motif becomes tyrosine phosphorylated upon DInR activation.

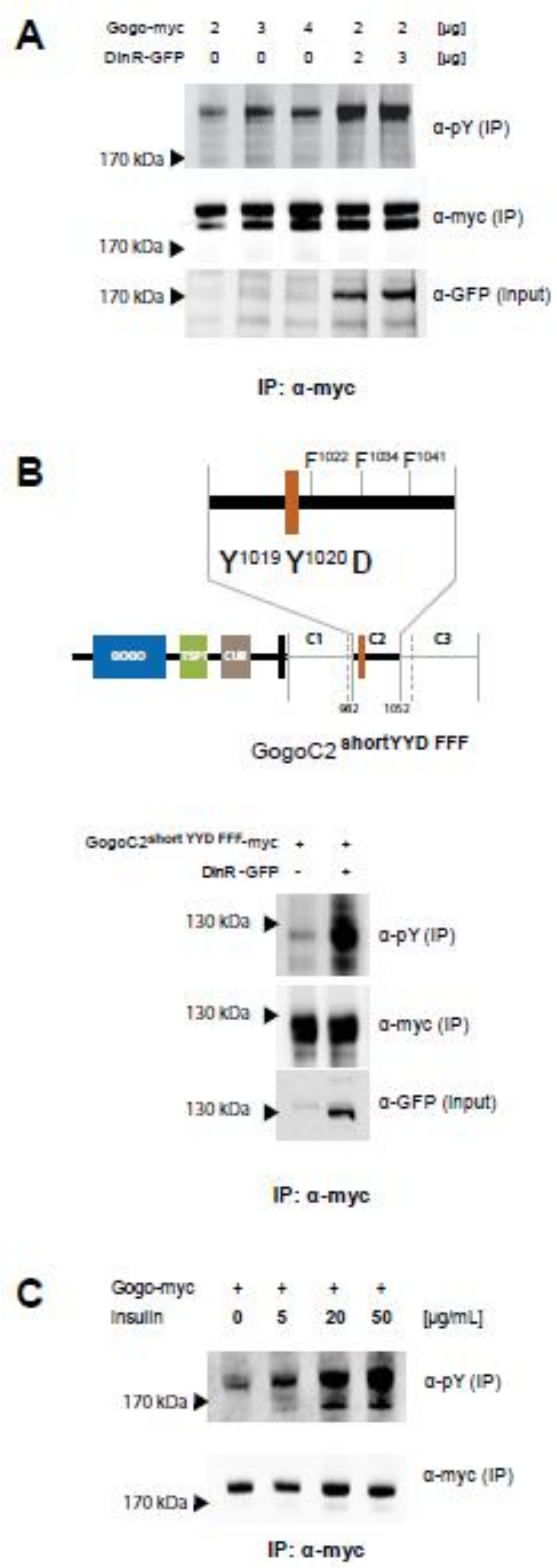

Figure 2-13: *dinr* positively regulates Gogo phosphorylation

(A-C) DInR signaling positively regulates Gogo YYD motif phosphorylation in S2 cells. *UAS-gogo-myc* and *UAS-dinr-GFP* constructs were co-transfected with *Act-Gal4* driver. Gogo-myc was immunoprecipitated (IP); pY signal was detected with the 4G10 antibody.

(A) DInR enhances Gogo phosphorylation in a dose-dependent manner. Indicated amounts of *UAS-Gogo-myc* and *UAS-dinr-GFP* were used for transfection. Gogo-myc in this case migrates as a double-band. The exact identity of this somewhat shorter form of Gogo is unknown, however it is occasionally observed in experiments. It could be a result of protein degradation or protein processing.

(B) DInR regulates specifically YYD motif phosphorylation. *UAS- Gogo*$^{short\ YYD\ FFF}$ construct has five tyrosine residues and only tyrosines in the YYD motif are intact whereas the other ones are mutated to phenylalanine. Phospho-tyrosine signal on the YYD motif is dramatically increased upon co-transfection with *UAS-dinr-GFP*.

(C) Gogo phosphorylation increases when insulin signaling is stimulated with human insulin. Insulin was applied for 20 hours at a concentration indicated in the panel.

2.13 *dinr* and *gogo* interact genetically in photoreceptor axon targeting

Since DInR can positively regulate Gogo phosphorylation in *Drosophila* S2 cells and, on the other hand, Gogo phospho- mimic causes R8 photoreceptor stopping at the M1 layer, it raises the possibility that DInR might influence the M1 layer targeting by enhancing Gogo phosphorylation. Is it possible to genetically manipulate Gogo phosphorylation by utilizing *dinr*?

To test the genetic interaction between *gogo* and *dinr*, I again took advantage of the *gogo* gain of function phenotype (blob formation at the M1 layer). Since a phosphomimetic version of Gogo (GogoDDD) does not allow the R8 axons to target the M3 layer and induces stopping at the surface of the medulla, the increase of Gogo phosphorylation by DInR overexpression should also affect the M1 targeting step. Interestingly, although *dinr* shows no gain of function phenotype in R8 cells when overexpressed alone (*GMR-Gal4, UAS-dinr*), it can strongly enhance the *gogo* gain of function phenotype when co-overexpressed (**Figure 2-14A-E**). The fraction of axons forming blobs is significantly increased when compared to single overexpression situation (**Figure 2-14D**). Further quantification of the blob phenotype showed that when *gogo* is overexpressed alone most of the blobs visible in R8 projection have a diameter varying between 0-10 μm^2 (92.7% of all blobs) and only small fractions of axons form blobs which are larger than 10 μm^2 (7.2%). However, when *dinr* is co-overexpressed with *gogo*, the blob size increases dramatically and the fraction of giant blobs larger than 10 μm^2 increases four-fold (from 7.2% to 31.9%, **Figure-14E**). Furthermore, single axon stopping at the M1 layer or terminating before reaching the M3 layer are visible.

Together, this demonstrates that *dinr* interacts genetically with *gogo* and is able to enhance the phenotype presumably related to Gogo phosphorylation (stronger adhesiveness to the M1 layer).

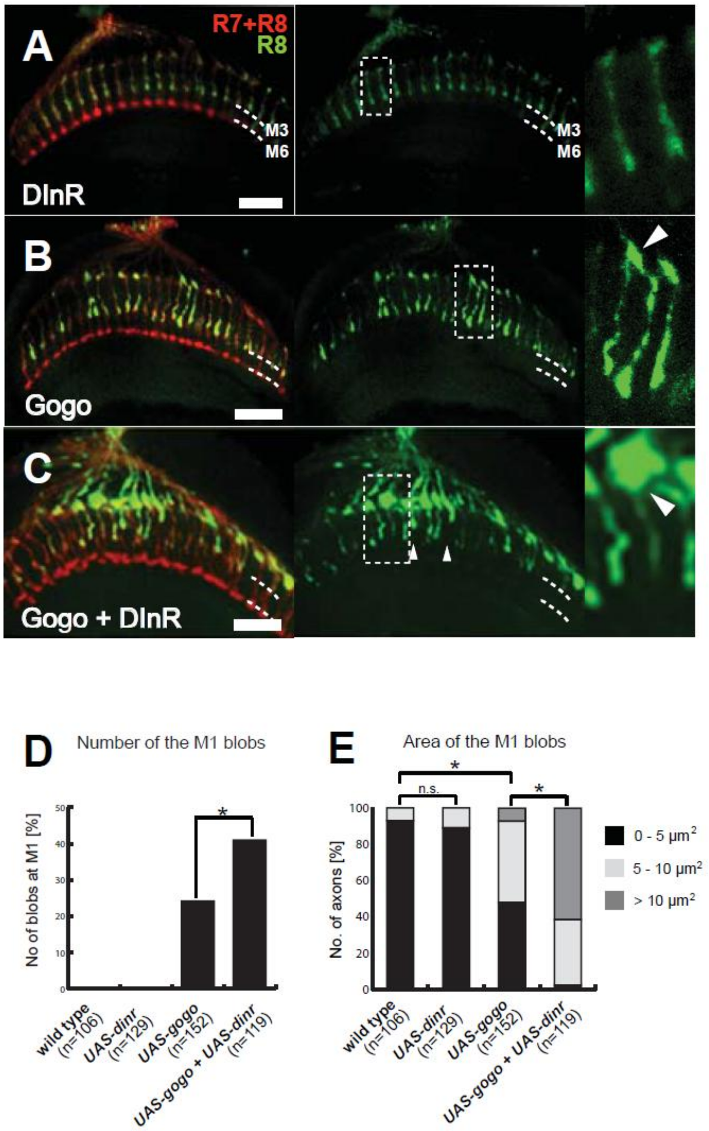
A
R7+R8
R8
M3
M6
DInR
B
Gogo
C
Gogo + DInR
D
Number of the M1 blobs
No of blobs at M1 [%]
0
10
20
30
40
50
*
wild type (n=106)
UAS-dinr (n=129)
UAS-gogo (n=152)
UAS-gogo + UAS-dinr (n=119)
E
Area of the M1 blobs
No. of axons [%]
0
20
40
60
80
100
*
n.s.
*
0 - 5 µm²
5 - 10 µm²
> 10 µm²

Figure 2-14: *gogo* interacts genetically with *dinr* during R8 axons targeting

(A) *dinr* does not affect photoreceptor targeting when expressed in the eye.

(B) When overexpressed in all photoreceptors, Gogo enhances R8 adhesion to the M1 layer visible in a blob formation phenotype (arrowhead).

(C) When Gogo and DInR are co-overexpressed the adhesive interaction with the M1 layer is strongly enhanced, and results in formation of giant blobs at the M1 layer and premature axon stopping (arrowheads).

(A-C) Expression of all constructs (*UAS*) was driven with *GMR-Gal4*. R8 axons were visualized with *Rh6-GFP* and all photoreceptors with mAb24B10.

(D) Quantification of the number of M1 blobs ($p < 0.001$, two-tailed t-test).

(E) Quantification of the M1 blob phenotype ($p < 0.001$, two-tailed t-test). The blobs area were calculated and classified into one of three categories: small (0 – 5 μm^2), intermediate (5 – 10 μm^2) or large (> 10 μm^2). Distribution of blobs within categories was plotted for each genotype tested and wild type flies.

2.14 DInR enzymatic activity is required for potentiating *gogo* overexpression phenotypes

Since DInR enhances Gogo phosphorylation when co-overexpressed in S2 cells and *dinr* enhances *gogo* gain of function phenotype, it is an intriguing question whether the genetic interaction between *gogo* and *dinr* requires DInR tyrosine kinase activity. If the interaction is kinase activity-dependent, it would support the model that DInR positively regulates Gogo phosphorylation directly or indirectly. To assess the *dinr* kinase activity requirement I took advantage of the available mutant *dinr* transgenic flies which show an impaired or enhanced enzymatic activity.

If *gogo* activity is indeed regulated by *dinr*, and if phosphorylation of Gogo explains the *gogo* overexpression phenotype, then the blob formation at the M1 layer should be significantly suppressed if *dinr* kinase activity is blocked. In order to assess the effect of DInR which lacks its enzymatic activity on Gogo, I utilized the available dominant negative *dinr* fly stock (DinR^{DN}). The K1409A substitution in the kinase domain of the Insulin Receptor results in a dominant negative protein variant (Wu et al., 2005). DinR^{DN} does not show any obvious mutant phenotype when overexpressed alone in all photoreceptor cells (*GMR-Gal4, UAS-dinr*^{DN}). Moreover, when co-overexpressed with Gogo, it can completely suppress the blob formation at the M1 layer, indicating that *dinr* activity is required for blob formation and thereby might influence the adhesion to the M1 layer during the mid pupal stages (**Figure 2-15A, B**).

Furthermore, I also tested the influence of the constitutively active form of DInR (DinR^{Act}) on *gogo* overexpression phenotype. The A1325D amino acid substitution in DInR mimics the human V938D protein variant (Longo et al., 1992). DInR^{Act} does not have any mutant phenotype when overexpressed alone in a wild type background. One of the possible reasons for this could be, that the endogenous levels of Gogo are not sufficient to evoke blob formation at the M1 layer, even if most of the Gogo protein would undergo phosphorylation (by DInR). However, when *gogo* is co-overexpressed with DInR^{Act} (*GMR-Gal4, UAS- dinr*^{Act}) the blob formation is enhanced when compared to situation when *gogo* is overexpressed alone, since almost all R8 axons form blobs (on contrary, *gogo-dinr* (wild type) results in large blob formation mostly in the middle part of the brain, **Figure 2-15C, D**). Additionally, many of the R8 axons fail to target the M3 layer and terminate before reaching their final destination, the M3 layer (7%, n = 659). Strikingly, a number of axons even stop at the medulla M1 layer (3%, n = 659).

Finally, if DInR modulates Gogo function by positively regulating the phosphorylation of the YYD motif, then the enhancement of the *gogo*-*dinr* co-overexpression phenotype should be suppressed when YYD motif is mutated to the non-phosphorylatable version, FFD. Indeed, the blob formation is significantly suppressed and the R8 axon morphology appears to be the same as wild type in this case (**Figure 2-16A, B**).

In summary, the presented above genetic analysis provides evidence that the enzymatic activity of *dinr* is involved in the interaction with *gogo*. Moreover, this genetical interaction involves the YYD motif. It further supports the possible involvement of *dinr* in modulating Gogo phosphorylation status and thereby axon pathfinding in the visual system.

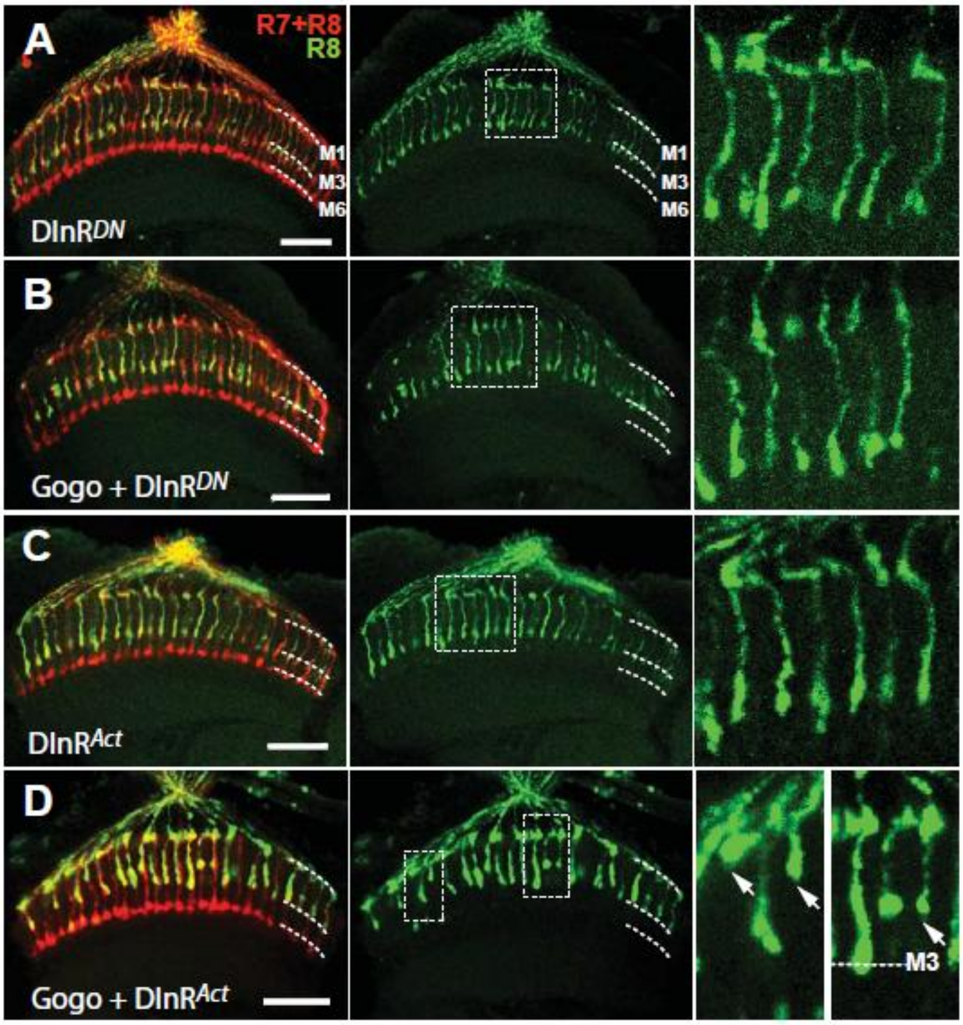

Figure 2-15: DInR enzymatic activity is required for potentiating Gogo overexpression phenotypes

(A-D) Genetic interaction between *dinr* and *gogo* depends on DInR enzymatic activity. *UAS-dinr* with impaired (*dinr*^{DN}) or enhanced (*dinr*^{Act}) activity were overexpressed alone (A, C respectively) and together with *UAS-Gogo* (B, D). Expression of all transgenes was driven by *GMR-Gal4*. R8 axons were visualized with *Rh6-GFP*, all photoreceptors are stained with mAb24B10. Dashed lines indicate medulla layers M1, M3 and M6; axons in the boxed area were magnified; Scale bar indicates 20 μm.

(A, B) DInR^{DN} overexpressed alone in photoreceptors does not affect R8 axons morphology (A). Furthermore, it suppresses completely M1 blob formation when co-overexpressed with Gogo (B).

(C, D) DInR^{Act} overexpressed alone in photoreceptors does not affect R8 axons morphology (C). However it enhances adhesive properties of R8 axon growth cones when co-overexpressed with Gogo (D); R8 cells form blobs at the M1 layer and terminate prematurely at M1 layer or between M1-M3 (arrows).

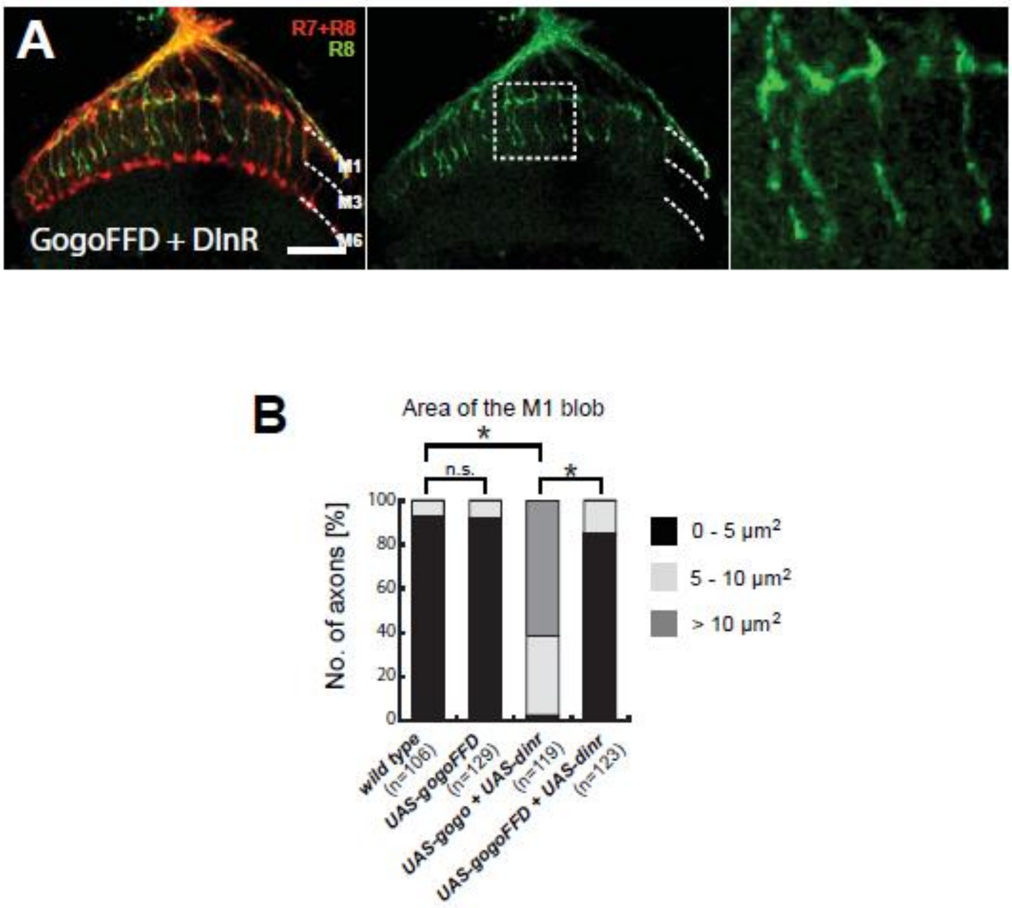
A
R7+R8
R8
M1
M3
M6
GogoFFD + DInR
B
Area of the M1 blob
*
n.s.
*
No. of axons [%]
100
80
60
40
20
0
0 - 5 μm²
5 - 10 μm²
> 10 μm²
wild type (n=106)
UAS-gogoFFD (n=129)
UAS-gogo + UAS-dinr (n=119)
UAS-gogoFFD + UAS-dinr (n=123)

Figure 2-16: Mutation in the YYD motif suppress the genetic interaction with *dinr*

(A) DInR does not enhance the *gogo* gain of function phenotype when the YYD is mutated to a non-phosphorylatable version (GogoFFD). Expression of both transgenes was driven by *GMR-Gal4*. R8 axons were visualized with *Rh6-GFP*, all photoreceptors are stained with mAb24B10. Dashed lines indicate medulla layers; axons in the boxed area were magnified; Scale bar indicates 20 µm.

(B) Quantification of the *dinr* - *gogo* genetic interaction ($p < 0.001$, two-tailed t-test). The blobs area were calculated and classified into one of three categories: small (0 – 5 µm^2), intermediate (5 – 10 µm^2) or large (> 10 µm^2). The distribution of blobs within categories was plotted for each genotype tested and wild type flies.

2.15 Loss of *dinr* does not affect R8 targeting

It has been reported that insulin receptor functions in axon guidance (R7 photoreceptors) in the *Drosophila* visual system, where DInR serves as a guidance receptor and acts *via* the adapter protein Dock/Nck (Song et al., 2003). In eye-brain complexes of the surviving transheterozygous hypomorphic allele *dinr*^{353}/*dinr*^{273} mosaic larvae, R-cells failed to expand to their termination points in the medulla. In adult animals in the null allele *dinr*^{ex15} mutant clones, gaps in the R7 layer and crossed fibers were observed (Song et al., 2003). However, the study from Song et al. does not give a direct answer whether *dinr* functions also in R8-cells axon guidance, since no specific markers for photoreceptor subtypes were available at that time. Thus I aimed to characterize the function of *dinr* in R8 targeting in more details by labeling specifically R8 cells which are mutant for *dinr*. If *dinr* is truly positively regulating Gogo phosphorylation, then in the situation when *dinr* is inactive, Gogo should be dephosphorylated and the observed phenotypes should resemble the features when *gogo*$^{-}$ phenotype is rescued by GogoFFD expression.

To determine whether *dinr* affects axon targeting in the visual system I utilized the FLP-FRT system to generate homozygous small cell patches mutant for *dinr* (*dinr*^{ex15}, null allele) in an otherwise wild type background (**Materials and Methods 4.2.8**). To obtain small *dinr*$^{-}$ clones in a wild-type background the *dinr*^{ex15} allele was placed in *trans* to the fluorescent marker KO (Kusabira-Orange) which expression was driven by the *GMR* promoter. After site-specific mitotic recombination (driven by the activity of *ey3.5*FLP), a heterozygous mother cell can give rise to two types of daughter cells in which the chromosome arms distal to the recombination site become homozygous: homozygous mutant (negatively labeled by the lack of *GMR-KO* expression) and homozygous wild type (expressing the fluorescence marker *GMR-KO*). Additionally, a small fraction of cells which are heterozygous is generated: they are labeled with *GMR-KO*. The use of *Rh6-GFP* marker (labeling R8 photoreceptors), and co-staining with antibody specific for all photoreceptor cells (mAb24B10) enables an easy identification of each subpopulation of cells. Although DInR signaling is involved in cell growth regulation and modulation of many aspects of cell physiology, single photoreceptors mutant for *dinr*^{ex15} could survive (**Figure 2-17A-J**). A detailed analysis revealed that all of the analyzed mutant axons have an altered morphology and the axonal process is very thin as compared to wild type axons (in average 2.5 µm and 5.9 µm in diameter respectively, n=10, **Figure 2-17K, L**). A possible explanation for this could be the crucial role of *dinr* in growth regulation. However, all analyzed R8 photoreceptors target the M3 layer (n=46 axons, 15 brains analyzed).

In summary, photoreceptor axons are able to survive upon removal of *dinr*, however they do not show any obvious guidance defects. The M3 layer targeting in this case resembles the wild type phenotype. It is consistent with the result which I obtained when *gogo*⁻ phenotype was rescued by a non-phosphorylatable form of Gogo (FFD). Thus, the signaling which regulates Gogo phosphorylation should include two components. On one hand DInR constitutively positively regulates Gogo phosphorylation. On the other hand an additional signaling is required to dephosphorylate Gogo.

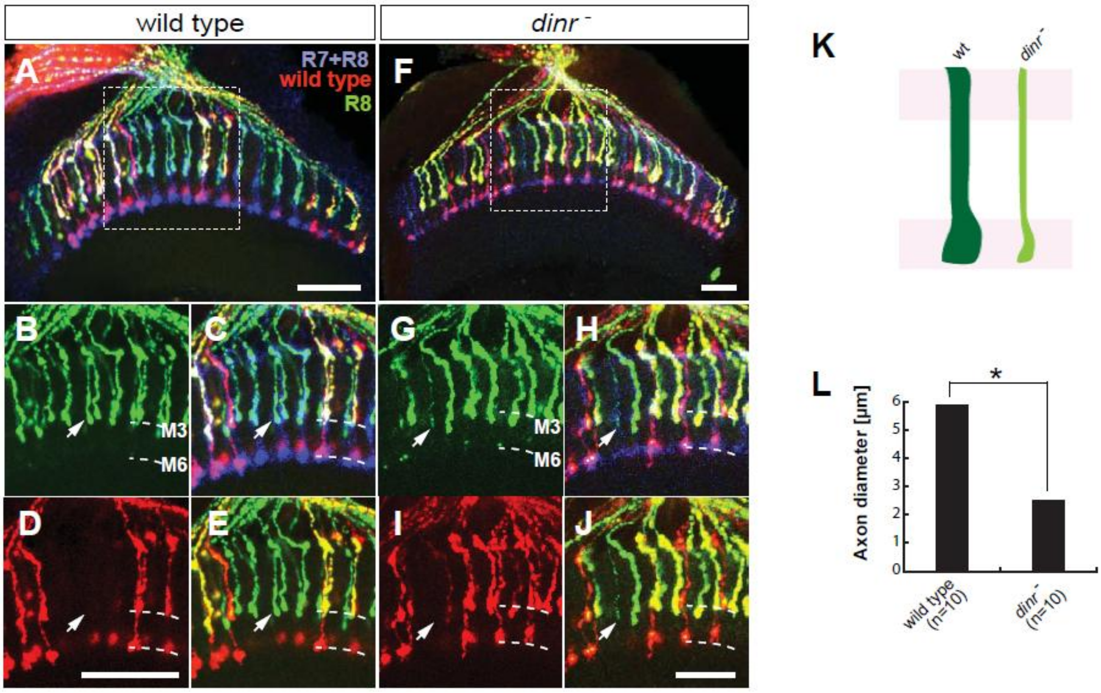

Figure 2-17: Loss of *dinr* does not affect R8 axon targeting

(A-J) R8 axons mutant for *dinr* taget normally the M3 layer. Small cell patches mutant for *dinr* (null allele *dinr*^{ex15} was used) and control clones were generated in an otherwise wild type background. All photoreceptors were stained with mAb24B10 (blue), R8 axons with *Rh6-GFP*, and all wild type axons express *GMR-KO* marker (red), cells within the clones are negatively labeled by the lack of *GMR-KO* expression (arrow). The boxed area is magnified and the dashed lines indicate the M3 and M6 layers, scale bar represents 20 µm.

(A-E) Wild type R8 axons within the control clone (FRT82B) terminate normally at the M3 layer and show a normal morphology (arrow).

(F-J) Axons mutant for *dinr* terminate at the appropriate layer (M3). However, they are abnormally thin (arrow).

(K) Schematic comparison of *dinr* mutant axon morphology with wild type process.

(L) Comparison of the axon diameter between R8 projections mutant for *dinr* and wild type, SD: 0.34 (wild type), 1.0 (mutant), ($p < 0.001$, two-tailed t-test).

2.16 Downregulation of insulin signaling suppresses R8 axons adhesion to the M1 layer

Insulin signaling positively regulates R8 axons adhesion to the M1 layer. However, lack of *dinr* activity does not result in incorrect targeting of R8 photoreceptors. Does it mean that the genetic interaction between *gogo* and *dinr* in photoreceptors is ectopic? If yes then insulin signaling should be dispensable for generation of the Gogo gain of function phenotype (blob formation at the M1 layer). On the other hand, if *dinr* endogenous activity somewhat contributes to the interaction with the temporary layer and formation of the blob phenotype, then the adhesive interaction between R8 cells and M1 layer should not enhance when Gogo activity increases (*UAS-Gogo*) and at the same time insulin signaling is downregulated. In order to verify this speculation I downregulated activity of the endogenous insulin signaling using two complementary approaches. First, one copy of *dinr* was removed from the fly (*dinr*^{ex15}/+). Second, one copy of *dilp1-5* (five out of seven *dilp* genes in *Drosophila*) were removed (*dilp1-4*^{1}, *5*^{3}/+). In each of this mutant backgrounds Gogo was overexpressed (*UAS-Gogo*) and the flies were tested for suppression of the blob phenotype (**Figure 2-18A-C**). In the control brains (*UAS-Gogo*) 30% of R8 axons form blobs at the M1 layer. This phenotype is dramatically suppressed in the situation when either one copy of *dinr* of *dilp1-5* were removed (*UAS-Gogo; dinr*^{ex15}/+: 12% and *UAS-Gogo; dilp1-4*^{1}, *5*^{3}/+: 6% of axons form blobs, **Figure 2-18D**). A similar suppression is visible in the blob size. In the control brains (*UAS-Gogo*) 43% of R8 axons form small blobs (0-5µm^2, **Figure 2-18E**). The blob size is suppressed when either one copy of *dinr* of *dilp1-5* were removed (*UAS-Gogo; dinr*^{ex15}/+: 62% and *UAS-Gogo; dilp1-4*^{1}, *5*^{3}/+: 59% of axons form small blobs (0-5µm^2).

To conclude, endogenous insulin signaling is involved in “Gogo signaling”.

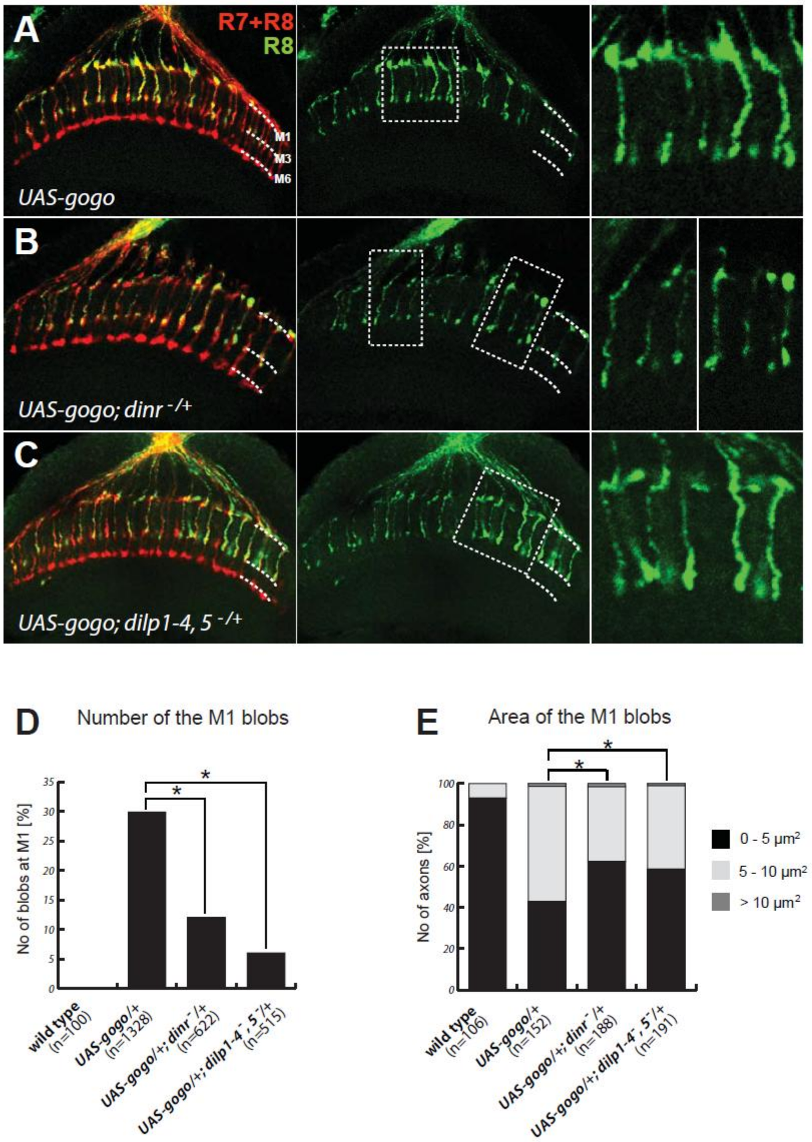

Figure 2-18: Downregulation of insulin signaling suppresses R8 axons interaction to the temporary layer

(A) Overexpression of Gogo results in blob formation at the M1 layer.

(B) When Gogo is overexpressed in a *dinr*^{ex15} heterozygous mutant background blob formation is suppressed.

(C) Similarly when Gogo is overexpressed in a *dilp1-4*^{1}, *5*^{3} heterozygous mutant background blob formation is suppressed.

(A-C) Expression of all constructs (*UAS*) was driven by *GMR-Gal4*. R8 axons are visualized with *Rh6-GFP*, all photoreceptors are stained with mAb24B10. The boxes areas are magnified (right) and the dashed lines indicate M1, M3 and M6 layers.

(D) The number of blobs formed at the M1 layer is significantly decreased when DInR or DILP's expression is downregulated ($p < 0.001$, two-tailed t-test).

(E) Upon downregulation of DInR and DILP's expression the blob size is suppressed and less blobs with the intermediate size (5-10 µm^2) size are formed which are typical for *gogo* overexpression.

3. Discussion

Gogo was shown to be (together with Fmi and Caps) one of the three cell-surface guidance molecules involved in synaptic layer selection by R8 photoreceptors in *Drosophila*. However, the exact way how Gogo acts in this process and how it collaborates with other guidance receptors is far from being understood. In this dissertation I aimed to shed some light on our understanding of Gogo activity at the molecular level. It was a challenging task since – besides the documented fact of a close collaboration with Fmi – no signaling pathways involving Gogo as a component are known. Furthermore, the identity of Gogo ligands and its binding partner(s) remains unknown. So far, there is only one direct binding partner of Gogo known, Hu-li tai shao (Hts, *Drosophila* adducing homolog). As Hts knock-out flies show a much weaker phenotype, more key elements in the "Gogo signaling pathway" remain to be discovered (Ohler et al., 2011).

Two main approaches were undertaken previously with the hope to characterize Gogo interaction network:

1) Candidate interaction partners were selected based on phenotypical similarities with *gogo*. This approach resulted in the identification of *fmi* as a key component of the "Gogo signaling" (Hakeda-Suzuki et al., 2011).

2) Potential binding partners were identified in a biochemical approach: tagged Gogo was overexpressed in *Drosophila* larvae and immunoprecipitated. The coimmunoprecipitated proteins were identified with mass spectroscopy and the candidate genes were further tested. This approach resulted in the identification of Hts as a binding partner (Ohler et al., 2011).

Based on the strong interaction with *fmi* one could imagine that studying the Fmi signaling in the visual system can be very helpful to understand Gogo function as well, since the two pathways may overlap. However, cytoplasmic deletion of Fmi does not disrupt axon targeting suggesting that Fmi signaling is not crucial for axon pathfinding in the visual system (Tomasi et al., 2008).

In this study I choose an approach alternative to the presented above: namely a search for unknown functional domains in Gogo. Although this attempt does not allow for a direct and immediate identification of the key signaling components, it may serve as a useful and fruitful starting point for further studies. Several scenarios were considered before the beginning of the experimental part of the project:

1) Once an essential sequence is characterized it might be used to create a constitutively active / dominant negative form of the gene. The modified gene can potentially create a specific mutant phenotype which could be used further in a search for enhancers or suppressors of this mutant phenotype.
2) The identified sequence can be used to create a “bait” which will be later used in a yeast-two-hybrid screen giving an opportunity to systematically search for proteins showing a physical interaction.

3.1 The functional elements in the Gogo cytoplasmic domain

Gogo has a cytoplasmic domain which was shown to be required for Gogo function (Tomasi et al., 2008). However, what are the functional elements within the cytoplasmic region was an unanswered question. This study shows that the middle part of the intracellular domain (C2 fragment, amino acids 954 – 1105) contains the necessary and sufficient elements for Gogo cytoplasmic function. Moreover, an even shorter deletion which covers amino acids 982 – 1052 is sufficient to partially rescue the *gogo*$^-$ phenotype. A detailed analysis showed that the conserved YYD tripeptide (Tyr^{1019}-Tyr^{1020}-Asp^{1021}) in the C2 fragment plays a key role for Gogo function. Mutations in the YYD motif can completely disrupt the molecular activity of Gogo *in vivo*. The functional requirement of this tripeptide is confirmed by the fact that it was well conserved during evolution among invertebrates and vertebrates as well. In summary the YYD tripeptide is necessary for Gogo.

Is the YYD motif the only functional element in Gogo cytoplasmatic domain? Several observations allow to answer negatively this question:

1) In a close proximity to the YYD motif there are several residues showing various degree of conservation as well. For instance the glutamic acid (E) Glu^{1016} in front of the YYD motif (**Figure 2-2**) shows a complete conservation among tested species. It suggests, that it could also play an essential role for Gogo function. Presumably, together with the YYD motif, it could be involved in binding to the downstream signaling molecules or in preserving the proper conformation of the Gogo protein.
2) Most probably elements outside of the YYD motif and its close proximity are required since the Gogo^{short} deletion shows a somewhat smaller rescuing ability than the complete C2 fragment.

Generation of series of Gogo mutants which contain mutations in the elements which could potentially have some function would be required in order to verify the impact of this elements for Gogo function.

Nevertheless, it is justified to conclude that the YYD is likely to be the “key element” for Gogo function in the cytoplasmic sequence.

3.2 Gogo is a tyrosine phosphorylated axon guidance receptor

Several studies have led to the view that tyrosine phosphorylation plays an important role in axon guidance and target recognition. Examples include Eph (Henkemeyer et al., 1996), Derailed (Callahan et al., 1995), Src family (Knoll and Drescher, 2004), Alk (Bazigou et al., 2007), Robo and Abl (Bashaw et al., 2000), Lar, and Ptp69D (Clandinin et al., 2001; Maurel-Zaffran et al., 2001).

In the present study I show that Gogo also undergoes *in vivo* a tyrosine specific phosphorylation. Furthermore, the phosphorylation site was mapped to the YYD motif. Two lines of evidence support the model that Gogo can be phosphorylated *in vivo*. First, I show that specifically the YYD motif is a phosphorylation site in *Drosophila* S2 cells. Second, Gogo undergoes a basal tyrosine-specific phosphorylation since I could detect a tyrosine-specific phosphorylation in Gogo isolated from the fly visual system (larval and pupal stages). An antibody raised against the YYD-phosphorylated Gogo enabled to further confirm the YYD motif as a phosphorylation site *in vivo*.

Studies on Gogo phosphorylation in S2 cell line revealed that additional tyrosine-phosphorylation site(s) are present in Gogo sequence. They are located in the C2 fragment. However their functional requirement remains to be investigated. In contrast to the YYD motif, the alternative phosphorylation sites are not conserved. Gogo lacking these three tyrosine residues can partially rescue the mutant phenotype. A partial rescue suggests that they could potentially have some regulatory function. In order to better understand their role, their functionality could be tested for instance by inserting mutations in these residues and testing their ability to rescue the *gogo*$^{-}$ phenotype.

Presented here data support the notion that the YYD motif is the essential tyrosine phosphorylation site.

3.3 The model

Here I propose a model in which the phosphorylation status of Gogo determines the protein activity and thus is critical for correct photoreceptor axon pathfinding: for both temporal and final layer targeting the YYD motif phosphorylation status is essential. The presented results suggest that Gogo is phosphorylated during the first targeting step (0 - 50% APF), followed by a dephosphorylation at the midpupal stage to allow the R8 axons to extend to their final layer. Thus my model predicts that the dephosphorylation is essential for Gogo activation (**Figure 3-1A**).

How does Gogo phosphorylation influence protein activity and thereby neuronal development? My experiments in which I utilized different Gogo forms having a Y-F mutation in the YYD motif, combined with the genetic interaction with *dinr*, clearly show that it is the dephosphorylated form of Gogo, which is the most active. The non-phospho-Gogo is functional during R8 targeting, since I could rescue *gogo*$^{-}$ mutant phenotype by expressing GogoFFD. On the contrary, phospho-mimetic Gogo does not rescue the mutant phenotype.

It is somewhat surprising that in order to become a functional protein Gogo has to be dephosphorylated. Moreover, even if it is constantly dephosphorylated the targeting of R8 axons occurs normally and without obvious defects. On the other hand similar examples are known from the literature. For instance Gogo inactivation upon phosphorylation in some aspects resembles the molecular regulation of Robo activity, since the dephosphorylated Robo shows the most activity in mediating repulsive signals during embryonic central nervous system axon guidance (Bashaw et al., 2000). Additionally, protein inactivation upon phosphorylation, although relatively rare, has been reported in biochemical pathways, for instance inactivation of transcriptional co-activator Yorkie by Warts (Saucedo and Edgar, 2007), and others (Johansen and Ingebritsen, 1986; Lin et al., 1990; Fang et al., 2000). Some possible explanations why Gogo undergoes phosphorylation, although it is not entirely necessary for axon guidance will be discussed later in this chapter (**Discussion 3.6**).

3.4 Gogo phosphorylation and visual system development

What are the consequences of lack of Gogo dephosphorylation? I was able to inactivate Gogo by either removing the YYD site (GogoΔYYD) or mimicking phosphorylation (GogoDDD). Both forms result in a very strong adhesiveness and stopping of growth cones at the M1 layer, suggesting the involvement of phosphorylation in the first targeting step (**Figure 3-1B**). Although Gogo dephosphorylation in necessary for leaving the M1 layer, it is not clear whether in a physiological situation phosphorylation contributes to adhesiveness to the M1 layer. For sure it is not entirely necessary, since axons expressing only the dephosphorylated Gogo (FFD) can still recognize the M1 layer in the pupal stages (**Figure 3-1C**). However, there might be some fine-tuning defects such as the location of the synapses along the R8 axons between M1 and M3 layers (not examined in this study).

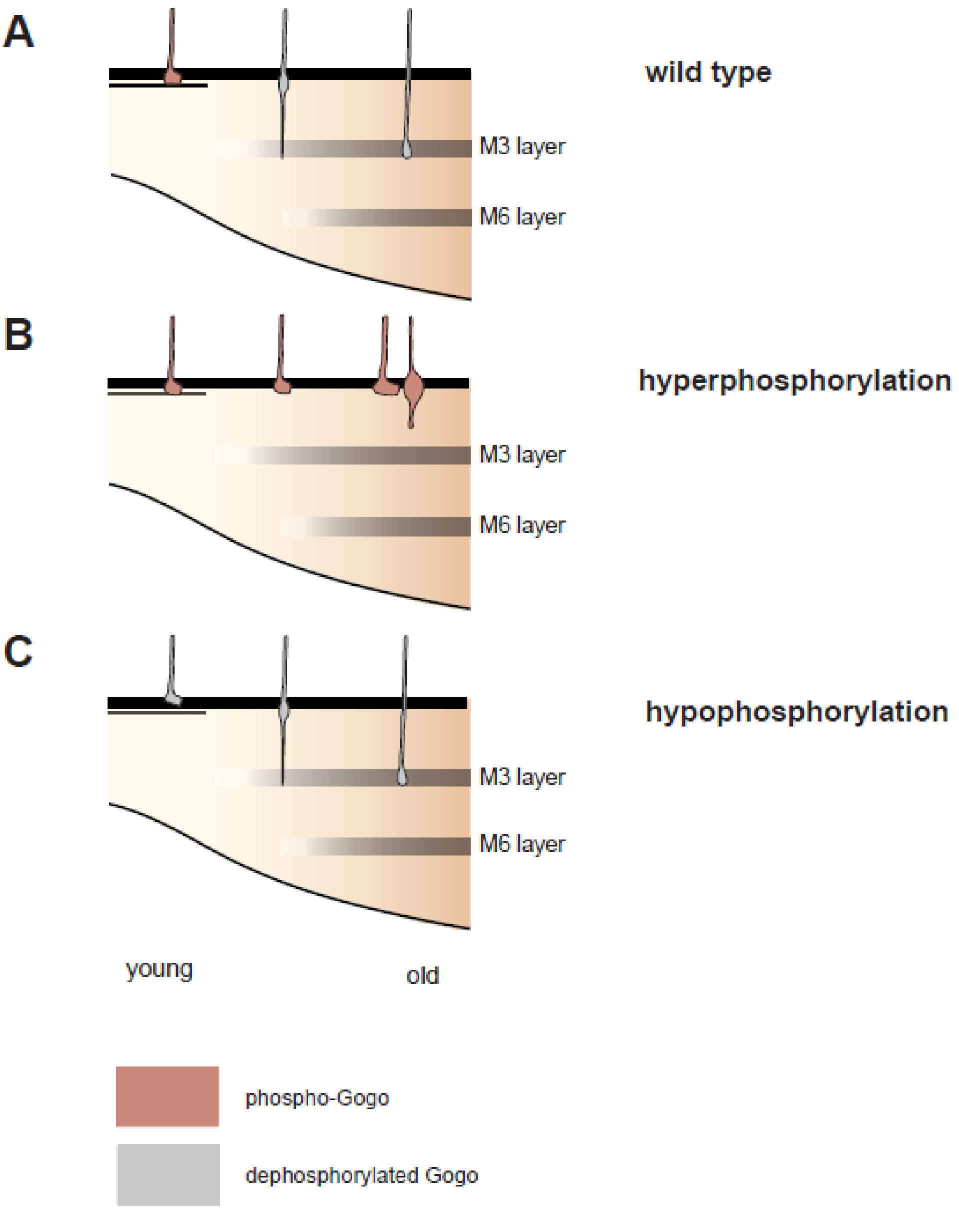
A
wild type
M3 layer
M6 layer
B
hyperphosphorylation
M3 layer
M6 layer
C
hypophosphorylation
M3 layer
M6 layer
young
old
phospho-Gogo
dephosphorylated Gogo

Figure 3-1: Model explaining R8 axons defects upon Gogo hyperphosphorylation

(A) In the presented model Gogo is phosphorylated at the beginning of the pupal development (red axons).

(B) However, it is obligatory that the phosphorylation is removed (grey axons) before the R8 processes start the targeting to the M3 layer. If the dephosphorylation is suppressed axons stalling at the medulla surface and blob formation occurs.

(C) Dephosphorylation provides a permissive signal allowing for M3 targeting. Thus even if Gogo is artificially constitutively dephosphorylated the targeting is normal

It is important to mention that GogoΔYYD behaves in all performed experiments similarly to the phospho mimics, GogoDDD. Why is that? What does it say about the YYD site phosphorylation? It is possible that multiple downstream molecules can bind to Gogo C2 fragment resulting in different types of signaling. Moreover, their binding could depend on YYD motif phosphorylation. For instance the signal to leave the M1 layer and target M3 could be mediated upon binding of factor “A”, which associates with Gogo only if it is dephosphorylated (signaling “A”). On the other hand there might exist signaling “B”, mediated by the presumptive factor “B” which stops the R8 axon at the M1 layer (**Figure 3-2**). In the presented here model binding of “A” and “B” to Gogo is mutually exclusive: “A” when bound to Gogo suppresses the interaction with “B”. “B” can only bind to Gogo when the YYD motif is phosphorylated or deleted. It is possible that phosphorylation and deletion of the YYD tripeptide result for instance in conformational change which makes it possible to bind “B”.

Gogo phospho-status is not only important for the interaction of R8 growth cones with their temporary layer, but defects in dephosphorylation can also result in mistargeting of the M3 layer. This is supported by the fact that GogoDDD (“phospho-Gogo”) does not show the proper cooperation with Fmi during final layer targeting. Therefore, Gogo has to be dephosphorylated to cooperate with Fmi in guiding photoreceptor axons to the M3 layer.

Manipulating Gogo activity status by inserting mutations in the YYD motif is able to induce very severe phenotypes in both *gogo*$^-$ and wild type background. On the other hand it is indispensable to confirm a scientific result by complementary experiments using different approaches. In Gogo case different phosphorylation status was controlled not only by inserting phospho- / non-phospho- mimicking mutations but also by modulating phosphorylation genetically using various mutants of the *dinr*. It was rewarding to see that hyperphosphorylation of Gogo by overexpressing *dinr* results not only in the strong adhesiveness to the M1 layer but also in occasional premature axon stopping (at the M1 layer or between M1-M3 layers). However, in this case the penetrance of the stopping phenotype was not as strong as when Gogo phospho- mimics are used. A possible explanation could be the fact that additional redundant mechanism can be present in R8 axons which modulate Gogo phosphorylation status.

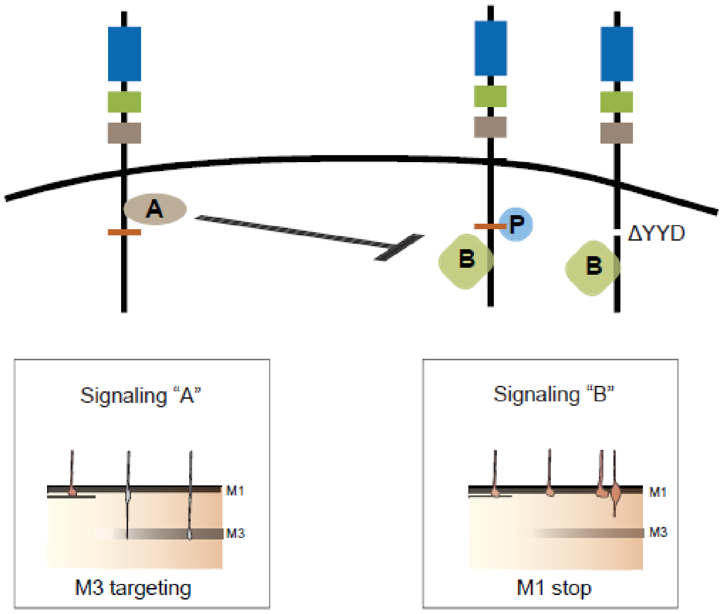

Figure 3-2: Signaling "A" and "B" model

Factors "A" and "B" both can bind to Gogo cytoplasmic domain. Binding of "A" is necessary to release the axon from the M1 layer and target to the M3 layer and it occurs only if the YYD motif is dephosphorylated. "A" suppresses the binding of "B". Red axons – phospho-Gogo; grey axons – non-phospho-Gogo.

3.5 *gogo* and *dinr*

The finding that Gogo is a tyrosine-phosphorylated protein raised the question about the nature of the cellular mechanisms that might regulate the phosphorylation status during development. To give an answer I searched for enzymes which might perform this function.

The *Drosophila* genome contains a relatively small number of tyrosine kinases (32) and phosphatases (21). I concentrated on candidate proteins which are expressed in the brain, are localized in the membrane and were implicated in axon guidance. Since the Gogo YYD motif phosphorylation is involved in formation of the characteristic overexpression phenotype, it was convenient to screen for suppression or enhancement of the M1 blobs when a kinase or phosphatase was co-overexpressed with *gogo*. The following genes were tested: *Abelson tyrosine kinase (abl), src42A, src42B, derailed (drl), epidermal growth factor receptor (egfr), Drosophila insulin-like receptor (dinr), eyes absent (eya), leukocyte-antigen-related-like* (*lar*), *protein tyrosine phosphatase*

69D (*ptp69D*)). The summary of observed phenotypes is included in the Appendix (**Table 5-1**).

From the above mentioned set of genes I identified *dinr* as a possible regulator of Gogo phosphorylation. All other tested candidates were excluded from a detailed analysis, since the overexpressed gene either did not enhance/suppress *gogo* gain of function phenotype, or resulted in an extensive cell death, or, finally, caused a severe axon guidance phenotype which was difficult to separate from a cell death phenotype (*egfr*).

DInR and the IIS [insulin/IGF (insulin-like growth factor)-signaling] have a well documented function in diverse aspects of physiology among various organisms including mammals. Most of the examples include processes linked to nutrition and energy demanding processes (growth, metabolism, reproduction and aging) (Saltiel and Kahn, 2001; Tatar et al., 2003; Edgar, 2006; Broughton and Partridge, 2009). Additionally there are evidence showing that IIS can modulate synaptic transmission (Wang et al., 2000) and even may be needed for learning and memory (Mayer et al., 1990; Craft et al., 1996; Wickelgren, 1998). In *Drosophila* DInR activates mostly the pathway involving the lipid kinase phosphatidylinositol 3-kinase (PI3K) and the protein kinase Akt/PKB. This pathway is mainly used to stimulate protein synthesis and thus cell growth (Stocker and Hafen, 2000).

DInR expression is enriched in R-cell projections and was reported to function in the fly photoreceptors axon guidance. DInR binds to Dock and triggers the Dock/Pak signaling – a well established pathway involved in axonal guidance in the fly (Garrity et al., 1996; Hing et al., 1999). These cellular events which regulate axon guidance most probably do not use the signaling pathways which are usually required for cell growth (PI3K/Akt). It has been reported that axons mutant for *dinr* fail to reach their targets. In the larvae axons cross and terminate prematurely, causing gaps and densely packed regions in the lamina plexus; in the medulla axons failed to expand resulting in a blunt ended morphology. In the adult eye-brain complexes with small cell clones mutant for *dinr* the projections of most of the axons are normal, however, gaps in R7 layer and fibers crosses are visible in areas associated with the *dinr* mutant clones (Song et al., 2003).

The ligands of DInR, called insulin-like peptides, DILPs, are encoded by 7 *dilp* genes. Studies based on gene knock-outs have shown synergy and compensation of expression between different DILPs (Gronke et al., 2010). DILPs are secreted into the circulatory system (Rulifson et al., 2002). Therefore, the insulin signaling most probably does not provide a directional cue for axonal growth cones and the exact mechanism of insulin signaling in retinal axon targeting remains unclear.

The DInR got my attention mainly because of its tyrosine kinase activity which makes it a possible modulator of Gogo phosphorylation. Is there any physiological relation between *gogo* and *dinr*? Two complementary approaches were used to verify this interaction: molecular studies involving the *Drosophila* S2 cell line and a series of genetic experiments exploiting the available loss and gain of function mutants. Using fly genetics, I have shown an interaction between *gogo* and *dinr* at the temporal target layer. When overexpressed together with *gogo*, *dinr* is able to strongly enhance the adhesiveness of photoreceptors to the M1 layer, including occasional axon stopping. In combination with the M1 stopping phenotype evoked by GogoΔYYD/DDD forms and our cell culture data showing that DInR positively regulates Gogo phosphorylation, these results provide evidence that the strong interaction with the M1 layer indeed is caused by Gogo phosphorylation. Why GogoDDD causes a much stronger adhesiveness to the M1 layer than Gogo phosphorylated by overexpressed DInR? A possible explanation is that, in contrary to GogoDDD form, DInR-dependent phosphorylation in this case is not complete. Alternatively, there are redundant mechanisms which can further modulate Gogo phosphorylation. Therefore only a small fraction of photoreceptors stop at the M1 layer, and the majority of axons form blob-like structures. In parallel approaches I could show that not only activation of DInR, but also stimulation of the insulin signaling by applying the ligand (insulin) results in enhanced Gogo phosphorylation.

In the study from Song et al. who reported the role of *dinr* for axonal guidance for the first time no specific markers for R7 and R8 photoreceptors were used. Thus no conclusions have been made about the *dinr* function in R8 cells. Presented in this work results show that, at least in the adult visual system, loss of *dinr* (small mutant cell clones) does not affect R8 axons targeting, but only affects the cell morphology (mutant axons are thinner than in the wild type situation). The notion that axon growth can occur properly even if the growth of the soma is suppressed (*dinr*$^{-}$*)* is not new. In fact, cell growth strictly depends on protein synthesis, whereas axon extension probably not (Holt and Campbell, 2001). For instance photoreceptors mutant for *chico* (the major DInR substrate) are smaller but their axons connect to the correct targets (Hafen et al., 1999; Song et al., 2003). What does it say about the relation between DInR activity and Gogo phosphorylation? My experiments with the non-phosphorylable Gogo form (FFD) show that even if Gogo is dephosphorylated throughout the development the targeting still occurs properly. Therefore, loss of *dinr* should not alter the targeting.

Presented in this dissertation results raise the question about the specificity of the interaction between *gogo* and *dinr in vivo*. Enhancement of the YYD motif phosphorylation upon IIS stimulation and genetic interactions do not allow to conclude a direct (physical) interaction. To test this for instance co-immunoprecipitation experiments would be required. However, even if DInR does not bind to Gogo, it can be speculated that DInR stimulates a series of signaling events, that as a result activate a kinase which then directly phosphorylates Gogo.

However, one could argue that since no physical interaction DInR - Gogo was presented so far, in a physiological situation DInR does not affect Gogo phosphorylation at all. Several arguments speak against this argument. The fact that blob formation at the M1 layer can be achieved when *gogo* is overexpressed (Tomasi et al., 2008) means that the factor responsible for phosphorylation of Gogo (presumably IIS) is in a sufficient concentration and shows sufficient activity to phosphorylate Gogo at a level which is enough to form the gain of function phenotype. However, when the level of endogenous IIS is genetically reduced, it is sufficient to significantly suppress the *gogo* overexpression phenotype. Thus, it means the IIS is the limiting factor for Gogo phosphorylation. Additionally, GogoFFD mutants can efficiently suppress the genetic interaction with DInR indicating that this interaction is specific. Therefore, the IIS activating signal, coming presumably from DILPs, does not have to provide a directional cue. So it is possible that insulin signaling orchestrates the guidance signals coming from instructive directional cues.

In mammals two types of InR are found in the brain: a peripheral type (glial cells), and a brain specific types found on neurons (Marks et al., 1988). It is tempting to speculate that since mammalian InR is present in the brain in neurons and glia (however in much lower levels) (Adamo et al., 1989) the IIS signaling requires similar mechanisms as in *Drosophila*.

3.6 Gogo dephosphorylation as a permissive signal in axon guidance

The presented data suggest a mechanism of Gogo activity modulation involving phosphorylation of the YYD motif. However, the dephosphorylation but not phosphorylation is required for proper axon targeting. Does it mean that the phosphorylation has no function? Which reasons could explain the fact that phosphorylation of a protein residue has evolved without having an axonal guidance function? One can imagine at least three possible explanations.

1) Gogo phosphorylation has a function for more fine-tuning effects (for instance in synaptic site formation). Thus presented here experimental approaches, which focus only on the guidance aspect, were not sufficient to observe them.
2) Gogo is not only expressed in photoreceptors but also in other parts of the body, for instance in the embryonic dendrites, where it has an axon guidance function as well. Thus it might be, that Gogo phosphorylation was conserved during evolution, because it has a critical function in other systems in *Drosophila*. If these speculations are true, then obviously a mechanism should have evolved, which enables an efficient dephosphorylation of Gogo in the visual system and thus allows for the targeting. Therefore, dephosphorylation of Gogo becomes a *sine qua non* requirement for the R8 targeting.
3) *dinr* could have evolved much earlier than *gogo* and has played an important role in proliferation, cell size control, metabolism regulation etc. Later in the evolution, *gogo* have evolved and it became involved in axon pathfinding regulation. However, for this process Gogo dephosphorylation mechanism was essential.

The cues that a growing axon encounters can be divided into instructive or permissive ones. Instructive cues usually have a restricted expression pattern and guide the axon by providing either attractive or inhibitory information to the growth cone. On the contrary, permissive signals usually steer in response to instructive cues (Bonner and O'Connor, 2001) or are needed to detect and to respond to extracellular guidance cues (Dickson, 2001). Here, I propose that IIS could be involved in ensuring the correct wiring of the nervous system by influencing the phosphorylation of a known regulator of photoreceptor axon guidance receptor Gogo. Gogo phosphorylation provides a signal which enhances the adhesive interaction with the M1 layer, whereas dephosphorylation could provide a permissive signal which allows the axon to leave the M1 layer and to project to the M3 targeting layer.

To understand the significance of insulin for R8 photoreceptor guidance, it has to be taken into account that the state of phosphorylation of a protein at any moment, and thus its activity, depends on the relative activities of the protein kinases and phosphatases that modify it. In this context, it would be rewarding to identify a phosphatase that mediates Gogo dephosphorylation and thereby is an essential component of Gogo activity regulation mechanism. A special attention was paid to test a possible genetic interaction between *gogo* and *lar* / *ptp69A*, since both of these phosphatases were implicated in various aspects of axon guidance in *Drosophila* photoreceptors (experiments performed by Satoko Suzuki, data not shown). However they did not reveal any obvious genetic interaction so far.

3.7 Concluding remarks

In summary, here I present evidence that a conserved tripeptide motif YYD located in the cytoplasmic domain of an axon guidance receptor Gogo is essential for its function. The YYD motif is a tyrosine phosphorylation site *in vivo*, and its phosphorylation is stimulated by IIS. These results reopen the question how insulin can contribute to various aspects of connectivity formation in the nervous system (Mayer et al., 1990; Craft et al., 1996; Wickelgren, 1998; Wang et al., 2000).

The proposed mechanism includes Gogo phosphorylation and presumptive dephosphorylation by a yet unknown phosphatase. The *dinr* can be considered as a possible positive regulator of Gogo phosphorylation. It provides an insight in how the developmental timing can be coordinated in the neuronal circuit wiring through phosphorylation-dephosphorylation mechanism.

Results included in this dissertation may serve as an inspiration for the future work since they allow to formulate several interesting questions. For instance the exact time course of Gogo phosphorylation status should be tested. Regarding the interaction with DInR one could perform a series of *in vitro* assays to further verify the specificity of this interaction. Finally, to further confirm the proposed in this Dissertation model the dephosphorylation mechanism should be elucidated.

4. Materials and Methods

4.1 Materials

4.1.1 Chemicals

All chemical used in this study were analytical grade.

Table 4-1: Chemicals

Chemical	Source
Acetic acid	Fluka
Agar-Agar	Roth
Agarose, high electroendosmosis	Biomol
Agarose NEEO Ultra – Qualität	Roth
Ampicillin	Sigma Aldrich
β-mercaptoethanol	Roth
Bacto-tryptone	Roth
Bromphenol blue	Merck
Dimethyl sulfoxide (DMSO)	Sigma
Ethanol absolute	Sigma Aldrich
EDTA	Sigma Aldrich
Fetal bovine serum	PromoCell GmbH
Formaldehyde (35%)	Roth
Glycerol	Merck
Heptane	Fluka

Hydrochloric acid (HCl)	Merck
Kanamycin	Sigma Aldrich
Isopropanol (2-propanol)	Sigma Aldrich
L-Glutamine 200mM	PAA Laboratories GmbH
Methanol	Sigma Aldrich
Milk powder	Roth
Nonided P-40 Substitute (NP-40)	Fluka
Phenolchloroform	Amresco
Recombinant human insulin	Invitrogen
Sodium chloride	Sigma
Sodium lauryl sulfate (SDS)	Roth
Sodium orthovanadate	Aldrich
Tris(hydroxymethyl)-aminomethane	Merck
Tris base	Sigma
Triton X-100	Roth
Tryptone	Sigma
Tween 20 (Polyoxyethylene 20) sorbitan monolaurate)	Sigma
Yeast extract	Sigma Aldrich

4.1.2 Buffers and solutions

Blocking solution: 5% (w/v) BSA in TBST (used for the anti-Phosphotyrosine antibody) or 5% (w/v) milk powder in PBS (used for all other antibodies)

2x Laemmli buffer: 100 mM Tris pH 6.8, 40 g/l SDS, 20% glycerol, 0.25 g/l bromphenol blue 200 mM β-mercaptoethanol

LB (Luria-Bertani)-Medium: 10 g/l bacto-tryptone, 5 g/l yeast extract, 5 g/l NaCl, pH 7.5. Medium was sterilized by autoclaving. If necessary, antibiotics were added after sterilizing (75 µg/ml ampicillin, 50 µg/ml kanamycin). For bacterial plates, 1.5% agar was added to the medium before autoclaving

Lysis buffer: 1% NP-40, 150 mM NaCl, 50 mM Tris, pH 7.5

PBT (0.1%): 0.1% (v/v) Triton X-100 in PBS
PBS-Tween (0.1%): 0.1% (v/v) Tween 20 in PBS

Phosphate buffered saline (PBS): 0.2g KCl, 0.2g KH_2PO_4, 1.15g Na_2HPO_4 and 8g NaCl in 1 l H_2O at pH 7.4

Solution A: 0.1M Tris HCl pH9.0, 0.1M EDTA pH 8.0, 1% SDS in water

TAE (50x): 484 g Tris base, 50 mM EDTA pH 8.0, 114.2 ml glacial acetic acid in 2 l water, pH 8.5 adjusted with glacial acetic acid.

TE: 10 mM Tris base pH 7.5, 50 mM EDTA pH 8.0 in water.

TBS: 24.23 g/l Tris base HCl, 80.06 g/l NaCl, pH 7.6

TBST: 0.1% (v/v) Tween 20 in TBS

4.1.3 Fly maintenance

Standard *Drosophila* medium:
For 50 l medium, 585 g agar was dissolved in 30 l of water by heating the mixture to the boiling point; meanwhile 5 kg corn flour, 925 g yeast, 500 soy flour, 4 kg molasses were mixed with water to obtain a homogeneous broth and as soon as the agar was dissolved they were mixed with agar. The mélange was filled up with water to 50 l and cooked at 96°C for 1,5 h. 315 ml propionic acid, 120 g methylparaben, 125 g niparsin/methylparaben, 1 l of 20% ethanol and 500 ml of 10% phosphatidic acid were added after the mixture had cooled down to 60°C.

Blue yeast paste:
Instant dry yeast (Femipan Inc.) was mixed with Instant blue *Drosophila* medium (Fisher Scientific) and water.

Apple-juice agar plates (for embryo collection)**:**

700 ml apple juice, 20 g agar in 1 l water

4.1.4 Equipment

Table 4-2: Equipment

Device	Model	Supplier
Fly maintenance		
Incubators	Unichromat 1500	Uniequip.
	Pervival	Percival
Drosophila transgenesis		
Pump for injection	Eppendorf FemtoJet micromanipulator	Eppendorf
Microscope	Axiovert S100	Zeiss
Micropipette puller	Flaming/Brown Micropipette puller, P-97	Sutter Instrument Co.
	Micro Grinder EG-400	Narshige
Cell culture		
Incubator (w/o CO_2)	FTC 90i	Uniequip.
Dissection stereomicroscope	Leica MS5, MZ95	Leica
Forceps		
Laminar air flow hoods	Hera Safe	Heraeus
Cell culture flasks	BD Falcon, 250 ml Polystyrene	BD Biosciences
Cell culture wells	6 well Cell Culture Cluster	Corning Inc.
Confocal microscope	Olympus FV1000	Olympus
Immunoblotting		
SDS runnung	XCell SureLock Electrophoresis Cell, Novex Mini Cell	Invitrogen
Imaging camera	Fusion FX7 camera	PeqLab
Imaging software	Fusion 15.12	PeqLab
Molecular biology		
Spectrophotometer	NanoDrop 1000	PeqLab
Thermocycler	Peltier Thermal Cycler	MJ Research

4.1.5 Consumables and other reagents

Table 4-3: Consumables and other reagents

Device	Model	Supplier
Microscopy and immunohistochemistry		
Cover glasses for microscopy	18x18 mm, 24x24 mm	Marienfeld
Microscope slides	76x26 mm, with frost end	Menzel-Gläser
Mounting medium	Vectashield Mounting Medium for Fluorescence, H-1000	Vector Laboratories Inc.
Biochemistry		
Gels	Tris-acetate gels (7%, 3-7%)	Invitrogen
Albumine, from bovine serum		Sigma
Transfer Buffer	NuPAGE Transfer Buffer (20x)	Invitrogen
SDS Running Buffer	NuPAGE MOPS SDS Running Buffer (20x)	Invitrogen
Nitrocellulose membrane	Hybond ECL Nitrocellulose membrane	Amersham
ECL solution		GE Healthcare
Protein marker	Prestained Protein MolecularWeight	Fermentas
Gateway clonase	Gateway LR Clonase Enzyme Mix	Invitrogen
Anti-myc agarose beads	EZview Red Anti-c-Myc Affinity Gel	Sigma
Cellfectin		Invitrogen
FuGENE transfection	FuGENE HD Transfection Reagent	Roche
Protease inhibitors	Complete mini protease cocktail	Roche
Molecular biology		
DNA polymerases	iProof High Fidelity DNA Polymerase	BioRad
	KOD DNA Polymerase	Novagen
Escherichia coli strains	DH5α, DB3.1	Invitrogen
Blades	Sterile Surgical Blade, no.19	Bayha
DNA loading buffer	6 x loading buffer	Fermentas
DNA marker	GeneRuler 1kb DNA Ladder	Fermentas
DNA isolation	QIAprep Spin Mini prep Kit, QIAGEN Plasmid Midi Kit, QIAGEN Plasmid Maxi Kit, QIAfilter Maxi Cartridges, QIAquick Gel Extraction Kit	Qiagen

Cell culture		
Schneider's media		PromoCell GmbH
Penicillin/Streptomycin	Penicillin/Streptomycin 100x	PAA Laboratories GmbH
Poly-L-lysine slides	µ-slide IV 0.4	IBIDI
Fly work, embryo injection		
Whatman Membrane Filters (embryo collection)	ME26/31, 0.6 µm, ø 50 mm	Whatman
Chloroxbleach	DanKlorix	DanKlorix
Borosilicate glass capillaries	GC 120TF-10	Harvard Apparatus Ltd
Silica gel	Silica Gel Orange 1-3 mm	Roth
Halocarbon oil	Voltalef 10S	Arkenia France
Scotch	Tesa Doppelband Fotostrip	Tesa
Apple juice		Albi GmbH & Co KG
Yeast		Femipan Inc
Blue fly food	Instant blue *Drosophila* Medium	Fisher Scientific

4.1.6 Antibodies

Primary antibodies for immunofluorescence (IF) and for western blotting (WB).

Table 4-4: Primary antibodies

Antigen	Host	Dilution	Supplier
anti-myc (4E10)	mouse	IF: 1:100 WB: 1:100	Santa Cruz
anti-Phosphotyrosine (4G10)	mouse	WB: 1:2000	Millipore
anti-GFP Alexa Fluor488-conjugated	rabbit	IF: 1:300	Invitrogen
anti-GFP (JL-8)	mouse	WB: 1:2000	Clontech
anti-24B10	mouse	IF: 1:50	DSHB
anti-*D*NCadherin (Ex#8)	rat	IF: 1:50	DSHB
anti-Gogo	rabbit	IF: 1:50	from T. Suzuki
anti-phospho-Gogo (Ab2795-D01)	rabbit	WB: 1:250	this study
anti-mCD8	rat	IF: 1:100	Invitrogen

The anti-Gogo antiserum was purified with the Melon Gel IgG Purification Kit (Pierce) and subsequently preabsorbed with *Drosophila* embryo in a 1:1 v/v ratio overnight at 4°C in order to reduce the binding of the antibody to unspecific antigens.

The rabbit polyclonal antibody Ab2795-D01 was generated by Peptide Institute Inc., Japan. The antigen peptides: ELEMDpYpYDYNVI, ELEMDpYYDYNVI, ELEMDYpYDYNVI were synthetized. A mixture of them was injected into rabbit. The serum was affinity purified on a custom made affinity column with the immobilized ELEMDYYDYNVI peptide (non-phosphorylated). Before use the antibody was preabsorbed in 1:1 v/v fixed *Drosophila* embryo overnight at 4°C in order to reduce the binding to unspecific antigens. Ab2795-D01 was used at 1:250 dilution for western blotting of immunoprecipitated Gogo.

Secondary antibodies for immunofluorescence and for western blotting.

Table 4-5: Secondary antibodies

Antigen	Host	Conjugate
mouse IgG	sheep	HRP (NA931V)
	goat	Alexa Fluor 488
	goat	Alexa Fluor 568
	goat	Alexa Fluor 633
rabbit IgG	goat	Peroxidase Conjugated Affinity Purified (H&L)
	goat	Alexa Fluor 488
	goat	Alexa Fluor 568
	goat	Alexa Fluor 633
rat IgG	goat	Alexa Fluor 633

All secondary antibodies for immunofluorescence were purchased from Invitrogen and diluted 1:300 in 0.1% PBT. Horseradish Peroxidase (HRP)-conjugated antibodies for western blotting were purchased from GE Healthcare and diluted 1:2000 (mouse). Anti-rabbit Peroxidase Conjugated Affinity Purified (H&L) from was used at for western blotting at 1:1000 dilution.

4.1.7 Fly stocks

Table 4-6: Fly stocks

Genotype	Source
w^{1118}	Bloomington Stock Center
w^{1118}/Y*hshid*	Takashi Suzuki
yw ; Pin/CyO, *y*+	Barry Dickson
w^{1118}/Y*hshid* ; Pin/CyO, *y*+	Takashi Suzuki
yw ; MKRS/TM6B, *y*+	Barry Dickson
y w^{1118}/Y*hshid*; Ly/TM6B, *y*+	Takashi Suzuki
w; Sco/CyO; MKRS/TM6B	Bloomington Stock Center
*yw ey*FLP2 c-*LacZ*; Sp/CyO, *y*+; MKRS/TM6B, *y*+	Takashi Suzuki
yw eyFLP2 c-*LacZ*; 3L *cl* FRT80B/TM6B, *y*+	Takashi Suzuki
w; *Rh6-GFP-myc*/TM3	Takashi Suzuki
*Rh6-GFP-myc ey*3.5 FLP; Pin/CyO	Satoko Suzuki
yw; *GMR-Gal4*	Barry Dickson
*ey*FLP2 glass-*LacZ Rh6-GFP*	Barry Dickson
yw; FRT82B	Takashi Suzuki
*yw ey*FLP2*; gogo[H1675]* FRT80/TM6B, *y*+	Takashi Suzuki
*ey*FLP2; *atonal-tau-myc*, *gogo[H869]* FRT80/TM6B, *y*+	Takashi Suzuki
w ; *UAS-gogo* T1	Barry Dickson
GMR-Gal4 UAS-gogo/ CyO	Tatiana Tomasi
GMR-mCD8-KO (SS39)	Satoko Suzuki
*yw ey*FLP2; FRT82B *GMR-mCD8-KO*/TM6	this study
yw; P{*UAS-InR.K1409A*}2	Bloomington Stock Center
yw; P{*UAS-InR.A1325D*}2	Bloomington Stock Center
FRT82B $dinr^{ex15}$/TM5	Leslie Pick
yw, $dilp6^{68}$; $dilp1\text{-}4^{1}$, 5^{4}/TM3 *Sb*	Linda Partridge
y v P{*nos-phiC31\int.NLS*}X; P{*CaryP*}attP40	Bloomington Stock Center
w; GMR-gogoC1-myc T1	Si-Hong Luu
w; GMR-gogoC2-myc T2a	Si-Hong Luu
w; GMR-gogoC3-myc T3b	Si-Hong Luu
w; GMR-gogoC1C2-myc T2	Si-Hong Luu
w; GMR-gogoC2C3-myc T2	Si-Hong Luu
w; GMR-gogoC1C3-myc T1	Si-Hong Luu

w; GMR-gogoC1C3-myc T2	Si-Hong Luu
w; *GMR-gogoFL*-P40 (116-21)	this study
w; *GMR-gogoΔYYD*-P40 (123-1)	this study
w; GMR-gogoFFD T4a	Si-Hong Luu
w; *GMR-gogoFYD*-P40 (126-14)	this study
w; *GMR-gogoYFD*-P40	this study
w; *GMR-gogoDDD*-P40 (117-1)	this study
w; *GMR-gogoYDD*-P40 (119-6, 119-8)	this study
w; *GMR-gogoDYD*-P40 (118-21)	this study
w; *GMR-gogoC2*$^{\text{short FFD}}$ -P40 (121-17)	this study
w; UAST-gogoFL-P40	this study (M. W.)
w; *UAST-gogoΔYYD*-P40	this study (M. W.)
w; *UAST-gogoFFD*-P40	this study (M. W.)
w; UAST-gogoFFD	Si-Hong Luu
w; *UAST-gogoFYD*-P40	this study (M. W.)
w; *UAST-gogoYFD*-P40	this study (M. W.)
w; *UAST-gogoDDD*-P40	this study (M. W.)
w; *UAST-gogoDYD*-P40	this study (M. W.)
w; *UAST-gogoYDD*-P40	this study (M. W.)
w; UAST-fmi-P40	this study (M. W.)

Note that for simplicity the following abbreviations were used in the table: *Rh6-GFP* (for *Rh6-mCD8-4xGFP-3xmyc*), *cl* (for *M(3)i[55])*.

4.1.8 Plasmids

Table 4-7: Plasmids

Description / name	No	Source
pActin-Gal4		Jürgen Knoblich
pMB6-1		Satoko Suzuki
pENTR-inr		Ernst Hafen
pUAST-KSWBgfpX		Stephan Ohler
pΔ23		Barry Dickson
pUAST-dinr-GFP		this study

pUASTattB		Konrad Basler
pUAST-gogo-myc	pSO045	Stephan Ohler
GMR-gogoΔYYD-myc	pSL008	Si-Hong Luu
GMR-gogoFFD-myc	pSL009	Si-Hong Luu
GMR-gogoDDD-myc	pSL010	Si-Hong Luu
UAST-gogoFFD-myc	pSO202	Stephan Ohler
UAST-gogoDDD-myc	pSO203	Stephan Ohler
UAST-gogoFL-attB	pGW54	this study (M. W.)
UAST-gogoΔYYD-attB	pGW34	this study (M. W.)
UAST-gogoFFD-attB	pGW32	this study (M. W.)
UAST-gogoFYD-attB	pGW36	this study (M. W.)
UAST-gogoYFD-attB	pGW37	this study (M. W.)
UAST-gogoDDD-attB	pGW33	this study (M. W.)
UAST-gogoDYD-attB	pGW35	this study (M. W.)
UAST-gogoYDD-attB	pGW45	this study (M. W.)
UAST-fmi-attB	pGW50	this study (M. W.)
UAST-gogoFL-^{9F}*-myc*	pKM84	this study
UAST-gogoC2^{shortFFD}*-myc-attB*	pKM110	this study
UAST-gogoC2$^{\text{short FFD-C}}$*-myc-attB*	pKM112	this study
UAST-gogoC2$^{\text{short FFD-N}}$ *-myc-attB*	pKM115	this study
UAST-gogoC2$^{\text{short YFD}}$*-myc-attB*	pKM140	this study
UAST-gogoC2$^{\text{short FYD}}$*-myc-attB*	pKM141	this study
UAST-gogoC2$^{\text{short FYD}}$*-myc-attB*	pKM140	this study
UAST-gogoC2$^{\text{short YFD}}$*-myc-attB*	pKM141	this study
GMR-gogoFL-attB	pKM116	this study
GMR-gogoΔYYD-attB	pKM123	this study
GMR-gogoFFD-attB	pKM124	this study
GMR-gogoFYD-attB	pKM126	this study
GMR-gogoYFD-attB	pKM125	this study
GMR-gogoDDD-attB	pKM117	this study
GMR-gogoDYD-attB	pKM118	this study
GMR-gogoYDD-attB	pKM119	this study
GMR-gogoC2$^{\text{short FFD}}$ *-myc-attB*	pKM121	this study
GMR-gogoC2 $^{\text{short FFD-C}}$*-myc-attB*	pKM127	this study
GMR-gogoC2 $^{\text{short FFD-N}}$ *-myc-attB*	pKM128	this study

4.1.9 Oligonucleotides

Table 4-8: Oligonucleotides

Name	Sequence	Purpose
KM3	GCGCGGTACCAATGGTTGCTTTTCACCAGCTGC	KpnI + C2:Y1F fwd
KM4	CCGATCCTGCATTGATCACATTGAAATCGAAGAAATCCATTTCAAGTTCTTCTTGATTTCC	C2:Y5 Y2.3.4F rev
KM4b	GCGCGGATCCATTCCAAGAAAGGAGCCCGGTGCCGATCCTGCATTGATCACATT	BamHI +C2:Y2.3.4F rev
KM5	GGAATGGATCCGGCTTTCCTTATCTGGATA	C2:Y2.3.4F fwd
KM6	CTTGGGCATCCGGATCTCCTCGAACAGCGGCTGCCGTTC	C2:Y7F rev
KM7	GGAGATCCGGATGCCCAAGTTCGGACACTTCCTAAGTCCAGCCAGTAACACGG	C2:Y8.9F fwd
KM8	GCGCTCTAGACACGGCCACTTCCTTTGACT	XbaI + C2:Y9 rev
KM11	GATCACATTGTAATCGAAGTAATCCATTTCAAGTTC	YYD->YFD rev
KM12	GAACTTGAAATGGATTACTTCGATTACAATGTGATC	YYD->YFD fwd
KM13	GATCACATTGTAATCGTCGTAATCCATTTCAAGTTC	YYD->YFD rev
KM14	GAACTTGAAATGGATTACGACGATTACAATGTGATC	YYD->YFD fwd
KM15	GATCACATTGTAATCGTAGAAATCCATTTCAAGTTC	YYD->FYD rev
KM16	GAACTTGAAATGGATTTCTACGATTACAATGTGATC	YYD->FYD fwd
KM17	GATCACATTGTAATCGTAGTCATCCATTTCAAGTTC	YYD->DYD rev
KM18	GAACTTGAAATGGATGACTACGATTACAATGTGATC	YYD->DYD fwd
KM28B	CCAATATGTGGTGCGATATCGGAAGTATCGCCTGAGAACCCGTAGTGTC	C2:Y1 fwd
KM29	GCGCTCTAGATTACGCCACCTCTTCGAATGGTG	C2:Y6 + stop rev
KM30B	CCAATATGTGGTGCGATATCGGAAGTATAGGACGACCAGTAATC	C2:YYD fwd
KM31	GCGCTCTAGATTACGGATCCATTCCAAGATAGGAGC	C2:Y5 + stop rev
KM32B	GACACTACGGGTTCTCAGGCGATACTTCCGATATCGCACCACATATTGG	C2:Y1 rev
KM33B	CCTTGGGATTACTGGTCGTCCTATACTTCCGATATCGCACCACATATTGG	TM + overlaps with KM30B rev
KM34	GCGCTCTAGATTATGTGTTGTCAGCCGTTGTGGACTTG	C2:Y9 + stop rev

KM35	GCGCAGATCTCGCCACCTCTTCGAATGGTG	C2:Y6 read through BglII rev
TS83	GCGCGGTACCATGCGGAAAAACTCAAAGGAAATG	KpnI + *gogo* 5’ fwd
TS84	GCGCAGATCTCACGGCCACTTCCTTTGACTTCGG	BglII + *gogo* 3’ read through rev
GW001	GCGCGGTACCCAAAATGCGGAAAAACTCAAAGGAAATG	KpnI + kozak + 5'gogo fwd
GW002	GCGCTCTAGATTACACGGCCACTTCCTTTGACTTC	XbaI + stop + 3'*gogo* rev
pCARYP_1	CTCGAGGGGATCCCCCTAGTACTGACGGA	verification of P40 flies
UAS_attB1	GGAAGAGCGCCCAATACGCAAACCGCCTCT	verification of P40 flies

For simplicity in the primer description tyrosines in the C2 section were numbered from Y1-Y9.

4.2 Methods

4.2.1 Molecular cloning

DNA gel electrophoresis

The DNA was mixed with the appropriate amount of 6 x DNA loading buffer and was separated on 1% agarose gels. The agarose was diluted in TAE buffer. A drop of ethidium bromide was added to the melted agarose before pouring. 1 x TAE was used as running buffer.

Polymerase chain reaction (PCR)

The iProof polymerase mix and the KOD Polymerase were used according to the manuals provided by the companies. iProof and KOD were always used in a 50 µl final volume reaction mix.

DNA restriction digestion and ligation

1-5 µg of plasmid DNA was digested always in a final volume of 20 or 50 µl of reaction mix supplied with the appropriate amount of 10 x Buffer and BSA provided with the restriction enzyme. The DNA was digested for 1-2 hours at 37°C. If the DNA had to be dephosphorylated 2-3 µl of CIP was used in the digestion mixture for 1 h at 37°C. The digested DNA was separated by DNA gel electrophoresis. If the DNA was subsequently used for ligation the bands of interest were cut from the gel using a sterile blade and purified using Qiagen Gel Extraction Kit as described in the manual provided by the company.

The ligation was performed for at least 2 h (up to overnight) at 18°C in 10 or 15 µl total volume of the ligation mix. 0.5 µl of T4 DNA ligase and the total amount of vector and insert DNA varying from 200-400 ng was used (the vector to insert molar ratio was varying from 1:3 to 1:6). All reagents were purchased form New Englad BioLabs unless stated otherwise.

Gateway cloning

The entry vectors were recombined with the destination vector, leading to generation of the expression clone. For the reaction 200 ng of each plasmid DNA was used, 2 µl of the LR Clonase Enzyme Mix supplied up with TE buffer up to 10 µl final volume.

Cloning strategies

The Gogo tyrosine mutations in the YYD motif (FYD, YFD, DYD, YDD, 9F) were generated by a overlap-PCR based approach. The primers inserting the mutations were: KM3-8 for 9F and KM11-18 for FYD, YFD, DYD, YDD. In each case the *gogo* amplifying primers from 5’ and 3’ site were TS83 and TS84. The final PCR product was digested with KpnI and BglII and cloned into *pMB6-1* vector (pBluescript SK+ with 4 x myc tag 3’ to the BglII site).

For *gogo* constructs which were not tagged at the C-terminus *gogo* in the *pMB6-1* plasmid was amplified by PCR using GW001 and GW002 primers and cloned with KpnI/XbaI into appropriate *UAST* or *GMR* vectors. For all myc-tagged constructs *gogo* sequence with 4 x myc from the *pMB6-1* vector was cloned with KpnI/XbaI into *UAST* or *GMR* vectors. For double digestions in KpnI and XbaI sites a KpnI isoschizomer Asp718 (Roche) with the provided BufferB in combination with XbaI was used.

For Gogo C2 section deletions the appropriate fragments of the C2 section were amplified by PCR. The template used for PCR was *GMR-gogoFFD*-attB. PCR-amplified *gogo* was cloned into *pMB6-1* to put the myc-tag and subsequently to the *UAST* or *GMR* vector.

For generation of $pUAST\text{-}gogoC2^{shortFYD}\text{-}myc$ and $pUAST\text{-}gogoC2^{shortYFD}\text{-}myc$ constructs pKM125 and pKM126 respectively were used as templates.

The *UAST-dinr-GFP* construct was generated as a product of a LR reaction (Gateway) between *pENTR-inr* and *pUAST-KSWBgfpX*.

4.2.2 Transformation and plasmid preparation

After the DH5α and DB3.1 cells were thaw from a -80°C stock on ice, the bacteria were incubated with 100-300 ng of DNA on ice for 5-15 min. The cells were heat-shocked at 42°C for 90 sec and immediately returned on ice for 1 min. 1 ml of LB media was added and the cells were recovered for 50 min at 37°C with 300 rpm shaking. After recovery cells were centrifuged for 3 min at 3000 rpm and resuspended in 100 μl of LB media. Afterwards, they were plated on LB plates containing selective antibiotics and incubated overnight at 37°C.

Single colonies were picked up from the Petri dish and grown in LB medium containing the proper antibiotic. The plasmids were purified using the Qiagen Kits as described in the manual provided by the company.

4.2.3 Cell culture and transfection

The Schneider's line 2 (S2) cells were maintained in a 25°C incubator without CO_2, in Schneider's medium supplemented with 10% heat-inactivated FBS, 2 mM L-glutamine, 100 units/ml penicillin, and 100 μg/ml streptomycin. Cells were passaged every 3-4 days at a 1:2,5 dilution.

For transient transfection, cells were seeded at about 10^6 cells/ml in 6-well plates (2 ml per well). After 16 h, cells were transfected with Cellfectin according to the manufacturer instructions. Per well, 2-4 μg of plasmid and 10 μl of Cellfectine were used. The DNA and Cellfectin were separately diluted in 100 μl of serum free medium (without antibiotics), mixed together, and incubated at room temperature for 30 min. Cells were washed with serum-free medium, 0.8 ml of serum free medium was added to each well, and the transfection mix was added dropwise. After 5-6 h incubation, the transfection mix was removed and cells were grown in complete medium (2 ml/well) for 48 h.

Alternatively, FuGENE HD Transfection Reagent was used for transfection: 10 µl of FuGENE reagent was added to 2-4 µg of plasmid DNA diluted in 90 µl of sterile water, mixed and incubated at room temperature for 15 min. The transfection mix was added dropwise to cells (in this case cells were not washed before and the media contained serum and antibiotics).

If the phosphorylation of a protein was subsequently detected, prior to cell lysis, sodium orthovanadate (a general phosphatase inhibitor) was added to the cell culture for 3 h (final concentration 2 mM).

For insulin treatment human recombinant insulin was added to the media 20 h prior to the cell lysis.

4.2.4 Cell aggregation assay and immunocytochemical staining

48 hr after transfection cells were diluted in cell culture medium 1:6 (total volume: 2 ml) and shaken for 2 hr on a rotary shaker. To concentrate the samples, cells were centrifuged at 1000 g for 30 sek, resuspended in 100 µl of medium and seeded on slides coated with poly-L-lysine (µ-slide IV 0.4, IBIDI) for 2 hr. For immunocytochemistry the medium was removed and cells were fixed for 30 min with 4% paraformaldehyde in PBS, washed twice with PBS, permeabilized with 0.1% Triton X-100 for 3 min and finally washed twice with PBS. The primary antibody was applied for 2 hr and subsequently cells were washed three times with PBS. Secondary antibody was applied for 1.5 hr.

4.2.5 Co-immunoprecipitation

48 h after transfection, cells were washed twice in PBS, and lysed with a dounce homogenizer in lysis buffer containing protease inhibitors. After centrifugation at 13,000 g for 15 min the supernatant was incubated with anti-myc agarose beads (typically 20 µl of beads/one well of transfected cells) for 2-3 hr at 4°C. The beads were washed with 500 µl of ice-cold lysis buffer, then once with 500 µl of 50 % v/v lysis buffer in PBS, and once with 500 µl of PBS. Next beads were incubated with Leammli

loading buffer at 65°C for 30 min. The beads were removed by centrifugation before loading on a Tris-acetate gel. For co-immunoprecipitation in larvae, about 65 mg of proteins were used (corresponding to approximately 40 dissected brains) and 25 µl of anti-myc agarose beads.

Additionally 2 mM orthovanadate was added to all solutions used for the immunoprecipitation (PBS, lysis buffer).

4.2.6 Immunoblotting

Protein samples were heated up to 65°C and subsequently centrifuged for 3min at 3000 rpm. The protein samples were separated by SDS-PAGE on a 7% or 3-7% Tris-acetate gel. The separated protein was blotted to a Hybond ECL Nitrocellulose membrane overnight at 4°C (90 mA/gel). Membranes were washed briefly with water and incubated with blocking solution for 1,5 h. Primary antibody was applied in blocking solution for 2 h at room temperature while rocking in a wet chamber on a shaker. The membrane was washed 3 x 10 min with PBS (depending on the antibody used). Secondary antibody was applied in PBS for 1-2 h at RT on a shaker. The membrane was washed 3 x 10 min with PBS and 1 x 10 min in 0.1% PBS-Tween 20. The membrane was incubated in 10ml of ECL solution for 1 min and exposed to Hyperfilm ECL or imaged with the Fusion FX7 imaging system. If the anti-phosphotyrosine antibody (4G10) was applied, TBST instead of PBS was used.

Anti-phosphotyrosine blots were quantified using ImageJ 1.44p. For the quantification of the phospho-band intensity the slight differences in loading between lines (quantified from the myc-control) were taken into account.

4.2.7 Fly maintenance

Flies were cultured in vials, or in bottles for expansion, with about 2 cm fly food covering the bottom part. For crosses and weak stocks the blue yeast paste was added. Vials/bottles were stored in incubators with controlled temperature and humidity (60-70%). Fly stocks were kept at 18°C and flies kept for expansion or fly crosses at 25°C unless otherwise stated. Flies were analyzed and collected using stereomicroscopes after anesthetization with CO_2.

4.2.8 *Drosophila* genetics

Reporter / Gene expression in photoreceptors

***ey*FLP**

Different *ey* (*eyeless*) enhancer fragments were used: *ey*FLP2 and *ey*3.5FLP.

***ey*FLP2:** *ey*FLP is a 258 bp eye-specific enhancer fragment from the *ey* gene upstream of the FLP cDNA (Newsome et al., 2000). *ey*FLP2 represents the transgene which is inserted on the X chromosome in a *yw* background. The *ey* enhancer fragment used in this *ey*FLP construct does not recapitulate the entire expression pattern of the *ey* gene, but is almost exclusively expressed in the visual system (Hauck et al., 1999). Expression begins in the 6-23 cell eye disc primordium in stage 15 embryos and is maintained until the final cell divisions in the approximately 15000-cell disc of the late third instar larvae. A lower level of expression can also be detected in the optic lobes, resulting in the generation of small mutant brain clones in mosaic animals. Mutant clone size induced with *ey*FLP2 in the retina without cell lethal mutation ranges from 20-30% (Newsome et al., 2000).

***ey*3.5FLP:** *ey*3.5FLP is a 3.5 kb eye-specific enhancer fragment from the *ey* gene cloned from eytTA vector (Bazigou et al., 2007). This clean *ey* enhancer does not show any brain expression.

***gmr* (*glass multiple reporter*)**

gmr enhancer is composed of five copies of a *Glass response element* from the *Rh1* gene and drives expression in all cells behind the morphogenetic furrow (Freeman, 1996, Hay et al., 1994).

rh4-mCD8-GFP-myc

rh4 (*rhodopsin4*) enhancer fragment which is specifically expressed in 70% of adult R7 (Fortini and Rubin, 1990; Newsome et al., 2000) was subcloned upstream of *mCD8GFPmyc* (Georg Dietzl, unpublished)

rh6-mCD8-GFP-myc

rh6 (*rhodopsin6*) enhancer fragment which is specifically expressed in 70% of adult R8 (Papatsenko et al., 2001) was subcloned upstream of *mCD8GFPmyc* (Georg Dietzl, unpublished).

atonal-tau-myc

atonal is strongly expressed in R8 cells after its formation (Jarman et al., 1994). A 2 kb R8-photoreceptor specific enhancer fragment derived from the *atonal* locus was used for the *atonal-tau-myc* reporter (Senti et al., 2003)

FLP/FRT system

Different *ey* enhancer fragments were used to induce mitotic recombination upon Flipase expression. In addition, mutant clone size was increased by inserting the *Minute* mutation M(3)i[55] (RpS17) onto the left arm of the 3rd chromosome in *trans* to the *gogo* mutant alleles. *Minute* mutations prevent the proliferation or survival of homozygous cells, and retard the proliferation of heterozygous cells (Morata and Ripoll, 1975). Using a cell lethal mutation with *ey*FLP2, almost the entire retina (90%) is homozygous mutant (Newsome et al., 2000).

Gal4/UAS system

Genes were overexpressed using the Gal4/UAS system (Brand and Perrimon, 1993) which allows for spatio-temporal control of gene expression. Gal4 is the yeast transcription activator protein and it can bind to the *UAS* (*Upstream Activation Sequence*) promoter and thereby activate gene transcription. *GMR-Gal4* was used a driver line to drive the expression of *UAS* constructs specifically in the photoreceptors.

4.2.9 *Drosophila* transgenesis

In order to transform the germline cells the DNA was microinjected into the syncytial blastoderm of *Drosophila* embryo at posterior side of the embryo before pole cell formation. These cells will later form the germline of the fly. In this way, “new” DNA can be internalized by P-element insertion during cell formation and is integrated into the genome of the pole cells. The injected plasmid contained a P-element with a promoter and the cDNA encoding the gene of interest with a marker gene *w+* (*white*) to identify transgenic flies, everything flanked by the inverted repeats.

P-element transformation

Involved the injection of the transposon-based construct with the w^{+} marker to w^{1118} host line. The construct encoding the gene of interest was mixed with a helper plasmid, *pΔ23*, encoding the integrase gene which enables the incorporation of the DNA into the genome of *Drosophila* (10 µg construct DNA + 1 µg *pΔ23* DNA in 15 µl water). Since the flies developing from the injected embryos do not show visible signs for successful germline transformation every hatched fly was crossed do w^{-} fly and the F1 generation was screened for the presence of the w^{+} marker (orange eye color). Transgenic flies were balanced and kept as a stock.

PhiC31 integrase-mediated transgenesis system

PhiC31 integrase-mediated transgenesis system is based on the site-specific bacteriophage PhiC31 integrase which mediates sequence-directed, irreversible integration between a bacterial attachment site (*attB*) and a phage attachment site (*attP*). The attB constructs were injected into a PhiC31-containing attP docking site embryos ($y^{1}w^{67c23}$; P{CaryP}attP40) (Markstein et al., 2008). The constructs are incorporated in the estimated CytoSite 25C7. The attB plasmid in this case was not co-injected with a helper plasmid since the injected embryos contain a transgene encoding for the PhiC31 integrase on the X chromosome (visible with the w^{+} marker). Since the flies developing from the injected embryos do not show visible signs for successful germline transformation every hatched male was crossed to w^{-} female and the F1 generation was screened for the presence of the w^{+} marker, but only in males (orange eye color), since F1 females have the w^{+} transgene encoded by the PhiC31 integrase gene on the X chromosome, which masks the w^{+} gene in the injected plasmid. Transgenic flies were balanced and kept as a stock.

For the confirmation of insertion the genomic DNA from transgenic flies was isolated and a PCR reaction was performed using the primers pCARYP_1 and UASattB1 (for both *GMR* and *UAS* constructs). For the PCR iProof polymerase was used with the following PCR program: 1) 98°C 2 min, 2) 98°C 15 sec, 3) 65°C 1 min, 4) 72°C 30 sec, 5) step2 for 35 more cycles, 6) 72°C 10 min, 7) 4°C forever.

Microinjection

For injection the extracted Midi/Maxiprep DNA (with or without addition of the helper plasmid DNA), diluted in water, was used at a concentration about 1 µg/µl. Borosilicate glass capillaries were pulled on a Suttner P-97 micropipette puller and opened on a Narishige EG-400 micropipette grinder. An Eppendorf FemtoJet with a micromanipulator mounted on a Zeiss Axiovert S100 Inverted Microscope was used for microinjections. *Drosophila* embryos were collected every 30 min on apple-juice agar plates, dechorionated with 50% chloroxbleach (about 90 sek.) and collected on a membrane filter (Whatman) using a glass vacuum filtration unit from Sartorius. On the membrane the embryos were arranged in short lines of 100-200 eggs. Each line was picked up with a 76 x 26 mm microscope slide that had been coated with glue (extracted from Scotch sticky tape with heptane) before. The coverslip was put for drying into a 12 cm Petri dish filled with silica gel at room temperature for 15-18 min. After drying the embryos were covered with halocarbon oil and microinjected. The coverslips with the injected embryos were placed into 12 cm Petri dishes together with moisturized paper towel. After two days at 18°C the larvae were collected and transferred into fly food vials supplemented with blue yeast paste. About two weeks later at 25°C the hatching adult flies are collected and screened for the presence of the w^+ marker.

Scotch heptane glue

Heptane and double-sided Scotch tape (about 2 m) (Scotch #665) were put together in a 50 ml falcone tube and were shaken for 1-2 days at room temperature. Heptane dissolves the glue from the tape resulting in quick evaporating glue.

4.2.10 Genomic DNA isolation

For genomic DNA isolation 5 adult flies were collected in a 1.5 ml eppendorf tube and put on ice. After adding 250 µl of Solution A flies were homogenized using a plastic homogenizer. Homogenized flies were incubated for 30 min at 70°C. Next 28 µl of 8M CH_3CO_2K was added and the samples were incubated for 30 min on ice. After spinning for 30 min at room temperature (13.000 rpm) the supernatant was transferred to a new tube. 250 µl of phenol-chloroform was added, after mixing and spinning at 13.000 rpm for 5 min the upper fraction was collected and transferred to a new tube. The DNA was precipitated by addition of 125 µl of isopropanol. The precipitated DNA was spun down by 15 min. of centrifugation at 13.000 rpm. The pellet was washed with 125 µl of 70% ethanol, spun down, dried at room temperature for 10-20 min. The DNA was diluted in 30 µl of water and the concentration was measured with a spectrophotometer.

4.2.11 Whole mount brain staining

Before brain dissection, adult flies were rinsed in 70% ethanol. Brains were dissected in PBS, they were kept on ice until fixation. Dissected brains were fixed for 30 min in 3.5% formaldehyde in PBS and washed 3 times for 10 min in 0.1% PBT. The primary antibodies were diluted in 0.1% PBT and applied overnight at 4°C. After washing the brains 3 x 10 min in 0.1% PBT, the secondary antibody diluted in 0.1% PBT was applied for 2-4 h. The brains were washed 3 x 10 min in 0.1% PBT and the Vectashield Mounting Medium was applied. The brains were mounted on a glass coverslip, imaged using the Olympus FV-1000 confocal microscope. Images were processed with Adobe Photoshop.

4.2.12 Assessment of the R8 photoreceptor axonal phenotypes

Figure 2-2B, **2-6**, **2-9F**, **2-13D**: the number of R8 axons stopping was calculated manually as a fraction of all GFP-expressing photoreceptors. **Figure 2-12D, 2-16D**: the number of R8 axons forming blobs was calculated manually as a fraction of all GFP-expressing axons. **Figure 2-7I**: the R8 axons stopping was clearly visible, however since R8 axons were overlapping before entering the medulla a precise quantification was not possible, thus the stopping was estimated as described previously (Hakeda-Suzuki et al., 2011) by comparing the number of M3 layer innervating axons between wild type and tested sample (wild type: 3.5 axons/µm). **Figure 2-12E**, **2-14B**, **2-15L**, **2-16E**: area of the M1 blob and diameter of R8 axons were calculated manually using the Olympus FV-1000 software.

4.2.13 Summary of experimental genotypes

Figure 2-1B *ey*FLP2 *glass-lacZ; Rh6-GFP*

Figure 2-1C *ey*FLP2 *glass-lacZ; gogo[H1675]* FRT80B/M(3)i[55], FRT80B

Figure 2-1D *ey*FLP2 *glass-lacZ; GMR-gogoFL* (IIA) / +; *gogo*[H1675] FRT80B / M(3)i[55], FRT80B

Figure 2-1E *ey*FLP2 *glass-lacZ; GMR-gogoC1-myc* (T1) / +; *gogo*[H1675] FRT80B / M(3)i[55], FRT80B

Figure 2-1F *ey*FLP2 *glass-lacZ; GMR-gogoC2-myc* (T2a) / +; *gogo*[H1675] FRT80B / M(3)i[55], FRT80B

Figure 2-1G *ey*FLP2 *glass-lacZ; GMR-gogoC3-myc* (T3b) / +; *gogo*[H1675] FRT80B / M(3)i[55], FRT80B

Figure 2-1H *ey*FLP2 *glass-lacZ; GMR-gogoC1C2-myc* (T2) / +; *gogo*[H1675] FRT80B / M(3)i[55], FRT80B

Figure 2-1I *ey*FLP2 *glass-lacZ; GMR-gogoC1C3-myc* (T1) / +; *gogo*[H1675] FRT80B / M(3)i[55], FRT80B

Figure 2-1J *ey*FLP2 *glass-lacZ; GMR-gogoC2C3-myc* (T2) / +; *gogo*[H1675] FRT80B / M(3)i[55], FRT80B

Figure 2-2C *ey*FLP2 *glass-lacZ; GMR-gogoFL*-P40 / +; *gogo[H1675]*, *Rh6-mCD8-4xGFP-3xmyc* FRT80B / M(3)i[55], *GMR-KO Gal80* FRT80B

Figure 2-2D *ey*FLP2 *glass-lacZ; GMR-gogoΔYYD*-P40 / +; *gogo[H1675]*, *Rh6-mCD8-4xGFP-3xmyc* FRT80B / M(3)i[55], *GMR-KO Gal80* FRT80B

Figure 2-2E *ey*FLP2 *glass-lacZ; GMR-gogoFFD-myc* (T4a) / +; *gogo[H1675]*, *Rh6-mCD8-4xGFP-3xmyc* FRT80B / M(3)i[55], *GMR-KO Gal80* FRT80B

Figure 2-2F *ey*FLP2 *glass-lacZ; GMR-gogoDDD*-P40 / +; *gogo[H1675]*, *Rh6-mCD8-4xGFP-3xmyc* FRT80B / M(3)i[55], *GMR-KO Gal80* FRT80B

Figure 2-2G *ey*FLP2 *glass-lacZ; GMR-gogoFYD*-P40 / +; *gogo[H1675]*, *Rh6-mCD8-4xGFP-3xmyc* FRT80B / M(3)i[55], *GMR-KO Gal80* FRT80B

Figure 2-2H *ey*FLP2 *glass-lacZ; GMR-gogoDYD*-P40 / +; *gogo[H1675]*, *Rh6-mCD8-4xGFP-3xmyc* FRT80B / M(3)i[55], *GMR-KO Gal80* FRT80B

Figure 2-2I *ey*FLP2 *glass-lacZ; GMR-gogoYFD*-P40 / +; *gogo[H1675], Rh6-mCD8-4xGFP-3xmyc* FRT80B / M(3)i[55], *GMR-KO Gal80* FRT80B
Figure 2-2J *ey*FLP2 *glass-lacZ; GMR-gogoYDD*-P40 / +; *gogo[H1675], Rh6-mCD8-4xGFP-3xmyc* FRT80B / M(3)i[55], *GMR-KO Gal80* FRT80B

Figure 2-6 *ey*FLP2 *glass-lacZ; GMR-gogoC2*^{shortFFD}*-P40* / +; *gogo[H1675], Rh6-mCD8-4xGFP-3xmyc* FRT80B / M(3)i[55], *GMR-KO Gal80* FRT80B

Figure 2-9A *GMR-Gal4 / UAS-gogoFL-P40; Rh6-mCD8-4xGFP-3xmyc* / +
Figure 2-9B *GMR-Gal4 / UAS-gogoΔYYD-P40; Rh6-mCD8-4xGFP-3xmyc* / +
Figure 2-9C *GMR-Gal4 / UAS-gogoDDD-P40; Rh6-mCD8-4xGFP-3xmyc* / +
Figure 2-9D *GMR-Gal4 / UAS-gogoDYD-P40; Rh6-mCD8-4xGFP-3xmyc* / +
Figure 2-9E *GMR-Gal4 / UAS-gogoYDD-P40; Rh6-mCD8-4xGFP-3xmyc* / +
Figure 2-9F *GMR-Gal4 / UAS-gogoFFD-P40; Rh6-mCD8-4xGFP-3xmyc* / +
Figure 2-9G *GMR-Gal4 / UAS-gogoFYD-P40; Rh6-mCD8-4xGFP-3xmyc* / +
Figure 2-9H *GMR-Gal4 / UAS-gogoYFD-P40; Rh6-mCD8-4xGFP-3xmyc* / +

Figure 2-10A *ey*FLP2 *glass-lacZ; atonal-tau-myc, gogo[D869]* FRT80B/M(3)i[55], FRT80B
Figure 2-10B *ey*FLP2 *glass-lacZ; GMR-gogoFL-P40 / +; atonal-tau-myc, gogo[D869]* FRT80B/M(3)i[55], FRT80B
Figure 2-10C *ey*FLP2 *glass-lacZ; GMR-gogoFFD-myc* (T4a) / +; *atonal-tau-myc, gogo[D869]* FRT80B/M(3)i[55], FRT80B

Figure 2-11A *GMR-Gal4 / UAS-gogoFL*-P40; *Rh4-mCD8-4xGFP-3xmyc* / +
Figure 2-11B *GMR-Gal4 / UAS-fmi*-P40; *Rh4-mCD8-4xGFP-3xmyc* / +
Figure 2-11C *GMR-Gal4, UAS-fmi*-P40 / *UAS-gogoFL*-P40; *Rh4-mCD8-4xGFP-3xmyc* / +
Figure 2-11D *GMR-Gal4, UAS-fmi*-P40 / *UAS-gogoFFD*-P40; *Rh4-mCD8-4xGFP-3xmyc* / +
Figure 2-11E *GMR-Gal4, UAS-fmi*-P40 / *UAS-gogoDDD*-P40; *Rh4-mCD8-4xGFP-3xmyc* / +

Figure 2-14A *ey*FLP2 *glass-lacZ, Rh6-mCD8-4xGFP-3xmyc* / Y; *GMR-Gal4 / UAS-dinr*
Figure 2-14B *eyFLP2 glass-lacZ, Rh6-mCD8-4xGFP-3xmyc* / Y; *GMR-Gal4, UAS-gogo* (T1) / +
Figure 2-14C *ey*FLP2 *glass-lacZ, Rh6-mCD8-4xGFP-3xmyc* / Y; *GMR-Gal4, UAS-gogo* (T1) */ UAS-dinr*

Figure 2-15A *ey*FLP2 *glass-lacZ, Rh6-mCD8-4xGFP-3xmyc* / Y; *GMR-Gal4 / UAS-InR.K1409A*
Figure 2-15B *ey*FLP2 *glass-lacZ, Rh6-mCD8-4xGFP-3xmyc* / Y; *GMR-Gal4, UAS-gogo* (T1) */ UAS-InR. K1409A*
Figure 2-15C *ey*FLP2 *glass-lacZ, Rh6-mCD8-4xGFP-3xmyc* / Y; *GMR-Gal4 / UAS-InR. A1325D*
Figure 2-15D *ey*FLP2 *glass-lacZ, Rh6-mCD8-4xGFP-3xmyc* / Y; *GMR-Gal4, UAS-Gogo* (T1) */ UAS-InR.A1325D*

Figure 2-16A *ey*FLP2 *glass-lacZ, Rh6-mCD8-4xGFP-3xmyc* / Y; *GMR-Gal4, UAS-Gogo* (T1) */ UAS-GogoFFD*

Figure 2-17A-E double (*ey*3.5FLP *glass-lacZ, Rh6-mCD8-4xGFP-3xmyc*) / +; FRT82 *GMR-mKO* / FRT82
Figure 2-17F-J double (*ey*3.5FLP *glass-lacZ, Rh6-mCD8-4xGFP-3xmyc*) / +; FRT82 *GMR-mKO* / FRT82 *dinr*^{ex15}

Figure 2-18A *ey*FLP2 *glass-lacZ, Rh6-mCD8-4xGFP-3xmyc* / Y; *GMR-Gal4, UAS-gogo* (T1) / +
Figure 2-18B *ey*FLP2 *glass-lacZ, Rh6-mCD8-4xGFP-3xmyc* / Y; *GMR-Gal4, UAS-gogo* (T1) / +; FRT82 *dinr*^{ex15} / +
Figure 2-18C *ey*FLP2 *glass-lacZ, Rh6-mCD8-4xGFP-3xmyc* / Y; *GMR-Gal4, UAS-Gogo* (T1) / +; *dilp1-4*^{1}, *5*^{3} / +

Figure 5-1A *GMR-gogoFL*-P40
Figure 5-1B *GMR-gogoΔYYD*-P40

Figure 5-1C	*GMR-gogoFFD*-T4a
Figure 5-1D	*GMR-gogoDDD*-P40
Figure 5-1E	*GMR-Gal4 / +; UAS-gogoFL*-P40
Figure 5-1F	*GMR-Gal4 / +; UAS-gogoΔYYD*-P40
Figure 5-1G	*GMR-Gal4 / +; UAS-gogoFFD*-P40
Figure 5-1H	*GMR-Gal4 / +; UAS-gogoDDD*-P40

5. Appendix

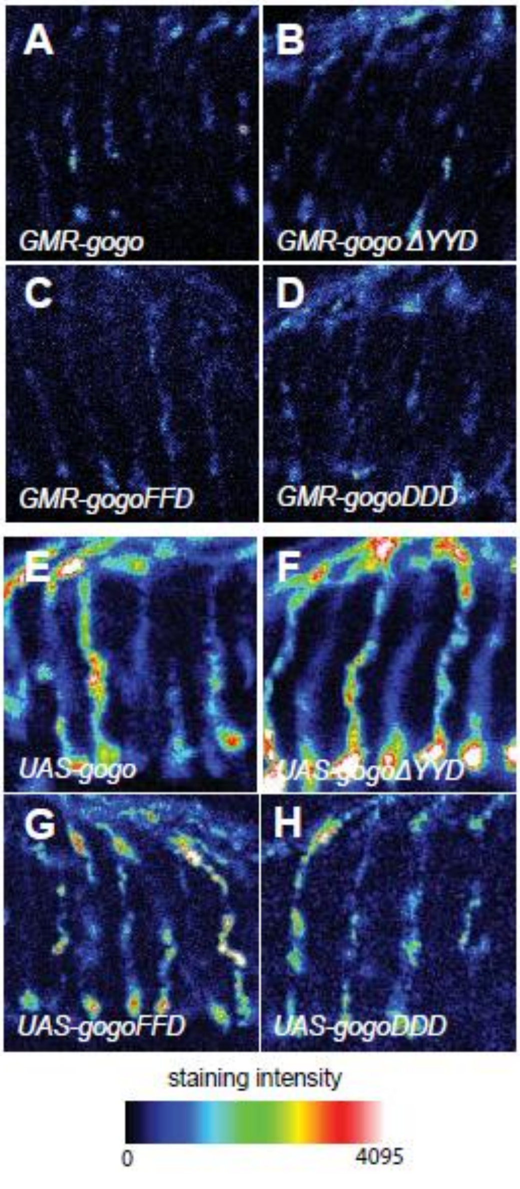
A
B
C
D
E
F
G
H
GMR-gogo
GMR-gogo ΔYYD
GMR-gogoFFD
GMR-gogoDDD
UAS-gogo
UAS-gogoΔYYD
UAS-gogoFFD
UAS-gogoDDD
staining intensity
0
4095

Figure 5-1: Gogo expression level comparison between different lines used in the study.

The expression levels was assessed based on the staining with the anti-Gogo antibody (the same staining conditions were used for the genotypes to be compared, see Materials and Methods). The scale (bottom) indicates the relative expression level; single confocal sections are shown.

(A-D) *gogo* constructs expression with the indicated genotype was driven with the *GMR* promoter. All constructs were inserted into the same locus (P40) except *GMR-gogoFFD* (T4a) which is a random insertion.

(E-H) *gogo* constructs (*UAS*) expression with the indicated genotype was driven with the *GMR-Gal4*. All of them were inserted into the same locus (P40).

Table 5-1: Candidate kinases tested for the enhancement of *gogo* gain of function phenotype

Gene	Transgene used	Source of the transgene	Overexpression *GMR-Gal4*	Co-overexpression *GMR-Gal4, UAS-gogo*
dinr	*UAS-dinr*	Bloomington	n.p.	M1 blobs enhanced
abl	*UAS-abl*	Takashi Suzuki	n.p.	Not enhanced
src64B	*UAS-src64B*	Bloomington	lethal	No R8 cells
src42A	*UAS-src42A.CA*	Bloomington	n.p.	Not enhanced
derailed	*UAS-drl*	Bloomington	n.p.	Not enhanced
egfr	*UAS-egfr*	Bloomington	n.p.	Cell death, axon guidance phenotype, M1 blobs enhanced
eyes absent	*UAS-eyeBII*	Bloomington	n.p.	Not enhanced

Kinases listed in the table were overexpressed alone (control) and in combination with *GMR-Gal4*, *UAS-gogo* and verified for enhancement or suppression of the M1 blob formation; n.p., no phenotype; *UAS-src42A.CA* – constitutively active form.

6. Bibliography

Adamo, M., Lowe, W. L., Leroith, D. and Roberts, C. T. (1989) 'Insulin-Like Growth Factor-I Messenger Ribonucleic-Acids with Alternative 5'-Untranslated Regions Are Differentially Expressed during Development of the Rat', *Endocrinology* 124(6): 2737-2744.

Alonso, A., Sasin, J., Bottini, N., Friedberg, I., Osterman, A., Godzik, A., Hunter, T., Dixon, J. and Mustelin, T. (2004) 'Protein tyrosine phosphatases in the human genome', *Cell* 117(6): 699-711.

Baba, K., Sakakibara, S., Setsu, T. and Terashima, T. (2007) 'The superficial layers of the superior colliculus are cytoarchitectually and myeloarchitectually disorganized in the reelin-deficient mouse, reeler', *Brain Res* 1140: 205-15.

Bashaw, G. J., Kidd, T., Murray, D., Pawson, T. and Goodman, C. S. (2000) 'Repulsive axon guidance: Abelson and Enabled play opposing roles downstream of the roundabout receptor', *Cell* 101(7): 703-15.

Bashaw, G. J. and Klein, R. (2010) 'Signaling from axon guidance receptors', *Cold Spring Harb Perspect Biol* 2(5): a001941.

Bazigou, E., Apitz, H., Johansson, J., Loren, C. E., Hirst, E. M., Chen, P. L., Palmer, R. H. and Salecker, I. (2007) 'Anterograde Jelly belly and Alk receptor tyrosine kinase signaling mediates retinal axon targeting in Drosophila', *Cell* 128(5): 961-75.

Benson, D. L., Colman, D. R. and Huntley, G. W. (2001) 'Molecules, maps and synapse specificity', *Nat Rev Neurosci* 2(12): 899-909.

Berger, J., Senti, K. A., Senti, G., Newsome, T. P., Asling, B., Dickson, B. J. and Suzuki, T. (2008) 'Systematic identification of genes that regulate neuronal wiring in the Drosophila visual system', *PLoS Genet* 4(5): e1000085.

Bonner, J. and O'Connor, T. P. (2001) 'The permissive cue laminin is essential for growth cone turning in vivo', *J Neurosci* 21(24): 9782-91.

Brand, A. H. and Perrimon, N. (1993) 'Targeted gene expression as a means of altering cell fates and generating dominant phenotypes', *Development* 118(2): 401-15.
Broughton, S. and Partridge, L. (2009) 'Insulin/IGF-like signalling, the central nervous system and aging', *Biochem J* 418(1): 1-12.

Butler, S. J. and Dodd, J. (2003) 'A role for BMP heterodimers in roof plate-mediated repulsion of commissural axons', *Neuron* 38(3): 389-401.

Callahan, C. A., Muralidhar, M. G., Lundgren, S. E., Scully, A. L. and Thomas, J. B. (1995) 'Control of neuronal pathway selection by a Drosophila receptor protein-tyrosine kinase family member', *Nature* 376(6536): 171-4.

Chapman, B. (2000) 'Necessity for afferent activity to maintain eye-specific segregation in ferret lateral geniculate nucleus', *Science* 287(5462): 2479-82.

Clandinin, T. R., Lee, C. H., Herman, T., Lee, R. C., Yang, A. Y., Ovasapyan, S. and Zipursky, S. L. (2001) 'Drosophila LAR regulates R1-R6 and R7 target specificity in the visual system', *Neuron* 32(2): 237-48.

Clandinin, T. R. and Zipursky, S. L. (2002) 'Making connections in the fly visual system', *Neuron* 35(5): 827-41.

Colamarino, S. A. and Tessier-Lavigne, M. (1995) 'The axonal chemoattractant netrin-1 is also a chemorepellent for trochlear motor axons', *Cell* 81(4): 621-9.

Craft, S., Newcomer, J., Kanne, S., DagogoJack, S., Cryer, P., Sheline, Y., Luby, J., DagogoJack, A. and Alderson, A. (1996) 'Memory improvement following induced hyperinsulinemia in Alzheimer's disease', *Neurobiology of Aging* 17(1): 123-130.

Demas, J., Sagdullaev, B. T., Green, E., Jaubert-Miazza, L., McCall, M. A., Gregg, R. G., Wong, R. O. and Guido, W. (2006) 'Failure to maintain eye-specific segregation in nob, a mutant with abnormally patterned retinal activity', *Neuron* 50(2): 247-59.

Dickson, B. J. (2001) 'Rho GTPases in growth cone guidance', *Curr Opin Neurobiol* 11(1): 103-10.

Dickson, B. J. (2002) 'Molecular mechanisms of axon guidance', *Science* 298(5600): 1959-64.

Edgar, B. A. (2006) 'How flies get their size: genetics meets physiology', *Nat Rev Genet* 7(12): 907-16.

Egea, J. and Klein, R. (2007) 'Bidirectional Eph-ephrin signaling during axon guidance', *Trends Cell Biol* 17(5): 230-8.

Fang, X., Yu, S. X., Lu, Y., Bast, R. C., Jr., Woodgett, J. R. and Mills, G. B. (2000) 'Phosphorylation and inactivation of glycogen synthase kinase 3 by protein kinase A', *Proc Natl Acad Sci U S A* 97(22): 11960-5.

Feldheim, D. A. and O'Leary, D. D. (2010) 'Visual map development: bidirectional signaling, bifunctional guidance molecules, and competition', *Cold Spring Harb Perspect Biol* 2(11): a001768.

Fernandez, R., Tabarini, D., Azpiazu, N., Frasch, M. and Schlessinger, J. (1995) 'The Drosophila insulin receptor homolog: a gene essential for embryonic development encodes two receptor isoforms with different signaling potential', *EMBO J* 14(14): 3373-84.

Fischbach K.F., D. A. P. M. (1989) 'The Optic Lobe of Drosophila melanogaster. Part I: A Golgi Analysis of Wild-Type Structure.', *Cell Tissue Res* 258(258): 441-475.

Fortini, M. E. and Rubin, G. M. (1990) 'Analysis of cis-acting requirements of the Rh3 and Rh4 genes reveals a bipartite organization to rhodopsin promoters in Drosophila melanogaster', *Genes Dev* 4(3): 444-63.

Freeman, M. (1996) 'Reiterative use of the EGF receptor triggers differentiation of all cell types in the Drosophila eye', *Cell* 87(4): 651-60.

Garrity, P. A., Rao, Y., Salecker, I., McGlade, J., Pawson, T. and Zipursky, S. L. (1996) 'Drosophila photoreceptor axon guidance and targeting requires the dreadlocks SH2/SH3 adapter protein', *Cell* 85(5): 639-50.

Gilbert, S. F. (1997) *Developmental Biology*: Sinauer Associates Inc. .

Gronke, S., Clarke, D. F., Broughton, S., Andrews, T. D. and Partridge, L. (2010) 'Molecular evolution and functional characterization of Drosophila insulin-like peptides', *PLoS Genet* 6(2): e1000857.

Grueber, W. B. and Sagasti, A. (2010) 'Self-avoidance and tiling: Mechanisms of dendrite and axon spacing', *Cold Spring Harb Perspect Biol* 2(9): a001750.

Hafen, E., Bohni, R., Riesgo-Escovar, J., Oldham, S., Brogiolo, W., Stocker, H., Andruss, B. F. and Beckingham, K. (1999) 'Autonomous control of cell and organ size by CHICO, a Drosophila homolog of vertebrate IRS1-4', *Cell* 97(7): 865-875.

Hakeda-Suzuki, S., Berger-Muller, S., Tomasi, T., Usui, T., Horiuchi, S. Y., Uemura, T. and Suzuki, T. (2011) 'Golden Goal collaborates with Flamingo in conferring synaptic-layer specificity in the visual system', *Nat Neurosci* 14(3): 314-23.

Harris, R., Sabatelli, L. M. and Seeger, M. A. (1996) 'Guidance cues at the Drosophila CNS midline: identification and characterization of two Drosophila Netrin/UNC-6 homologs', *Neuron* 17(2): 217-28.

Hauck, B., Gehring, W. J. and Walldorf, U. (1999) 'Functional analysis of an eye specific enhancer of the eyeless gene in Drosophila', *Proc Natl Acad Sci U S A* 96(2): 564-9.

Hay, B. A., Wolff, T. and Rubin, G. M. (1994) 'Expression of baculovirus P35 prevents cell death in Drosophila', *Development* 120(8): 2121-9.

Henkemeyer, M., Orioli, D., Henderson, J. T., Saxton, T. M., Roder, J., Pawson, T. and Klein, R. (1996) 'Nuk controls pathfinding of commissural axons in the mammalian central nervous system', *Cell* 86(1): 35-46.

Hiesinger, P. R., Zhai, R. G., Zhou, Y., Koh, T. W., Mehta, S. Q., Schulze, K. L., Cao, Y., Verstreken, P., Clandinin, T. R., Fischbach, K. F. et al. (2006) 'Activity-independent prespecification of synaptic partners in the visual map of Drosophila', *Curr Biol* 16(18): 1835-43.

Hing, H., Xiao, J., Harden, N., Lim, L. and Zipursky, S. L. (1999) 'Pak functions downstream of Dock to regulate photoreceptor axon guidance in Drosophila', *Cell* 97(7): 853-63.

Hofmeyer, K., Maurel-Zaffran, C., Sink, H. and Treisman, J. E. (2006) 'Liprin-alpha has LAR-independent functions in R7 photoreceptor axon targeting', *Proc Natl Acad Sci U S A* 103(31): 11595-600.

Hofmeyer, K. and Treisman, J. E. (2009) 'The receptor protein tyrosine phosphatase LAR promotes R7 photoreceptor axon targeting by a phosphatase-independent signaling mechanism', *Proc Natl Acad Sci U S A* 106(46): 19399-404.

Holt, C. E. and Campbell, D. S. (2001) 'Chemotropic responses of retinal growth cones mediated by rapid local protein synthesis and degradation', *Neuron* 32(6): 1013-1026.

Huberman, A. D., Clandinin, T. R. and Baier, H. (2010) 'Molecular and cellular mechanisms of lamina-specific axon targeting', *Cold Spring Harb Perspect Biol* 2(3): a001743.

Jarman, A. P., Grell, E. H., Ackerman, L., Jan, L. Y. and Jan, Y. N. (1994) 'Atonal Is the Proneural Gene for Drosophila Photoreceptors', *Nature* 369(6479): 398-400.

Jiang, Y., Obama, H., Kuan, S. L., Nakamura, R., Nakamoto, C., Ouyang, Z. and Nakamoto, M. (2009) 'In vitro guidance of retinal axons by a tectal lamina-specific glycoprotein Nel', *Mol Cell Neurosci* 41(2): 113-9.

Johansen, J. W. and Ingebritsen, T. S. (1986) 'Phosphorylation and inactivation of protein phosphatase 1 by pp60v-src', *Proc Natl Acad Sci U S A* 83(2): 207-11.

Kidd, T., Brose, K., Mitchell, K. J., Fetter, R. D., Tessier-Lavigne, M., Goodman, C. S. and Tear, G. (1998) 'Roundabout controls axon crossing of the CNS midline and defines a novel subfamily of evolutionarily conserved guidance receptors', *Cell* 92(2): 205-15.

Klein, R. (2004) 'Eph/ephrin signaling in morphogenesis, neural development and plasticity', *Curr Opin Cell Biol* 16(5): 580-9.

Klein, R. (2009) 'Bidirectional modulation of synaptic functions by Eph/ephrin signaling', *Nat Neurosci* 12(1): 15-20.

Knoll, B. and Drescher, U. (2004) 'Src family kinases are involved in EphA receptor-mediated retinal axon guidance', *J Neurosci* 24(28): 6248-57.

Kolodkin, A. L. and Tessier-Lavigne, M. (2011) 'Mechanisms and molecules of neuronal wiring: a primer', *Cold Spring Harb Perspect Biol* 3(6).

Lai Wing Sun, K., Correia, J. P. and Kennedy, T. E. (2011) 'Netrins: versatile extracellular cues with diverse functions', *Development* 138(11): 2153-69.

Langley, J. N. (1892) 'On the origin from the spinal cord of the cervical and upper thoracic sympathetic fibres, with some observations on white and grey rami communications. ', *Philos Trans R Soc Land B Biol Sci* 183(183): 85-124.

Lee, C. H., Herman, T., Clandinin, T. R., Lee, R. and Zipursky, S. L. (2001) 'N-cadherin regulates target specificity in the Drosophila visual system', *Neuron* 30(2): 437-50.

Lee, R. C., Clandinin, T. R., Lee, C. H., Chen, P. L., Meinertzhagen, I. A. and Zipursky, S. L. (2003) 'The protocadherin Flamingo is required for axon target selection in the Drosophila visual system', *Nat Neurosci* 6(6): 557-63.

Lin, A. N., Barnes, S. and Wallace, R. W. (1990) 'Phosphorylation by protein kinase C inactivates an inositol 1,4,5-trisphosphate 3-kinase purified from human platelets', *Biochem Biophys Res Commun* 170(3): 1371-6.

Liu, G., Beggs, H., Jurgensen, C., Park, H. T., Tang, H., Gorski, J., Jones, K. R., Reichardt, L. F., Wu, J. and Rao, Y. (2004) 'Netrin requires focal adhesion kinase and Src family kinases for axon outgrowth and attraction', *Nat Neurosci* 7(11): 1222-32.

Longo, N., Shuster, R. C., Griffin, L. D., Langley, S. D. and Elsas, L. J. (1992) 'Activation of insulin receptor signaling by a single amino acid substitution in the transmembrane domain', *J Biol Chem* 267(18): 12416-9.

Maher, P. A. and Pasquale, E. B. (1988) 'Tyrosine phosphorylated proteins in different tissues during chick embryo development', *J Cell Biol* 106(5): 1747-55.

Marks, J. L., Maddison, J. and Eastman, C. J. (1988) 'Subcellular-Localization of Rat-Brain Insulin Binding-Sites', *Journal of Neurochemistry* 50(3): 774-781.

Markstein, M., Pitsouli, C., Villalta, C., Celniker, S. E. and Perrimon, N. (2008) 'Exploiting position effects and the gypsy retrovirus insulator to engineer precisely expressed transgenes', *Nat Genet* 40(4): 476-83.

Mast, J. D., Prakash, S., Chen, P. L. and Clandinin, T. R. (2006) 'The mechanisms and molecules that connect photoreceptor axons to their targets in Drosophila', *Semin Cell Dev Biol* 17(1): 42-9.

Maurel-Zaffran, C., Suzuki, T., Gahmon, G., Treisman, J. E. and Dickson, B. J. (2001) 'Cell-autonomous and -nonautonomous functions of LAR in R7 photoreceptor axon targeting', *Neuron* 32(2): 225-35.

Mayer, G., Nitsch, R. and Hoyer, S. (1990) 'Effects of Changes in Peripheral and Cerebral Glucose-Metabolism on Locomotor-Activity, Learning and Memory in Adult Male-Rats', *Brain Res* 532(1-2): 95-100.

Meinertzhagen, I. A. and O'Neil, S. D. (1991) 'Synaptic organization of columnar elements in the lamina of the wild type in Drosophila melanogaster', *J Comp Neurol* 305(2): 232-63.

Moore, S. W., Tessier-Lavigne, M. and Kennedy, T. E. (2007) 'Netrins and their receptors', *Adv Exp Med Biol* 621: 17-31.

Morata, G. and Ripoll, P. (1975) 'Minutes: mutants of drosophila autonomously affecting cell division rate', *Dev Biol* 42(2): 211-21.

Morey, M., Yee, S. K., Herman, T., Nern, A., Blanco, E. and Zipursky, S. L. (2008) 'Coordinate control of synaptic-layer specificity and rhodopsins in photoreceptor neurons', *Nature* 456(7223): 795-9.

Nern, A., Nguyen, L. V., Herman, T., Prakash, S., Clandinin, T. R. and Zipursky, S. L. (2005) 'An isoform-specific allele of Drosophila N-cadherin disrupts a late step of R7 targeting', *Proc Natl Acad Sci U S A* 102(36): 12944-9.

Newsome, T. P., Asling, B. and Dickson, B. J. (2000) 'Analysis of Drosophila photoreceptor axon guidance in eye-specific mosaics', *Development* 127(4): 851-60.

Ohler, S., Hakeda-Suzuki, S. and Suzuki, T. (2011) 'Hts, the Drosophila homologue of Adducin, physically interacts with the transmembrane receptor Golden goal to guide photoreceptor axons', *Dev Dyn* 240(1): 135-48.

Papatsenko, D., Nazina, A. and Desplan, C. (2001) 'A conserved regulatory element present in all Drosophila rhodopsin genes mediates Pax6 functions and participates in the fine-tuning of cell-specific expression', *Mech Dev* 101(1-2): 143-53.

Petrovic, M. and Hummel, T. (2008) 'Temporal identity in axonal target layer recognition', *Nature* 456(7223): 800-3.

Raper, J. and Mason, C. (2010) 'Cellular strategies of axonal pathfinding', *Cold Spring Harb Perspect Biol* 2(9): a001933.

Rulifson, E. J., Kim, S. K. and Nusse, R. (2002) 'Ablation of insulin-producing neurons in flies: growth and diabetic phenotypes', *Science* 296(5570): 1118-20.

Sakakibara, S., Misaki, K. and Terashima, T. (2003) 'Cytoarchitecture and fiber pattern of the superior colliculus are disrupted in the Shaking Rat Kawasaki', *Brain Res Dev Brain Res* 141(1-2): 1-13.

Salecker, I., Hadjieconomou, D. and Timofeev, K. (2011) 'A step-by-step guide to visual circuit assembly in Drosophila', *Current Opinion in Neurobiology* 21(1): 76-84.

Salinas, P. C. and Zou, Y. (2008) 'Wnt signaling in neural circuit assembly', *Annu Rev Neurosci* 31: 339-58.

Saltiel, A. R. and Kahn, C. R. (2001) 'Insulin signalling and the regulation of glucose and lipid metabolism', *Nature* 414(6865): 799-806.

Sanes, J. R. and Zipursky, S. L. (2010) 'Design principles of insect and vertebrate visual systems', *Neuron* 66(1): 15-36.

Saucedo, L. J. and Edgar, B. A. (2007) 'Filling out the Hippo pathway', *Nat Rev Mol Cell Biol* 8(8): 613-21.

Senti, K. A., Usui, T., Boucke, K., Greber, U., Uemura, T. and Dickson, B. J. (2003) 'Flamingo regulates R8 axon-axon and axon-target interactions in the Drosophila visual system', *Curr Biol* 13(10): 828-32.

Shinza-Kameda, M., Takasu, E., Sakurai, K., Hayashi, S. and Nose, A. (2006) 'Regulation of layer-specific targeting by reciprocal expression of a cell adhesion molecule, capricious', *Neuron* 49(2): 205-13.

Siebert, M., Banovic, D., Goellner, B. and Aberle, H. (2009) 'Drosophila motor axons recognize and follow a Sidestep-labeled substrate pathway to reach their target fields', *Genes Dev* 23(9): 1052-62.

Song, J., Wu, L., Chen, Z., Kohanski, R. A. and Pick, L. (2003) 'Axons guided by insulin receptor in Drosophila visual system', *Science* 300(5618): 502-5.

Sperry, R. W. (1963) 'Chemoaffinity in the orderly growth of nerve fiber patterns and connections. ', *Proc Natl Acad Sci U S A* 50(50): 703-710.

Stocker, H. and Hafen, E. (2000) 'Genetic control of cell size', *Curr Opin Genet Dev* 10(5): 529-35.

Takemura, S. Y., Lu, Z. and Meinertzhagen, I. A. (2008) 'Synaptic circuits of the Drosophila optic lobe: the input terminals to the medulla', *J Comp Neurol* 509(5): 493-513.

Tarrant, M. K. and Cole, P. A. (2009) 'The chemical biology of protein phosphorylation', *Annu Rev Biochem* 78: 797-825.

Tatar, M., Bartke, A. and Antebi, A. (2003) 'The endocrine regulation of aging by insulin-like signals', *Science* 299(5611): 1346-51.

Tayler, T. D. and Garrity, P. A. (2003) 'Axon targeting in the Drosophila visual system', *Curr Opin Neurobiol* 13(1): 90-5.

TessierLavigne, M. and Goodman, C. S. (1996) 'The molecular biology of axon guidance', *Science* 274(5290): 1123-1133.

Ting, C. Y. and Lee, C. H. (2007) 'Visual circuit development in Drosophila', *Curr Opin Neurobiol* 17(1): 65-72.

Ting, C. Y., Yonekura, S., Chung, P., Hsu, S. N., Robertson, H. M., Chiba, A. and Lee, C. H. (2005) 'Drosophila N-cadherin functions in the first stage of the two-stage layer-selection process of R7 photoreceptor afferents', *Development* 132(5): 953-63.

Tomasi, T., Hakeda-Suzuki, S., Ohler, S., Schleiffer, A. and Suzuki, T. (2008) 'The transmembrane protein Golden goal regulates R8 photoreceptor axon-axon and axon-target interactions', *Neuron* 57(5): 691-704.

Tran, T. S., Kolodkin, A. L. and Bharadwaj, R. (2007) 'Semaphorin regulation of cellular morphology', *Annu Rev Cell Dev Biol* 23: 263-92.

Wang, K. H., Brose, K., Arnott, D., Kidd, T., Goodman, C. S., Henzel, W. and Tessier-Lavigne, M. (1999) 'Biochemical purification of a mammalian slit protein as a positive regulator of sensory axon elongation and branching', *Cell* 96(6): 771-84.

Wang, Y. T., Man, H. Y., Lin, J. W., Ju, W. H., Ahmadian, G., Liu, L. D., Becker, L. E. and Sheng, M. (2000) 'Regulation of AMPA receptor-mediated synaptic transmission by clathrin-dependent receptor internalization', *Neuron* 25(3): 649-662.

Wickelgren, I. (1998) 'Tracking insulin to the mind', *Science* 280(5363): 517-519.

Wu, Q., Zhang, Y., Xu, J. and Shen, P. (2005) 'Regulation of hunger-driven behaviors by neural ribosomal S6 kinase in Drosophila', *Proc Natl Acad Sci U S A* 102(37): 13289-94.

Xia, F., Li, J., Hickey, G. W., Tsurumi, A., Larson, K., Guo, D., Yan, S. J., Silver-Morse, L. and Li, W. X. (2008) 'Raf activation is regulated by tyrosine 510 phosphorylation in Drosophila', *PLoS Biol* 6(5): e128.

Xiao, T. and Baier, H. (2007) 'Lamina-specific axonal projections in the zebrafish tectum require the type IV collagen Dragnet', *Nat Neurosci* 10(12): 1529-37.

Xiao, T., Roeser, T., Staub, W. and Baier, H. (2005) 'A GFP-based genetic screen reveals mutations that disrupt the architecture of the zebrafish retinotectal projection', *Development* 132(13): 2955-67.

Yamagata, M. and Sanes, J. R. (2005) 'Versican in the developing brain: lamina-specific expression in interneuronal subsets and role in presynaptic maturation', *J Neurosci* 25(37): 8457-67.

Yazdani, U. and Terman, J. R. (2006) 'The semaphorins', *Genome Biol* 7(3): 211.

Yonekura, S., Xu, L., Ting, C. Y. and Lee, C. H. (2007) 'Adhesive but not signaling activity of Drosophila N-cadherin is essential for target selection of photoreceptor afferents', *Dev Biol* 304(2): 759-70.

Zang, M., Gong, J., Luo, L., Zhou, J., Xiang, X., Huang, W., Huang, Q., Luo, X., Olbrot, M., Peng, Y. et al. (2008) 'Characterization of Ser338 phosphorylation for Raf-1 activation', *J Biol Chem* 283(46): 31429-37.

Acknowledgements

I am grateful to Dr. Takashi Suzuki for giving me the opportunity to work in his lab and for supervising my work. Thanks for making it possible for me to change the project during the PhD.

I would like to thank to Prof. Rűdiger Klein and Dr. Ilona Kadow as members of my thesis committee - for helpful suggestions, availability. I especially thank Prof. Klein for being my official Doktorvater.

I am indebted to all the people I could meet in the lab during the last four years… your presence, words, comments helped me to go through everything. Thanks to all of you! I would like to list at least some of the things I especially appreciate.

I am grateful to:
Dr. Atsushi Sugie - for showing how to work with passion, tranquility and persistence.
Cristina Organisti - for bringing so much smile, sun and optimism to our lab.
Grace Wang - for helping me so much with the experiments. Without her help it would take certainly much longer. Thanks for your enthusiasm and involvement.
Irina Hein - for the unforgettable discussions (fights?) on the "life philosophy" and religion – we never reached the consensus - but they were indeed stimulating! We have to do more…
Michael Sauter - the most relaxed guy I ever met. Thanks for your readiness to help me with flies and cloning.
Dr Sandra Berger-Műller - we spend together our PhD time from the very first day, thanks for teaching me biochemistry, being always helpful, for providing the "French accents" in the lab, which I liked so much and for correcting my manuscript.
Dr Satoko Suzuki - for giving me help always, generously and immediately whenever I asked.

I would like to thank the previous lab members for their kindness and readiness to help: Stephan Ohler, Jing Shi, Dr. Tatiana Tomasi, Franziska Götschel, all the people I meet in the Institute in the neighboring labs and of course last but not least Si-Hong Luu who actually started this project in the lab during his Diploma. I am grateful to Marion Hartl for a careful correction of the thesis and for so much "positive attitude" she was always spreading around.

Special thanks go to my friends who stayed on my side during the time of my PhD: Marta, Marta, Hristina, Ola and Marcin, Iv… for sharing years of their lives full of happiness, worries, hopes and struggles with me.

****

I would like to feature Kalina, who accompanied so many moments in my live - for so many reasons which cannot be listed here. Grazie con tutto il cuore.

****

Szczególnie dziękuję mojej najbliższej Rodzinie: Mamie, Dziadkom, Elwirze… za obecność, wiarę we mnie i dom. Bez ich wysiłku mój doktorat z całą pewnością nie byłby możliwy.

Curriculum vitae

Personal information

Name:	Klaudiusz Łukasz Mann
Date of birth:	03.08.1983
Place of birth:	Pyskowice, Poland

Educational background

X 2007 – present	Ph.D. at the Max Planck Institute of Neurobiology (Munich, Germany)
X 2006 – II 2007	Diploma thesis project at the Ludwig-Maximilians-Universität München, Germany (project supervisor: Günther Woehlke, PD, Ph.D.). Title: Properties of KIF5A, neuronal conventional kinesin, mutant proteins linked to Hereditary Spastic Paraplegia
X 2002 – VI 2007	Diploma in Biology at the Jagiellonian University, Poland; specialization: cell biology (supervisor: Marta Michalik, PhD)

Publications and scientific communications

- Ebbing, B., Mann, K., Starosta, A., Jaud, J., Schöls, L., Schűle, R., Woehlke, G. (2008) Effect of spastic paraplegia mutations in KIF5A kinesin on transport activity. Hum Mol Genet 17(9): 1245-52
- Mann, K., Wang, M., Luu, S.H., Ohler, S., Hakeda-Suzuki, S., Suzuki, T., A putative tyrosine phosphorylation site of the cell surface receptor Golden goal is involved in synaptic layer selection in the visual system. Development 139(4):760-71
- 1st Asia-Pacific Drosophila Research Conference, Taipei, Taiwan (2011) – poster presentation
- Cold Spring Harbor Laboratory conference on “Axon Guidance, Synaptic Plasticity and Regeneration”, New York, USA (2010) – poster presentation
- European *Drosophila* Research Conference, Nice, France (2009) – poster presentation